1-1-2013

Development and Figures of Merit of Microextraction and Ultra-Performance Liquid Chromatography for Forensic Characterization of Dye Profiles on Trace Acrylic, Nylon, Polyester, and Cotton Textile Fibers

Scott James Hoy
University of South Carolina

Development and Figures of Merit of Microextraction and Ultra-Performance Liquid Chromatography for Forensic Characterization of Dye Profiles on Trace Acrylic, Nylon, Polyester, and Cotton Textile Fibers

By

Scott J. Hoy

Bachelor of Science
Georgia Institute of Technology, 2005

Submitted in Partial Fulfillment of the Requirements

For the Degree of Doctor of Philosophy in

Chemistry and Biochemistry

College of Arts and Sciences

University of South Carolina

2013

Accepted by:

Stephen L. Morgan, Major Professor

Scott R. Goode, Committee Member

Michael L. Myrick, Committee Member

James M. Chapman, Committee Member

Lacy Ford, Vice Provost and Dean of Graduate Studies

DEDICATION

This work is dedicated to my family for their unwavering love and support.

ABSTRACT

Methodology for the microextraction of basic dyes on acrylic, acid dyes on nylon, disperse dyes on polyester, and reactive dyes, direct dyes, and indigo on cotton textile fibers is reported. Although these processes are destructive to the fiber evidence, the ability to analyze dye extracts from sub-millimeter fiber lengths of single fibers, coupled with detection limits in the hundred picogram range by ultra-performance liquid chromatography (UPLC) with both diode array detection (DAD) and tandem mass spectrometry (MS-MS) makes routine forensic characterization feasible.

Microextraction, followed by UPLC, can often distinguish similar fibers containing different, but similar, dyes with the combination of retention time matching, UV/visible spectral comparison, and structural analysis by mass spectrometry. This work focuses on determining the optimum extraction conditions for each dye class and developing chromatographic methods with suitable resolution and sensitivity for trace analysis. Analysis of fibers as small as 1 mm in length is the target sample size to minimize destruction of fiber evidence. Analytical figures of merit and validation statistics, including extraction reproducibility, linearity, limits of detection and quantitation, and UPLC precision, are reported.

The analysis of cotton fibers is challenging because they can be dyed with three different classes of dye, each requiring a different method for extraction and analysis. Reactive dyes present a unique challenge because they are chemically bound to the cellulose structure of the fiber. Release of these dyes from cotton requires breaking of the covalent bond using hot sodium hydroxide. The resulting hydrolysis reactions can also cleave amide bonds and possibly other chemical bonds in the dye molecule. The various

structural changes that can take place leads, in many cases, to production of multiple reaction products from a single dye. We demonstrate successful extraction of reactive dyes from single 1 mm cotton fibers with detection limits as low as 3.3 pg. Systematic experiments at varying reaction conditions, with product analysis by mass spectrometry, were also performed to characterize the degradation of reactive dyes under hydrolysis, and to facilitate interpretation of reactive dye extractions.

The concept of the sensitivity ratio as an analytical performance characteristic was introduced by John Mandel of the National Bureau of Standards in 1954, but has been not been widely applied in analytical chemistry. The basis for Mandel sensitivity is reviewed here, along with examples of its use. Because the sensitivity ratio is independent of the scale in which measurements are expressed, it is a useful tool for comparisons of variability between different analytical methods.

TABLE OF CONTENTS

LIST OF TABLES

LIST OF FIGURES

CHAPTER ONE

TRACE CHEMICAL ANALYSIS OF DYES EXTRACTED FROM FORENSIC EVIDENCE FIBERS: A REVIEW

INTRODUCTION

Trace fiber evidence has been probative in cases ranging from the 1963 JFK assassination,[1] to the Atlanta Child murders[2] of the early 1980s, and the 2002 Washington, DC, sniper case.[3] The fiber examiner typically performs a series of comparisons of the questioned fiber to a known fiber in an attempt to exclude the possibility that a 'questioned' fiber and 'known' fiber could have originated from a common source. If the two fibers can be shown to be substantially different, then the hypothesis that the two fibers originated from a common source can be discounted. The comparison of an 'unknown' to a 'known' fiber is illustrated by the testimony of FBI fiber examiner Paul Stombaugh before the Warren Commission.[1] A tuft of fibers that appeared to match fibers from Oswald's shirt was found caught on a jagged edge of Oswald's rifle stock. Stombaugh testified "there is no doubt in my mind that these fibers could have come from this shirt. There is no way, however, to eliminate the possibility of the fibers having come from another identical shirt." Whenever the hypothesis of a common source for two fibers cannot be rejected, evidence may have probative value, and investigative leads could evolve from the suggested association between victim and suspect. The history of fiber examinations is characterized by a search for increased discrimination to render trace evidence more specific and discriminating. Significance of fiber evidence and discrimination are expanded by combinatorial possibilities of fiber types and dyes.[4-9] If dye formulations on trace fibers can be reliably profiled at trace levels, match exclusions can be made with higher reliability, and "results consistent with" will have increased significance. Separation and detection of individual dye components provides a qualitative and semi-quantitative fiber dye 'fingerprint.' Determining the

number and relative amounts of dyes present, and characterizing those dyes at the molecular level by UV/visible absorbance and MS, offers an entirely new level of discrimination. Such information may also open the possibility of tracing specific dye formulations to the dye manufacturer.

Our work has focused on manufactured fibers (nylon, acrylic, and polyester), and the natural fiber, cotton, because of their prevalence in case work.[10,11] Understanding the chemistry and industrial processes involving fibers and dyes is a starting point for design of extraction methods, for developing improved analysis methods, and for correct data interpretation.[4,12] In manufacturing, raw fibers are treated to remove contaminants and lubricants, or to change morphology; fabrics may be bleached; cotton is mercerized to change its morphology and increase dye uptake; nylon and polyester are heat-set to stabilize distortion and to improve dyeability. Fabrics may be flame-treated to remove surface fuzz, or desized by enzymes to remove weaving aids (*e.g.*, lubricants). Fibers are dyed with processes appropriate for their chemistry (acid dyes, basic dyes, direct dyes, azoic dyes, mordant dyes, sulfur dyes, vat dyes, reactive dyes, disperse dyes, and pigments). Dyes may be loosely associated with fibers (direct dyes on cotton are held by Van der Waals forces and hydrogen bonding), bound by salt linkages (acid dyes on nylon, basic dyes on acrylic), or covalently bonded (reactive dyes on cotton). Dyes may be dispersed through the fiber (*e.g.*, on polyester), mechanically trapped through redox processes (vat dyes on cotton), applied during melt spinning (pigment coloration of nylon, polyolefins, and polyester), or adhered to surfaces with adhesives (pigment dyeing of bedding and apparel fabrics). Fabrics are often finished to impart aesthetic and

performance properties, such as stay-press finishing and water-proofing. Preprocessing, dyeing, and finishing all may leave residues on fibers that are useful for discrimination.

Dyes are conjugated molecules, generally consisting of aromatic and/or unsaturated compounds that are either derived from natural sources or are made synthetically. Dyes are often classified according to their application method (*e.g*., reactive, disperse, and vat) and their chemical constitution (*e.g*., azo, anthraquinone, metal complex azo). Knowledge of the chemistry of both fibers and dyes is relevant to the extraction of dyes from fibers and to development of appropriate methods of analysis. To extract dye from fiber, the dye's substantivity for the fiber (affinity via intermolecular interactions) must be reduced, then the dye is solvated and transported from the fiber into the extractant. Wiggins[13] summarized solvents for dye extraction. Thin layer chromatography (TLC) of dyes has been widely used in forensic labs.[4-6,13-27] Gaudette[14] mentions that some dyes on 2 mm fibers can be analyzed by TLC, but light-colored fibers may require more than 100× that length. Of 64 fibers listed by polymers, dyes, and color intensities, only 17% of those fibers could be analyzed at 2 mm lengths, 30% at 5 mm, and 61% at 10 mm. For applicability to casework relevant sample sizes, optimizing extraction protocols is critical.

Stefan, *et al*. and Dockery, *et al*. employed experimental design[30-33] to optimize extraction of acid dyes on nylon, basic dyes on acrylic, disperse dyes on polyester, and direct, reactive, and indigo vat dyes on cotton. As an example, with acid dyes on nylon, 10 mixtures of water: pyridine: aqueous ammonia were prepared in duplicate by a laboratory robot, in vials on a 96-well plate. Identical 10-cm fibers were extracted and the absorbance of extracts were measured by a plate reader.[30] In the fitted model, a diagonal

ridge of high extraction response runs across the surface from 50:50 pyridine:water to 50 :50 pyridine/ammonia. Of the pure solvents, water gives the best extraction, although the amount of dye extracted is low. Pyridine does not dissolve the dye completely; the solubility of the dye in water is four times higher than that in pyridine. However, pure water is not sufficiently basic to deprotonate the nylon amine end groups and to release acid dyes completely from nylon. Although aqueous ammonia dissolves acid dyes better than does pure pyridine, aqueous ammonia lacks the organic content necessary to fully extract the organic anions of acid dyes. The diagonal ridge runs across the ternary solvent triangle at constant pyridine content of about 45-50%. For extraction of the anthraquinone Acid Blue 45 dye from nylon, the predicted optimum is at a solvent composition of 42% pyridine/58% water. These extraction conditions were confirmed for two other subclasses of acid dyes (azo, and metal complex azo dyes) and produce complete extraction of the tested dyes.[30] All extraction protocols that we have developed can be done in reasonable times (30-60 min, even if done manually).

LC, CE, and MS are established in applications from drug identification to DNA analysis and forensic toxicology. CE and LC methods offer efficiency, selectivity, short analysis time, low organic solvent consumption, low required sample, and relatively low running costs. CE is well suited for dye analysis because many dyes are ionized, depending on their pK_a and buffer solution pH, however a comprehensive separation method by CE is problematic due to a number of non-ionizing dyes (disperse dyes on polyester, vat dyes on cotton). HPLC is theoretically superior to CE because dye species need not be ionic or ionizable, and offers mobile and stationary phase tunability. Sirén and Sulkava[34] used CE and UV/visible diode array detection (DAD) for analysis of black

dyes from cotton and wool fibers. Xu, *et al.*[35] employed CE to separate reactive, acid, direct, azoic and metal complex dyes extracted from cotton, wool, polyacrylic, polyester, and polyamide fibers; sample stacking was used to improve detection limits. Environmental or industrial applications dominate the dye extract analysis literature.[36-47]

Minor peaks are often observed in separations of dye extracts using any separation technique. These contaminants in the "pure" dyestuffs and side products from incomplete dye synthesis may be signatures of the manufacturing process. Purified component dyes are neither required nor economically feasible on a commercial scale as long as the dyes possess the desired properties. Whether patterns of trace contaminants can be related to manufacturing processes is worth investigating in discussions with industrial manufacturers. However, whether such trace patterns can be reliably used to associate a fiber with a manufacturer is unlikely. The relative amounts of dyes can be correlated with the quantitative dye formulation from the manufacturer might be of forensic significance, if such information were obtainable. Additionally, environmental changes associated with a questioned fiber could affect the quality of such information for comparative purposes.

UV/visible detection of dyes from short single fiber lengths can be difficult. One cm of nylon fiber dyed with commercial levels of an acid dye was extracted with 60:40 water:pyridine and the extract was dried down and reconstituted with 190 μL of water prior to CE injection. The absorbance of 3 mAU at the peak maximum produced unreliable spectra. Wheals, *et al.*[49] reported HPLC detection limits of 200 pg/dye, but also found that extracts of short fibers of light shades often yielded insufficient dye. Minor dye components sometimes discriminated fibers even when major components were indistinguishable. Laing, *et al.*[50] analyzed acid dyes by LC with UV/visible diode

array detection (DAD), but did not show analysis of very short fibers. The target size for forensically relevant fibers derives in part from fiber examinations and population studies reporting that recovered fibers are often as small as 2 mm in length, depending on the degree of dyeing.[50-52] Clearly, methods for the analysis of dyes extracted from fibers require high sensitivity for applicability to forensic casework. Other studies have also reported that UV/visible detection provides neither sufficient sensitivity, nor discrimination, for analysis of trace fiber extracts from structurally-related dyes.[53-58]

The coupling of separations to mass spectrometry for analysis of dye extracts represents a state-of-the-art approach to forensic dye identification. LC-MS, and more often LC-MS/MS, is the benchmark analytical approach for chemical quantitation in virtually all biological fluids. Analysis of dye extracted from single fibers of 2-10 mm in length has been achieved by Xu, *et al*.[55] by sample-induced isotachophoresis with micellar elecktrokinetic capillary chromatography, by Tuinman, *et al*. [56] who directly infused dyes into electrospray MS, and by other researchers with LC or CE coupled to MS.[30-33,48,53-58] Huang, *et al*.[57] demonstrated LC-MS identification of dyes with 22 reference dyes and 10 dyes extracted from fibers. Significantly, this paper showed MS discrimination of dyes that were not reliably identified by HPLC/DAD.[58] Pawlak, *et al*. used HPLC-MS to successfully identify several natural blue dye compounds from a tapestry fiber and concluded that several compounds exhibited complex fragmentation patterns due to chromatographic conditions using ESI-MS.[59] Zhang, *et al*. investigated alternative methods to HCl extraction for six flavonoid and mordant dyes on silk and used HPLC/ESI-MS to identify and quantify extracts for comparison.[60] ESI appears to be the ionization method of choice for most dye classes, however Szostek, *et al*. reported

difficulty in ionizing indigotin and brominated indigotin dyes by ESI but demonstrated successful ionization using APCI.[61] Several wool dyes were extracted from historic textiles and analyzed using HPLC and tandem ESI-MS (ion trap MS-MS) by Petroviciu, *et al*. who also noted that most MS literature on dyes focuses on molecular ion identification, and highlighted the importance of the availability of standards to build databases for unambiguous dye identification.[62] The importance of method optimization for fiber extract analysis was highlighted by Rafaëlly, *et al*. who cited the challenges of small extract quantities and commercial availability of dyestuff standards. They concluded that the superior sensitivity and structural elucidation properties of MS were sufficient to overcome low concentrations of extracts.[63]

Conventional HPLC uses 4-5 mm ID columns of 10-25 cm length; injected dyes are diluted by band broadening and relatively large samples are needed. Only a small number of papers in the forensic literature have applied HPLC to dye extracts; one notable paper is that of Laing, *et al*., who used diode array detection for acid dyes.[64] Ultra-performance liquid chromatography (UPLC), introduced commercially in 2004-2005, uses high pressures (>10,000 psi), smaller column particles (<2 µm), short columns (~5 cm), and minimal sample (~100 µL) to obtain high speed, resolution, and sensitivity. UPLC has rapidly become an established instrumental analysis technique, especially in areas requiring sample throughput (speed of analysis) and high resolution. Decreasing column particle size allows for columns to be packed tighter and more uniformly, resulting in reduced band broadening due to eddy diffusion. Smaller particles also provide a shorter pathway into and out of the stationary phase, yielding less band broadening due to mass transfer. Finally, the shorter column length of small particle columns allows for faster

separation times and thus reduces band broadening due to longitudinal diffusion within the column. Together, these three factors produce increased plate count and flatten the van Deemter curve at high flow rates. As a result, UPLC chromatographic peaks are narrower, and flow rates can be effectively doubled over that in HPLC columns with 5 µ particles without the penalty of band broadening and decreased resolution. However, the small UPLC particle sizes used requires the high pressures mentioned above to achieve flow through packed columns.

When compared to HPLC separations, UPLC separations produce a narrower, and thus more concentrated, analyte band allowing for lower limits of detection by UV/visible analysis. A comparison of detection limits of several food dyes characterized by HPLC-DAD and UPLC-DAD shows similar detection limits at first glance, however the required injection volume to achieve these levels by HPLC was 20 µL versus 3 µL for UPLC.[65,66] These results are summarized in Table 1.1.

The HPLC-DAD literature for dye analysis is abundant with refined analysis techniques while literature for UPLC-DAD of dyes is very scarce and underdeveloped. Achieving comparable limits of detection at lower injection volumes by UPLC suggests the possibility of lowering those limits through higher volume injections and optimizing the methodology. The UPLC-DAD LOD results listed in Table 1.1 were reported by Ji, *et al*. They also reported LOD values using UPLC-MS-MS, and their results indicate that Tartrazine, Amaranth, Indigo Carmine, Allura Red AC, and Sunset Yellow FCF are more sensitive to UV/visible analysis than tandem mass spectrometry.[65]

A recent search on *Science Direct* (only Elsevier journals) found 1,334 articles on UPLC, many of which were in biomedical and environmental applications; forensic

applications of UPLC were targeted mostly in toxicology and drug identification. These applications typically report UPLC analysis times of 30 s to 1-3 min, and detection limits in the range of pg of analyte injected using MS detection. For example, UPLC TOF-MS was used to analyze liver blood from a poisoning case involving Bromo-Dragonfly drug.[67] Another forensic application involved post-mortem analysis of ethyl glucuronide (EtG) as an alcohol metabolite in hair; with an evaporative light scattering detector, levels of EtG at just above 30 pg/mg were detected.[68] A review of applications of LC/MS, including some UPLC discussion, was published by Wood, *et al*.[69]

It has been observed that use of trace evidence and testimony of examiners has decreased in recent years, perhaps due to "over-reliance on nuclear DNA, latent print, and mitochondrial DNA evidence."[3] Fiber evidence is also maligned in popular forensic books with phrases such as "hanging by a thread" and "an inexact science" implying fiber comparisons are entirely "subjective."[70,71] While the identification of particular dye formulations or the presence of less common characteristics resulting from environmental exposure or laundering may impart distinctiveness to fibers, fibers cannot be individualized from other exemplars of their class. Other significant questions raised in the 2009 National Academy of Sciences report[72] include the following:

(1) Scientific Working Group for Materials Analysis (SWGMAT) "has produced guidelines, but no set standards, for the number and quality of characteristics that must correspond in order to conclude that two fibers came from the same manufacturing batch. There have been no studies of fibers (*e.g*., the variability of their characteristics before and after manufacturing) on which to base such a threshold."[73]

(2) “Similarly, there have been no studies to inform judgments about whether environmentally related changes discerned in particular fibers are distinctive enough to reliably individualize their source.”

(3) “[T]here have been no studies that characterize either reliability or error rates in the procedures.”

Optical microscopy (color and morphology), polarized light microscopy (retardation and birefringence indices for generic class), UV/visible microspectrophotometry (visible spectrum of the fiber and dyes), and infrared spectroscopy (polymer type) are irreplaceable as screening tools for excluding fiber matches. Fast nondestructive methods are preferred, but these techniques do not identify dyes. Two textile fibers dyed with mixtures of several, possibly different, dyes might be formulated by different manufacturers to achieve a particular (common) color. These fibers could be visually indistinguishable and exhibit very similar UV/visible spectra. Visual comparison of shapes of peak, valleys, and rising or falling portions of the spectra may indeed reveal subtle differences. However, judgment of the practical significance of these differences is often subjective, and the spectra usually represent unresolved mixtures of several unidentified dyes. Identification of separated dye components can increase the reliability of fiber examinations by providing informative discriminating information on dye characterization and possibly identification. Stoney stated the case well: “Failure to use state of the art techniques for fibre identification and comparison can lead to a reduction in evidential value, as the number of potential alternative sources will rise considerably if all comparative possibilities are not exhausted.”[74]

The development and validation of reliable microextraction protocols followed by sensitive trace analyses by chromatography and mass spectrometry is the subject of the research presented in this dissertation.

REFERENCES

(1) *The Warren Commision Report*. St. Martin's Press, New York, 1964; p. 592.

(2) Deadman, H. *Fiber evidence and the Wayne Williams trial*, US Government Document J1.14/8a:F44, Federal Bureau of Investigation, US Department of Justice, FBI Law Enforcement Bulletin, March and May, 1984.

(3) Oien, C. T. *Case management issues from crime scene to courtroom*. Trace Evidence Symposium, Clearwater, FL, 2007 [URL: http://nfstc.org/projects/trace/].

(4) Robertson J.; Grieve, M., Eds., *Forensic Examination of Fibres*. 2nd edition. London: Taylor & Francis: 1999.

(5) Eyring, M. B.; Gaudette, B. D. An introduction to the forensic aspects of textile fiber examinations. Chapter 6 in: *Forensic Science Handbook*, vol. 2, R. Saferstein, Ed.; Prentice Hall: Englewood Cliffs, NJ, 2005.

(6) Grieve, M. Interpretation of fibres evidence. Chapter 13 in: *Forensic Examination of Fibres*, 2nd edition, Robertson J.; Grieve, M., Eds.; Taylor & Francis: London, 1999.

(7) Wiggins, K.G.; Cook, R.; Turner, Y.J. Dye batch variation in textile fibers. J. *Forensic Sci*. **1988**, *33*, 998-1007.

(8) Wiggins, K.; Holness, J. A further study of dye batch variation in textile and carpet fibres. *Science & Justice* **2005**, 45, 93-96.

(9) National Research Council of the National Academies. *Forensic Analysis: Weighing Bullet Lead Evidence*. The National Academies Press: Washington, DC, 2004.

(10) Rendle, D. F.; Wiggins, K. G. Forensic analysis of textile fibre dyes. *Review of Progress in Coloration and Related Topics* **1995,** *25*, 29-34.

(11) Webb-Salter, M.; Wiggins, K. G. Aids to Interpretation, in: *Forensic Examination of Fibres*. 2nd edition, J. Robertson, M. Grieve, Eds., Taylor & Francis: London, 1999; pp. 364-378.

(12) Needles, H. L. *Textile Fibers, Dyes, Finishes, and Processes: A Concise Guide*. Noyes Publications: Park Ridge, NJ, 1986.

(13) Wiggins, K. G. Thin layer chromatographic analysis for fibre dyes. Chapter 11 in: *Forensic Examination of Fibres*, 2nd edition, Robertson J.; Grieve, M., Eds.; Taylor & Francis: London, 1999.

(14) Gaudette, B. D. The forensic aspects of textile fiber examination. Chapter 5 in: *Forensic Science Handbook*, vol. 2, R. Saferstein, Ed.; Prentice Hall: Englewood Cliffs, NJ, 1988.

(15) Macrae, R.; Dudley, R. J.; Smalldon, K. W. The characterization of dyestuffs on wool fibers with special reference to microspectrophotometry. *J. Forensic Sci*. **1979**, *24*, 117-129.

(16) Resua, R. A semi-micro technique for the extraction and comparison of dyes in textile fibers. *J. Forensic Sci*. **1980**, *25*, 168-173.

(17) Shaw, I. C. Micro-scale thin-layer chromatographic method for the comparison of dyes stripped from wool fibers. *Analyst* **1980**, *105*, 729-730.

(18) Home, J. M.; Dudley, R. J. Thin-layer chromatography of dyes extracted from cellulosic fibers. *Forensic Sci.Int*. **1981**, *17*, 71-78.

(19) Beattie, B.; Roberts, H.; Dudley, R. J. The extraction and classification of dyes from cellulose acetate fibers. *J. Forensic Sci. Soc*. **1981**, *21*, 233-237.

(20) Hartshorne, A. W.; Laing, D. K. The dye classification and discrimination of colored polypropylene fibers. *Forensic Sci.Int*. **1984**, *25*, 133-141.

(21) Wiggins, K. G.; Crabtree, S. R.; March, B. M. The importance of thin layer chromatography in the analysis of reactive dyes released from wool fibers. *J. Forensic Sci.* **1996**, *41*, 1042-1045.

(22) Laing, D. K.; Boughey, L.; Hartshorne, A. W. The standardization of thin layer chromatographic systems for comparison of fiber dyes. *J. Forensic Sci. Soc*. **1990**, *30*, 299-307.

(23) Laing, D. K.; Hartshorne, A. W.; Bennett, D. C. Thin layer chromatography of azoic dyes extracted from cotton fibers. *J. Forensic Sci. Soc*. **1990**, *30*, 309-315.

(24) Rendle, D. F.; Wiggins, K. G. Forensic analysis of textile fibre dyes. *Review of Progress in Coloration and Related Topics* **1995**, *25*, 29-34.

(25) Rendle, D. F.; Crabtree, S. R.; Wiggins, K. G.; Salter, M. T. Cellulase Digestion of Cotton Dyed with Reactive Dyes and Analysis of the Products by Thin-Layer Chromatography. *J. Soc. Dye. Colour* **1994**, *110*, 338-341.

(26) Crabtree, S. R.; Rendle, D. F.; Wiggins, K. G.; Salter, M. T. The Release of Reactive Dyes from Wool Fibers by Alkaline- Hydrolysis and Their Analysis by Thin-Layer Chromatography. *J. Soc. Dye. Colour* **1995**, *111*, 100-102.

(27) Beattie, I.B.; Dudley, R.J.; Smalldon, K.W. The extraction and classification of dyes on single nylon, polyacrylonitrile and polyester fibers. *J. Soc. Dye. Colour* **1979**, *95*, 295-302.

(28) Smith, W. F. *Experimental Design for Formulation*. Cambridge University Press: New York, 2005.

(29) Deming, S. N.; Morgan, S. L. *Experimental Design: A Chemometric Approach*, 2nd ed. Elsevier Science Publishers: Amsterdam, 1993.

(30) Stefan, A. R., Dockery C. R., Nieuwland, A. A., Roberson, S. N., Baguley, B. M., Hendrix, J. E., Morgan, S. L. Forensic analysis of anthraquinone, azo, and metal complex acid dyes from nylon fibers by micro-extraction and capillary electrophoresis. *Anal. Bioanal. Chem*. **2009**, *394*, 2077-2085.

(31) Stefan, A. R., Dockery, C. R., Baguley, B.M., Vann, B. C., Nieuwland, A. A., Hendrix, J. E., Morgan, S. L. Microextraction, capillary electrophoresis, and mass spectrometry for forensic analysis of azo and methine basic dyes from acrylic fibers. *Anal. Bioanal. Chem*.**2009**, *394*, 2087-2094.

(32) Hartzell-Baguley, B.; Stefan, A. R.; Dockery, C. R.; Hendrix, J. E.; Morgan, S. L. Non-aqueous capillary electrophoresis of azo and anthraquinone disperse dyes extracted from polyester fibers for forensic analysis. *Anal. Bioanal. Chem*., **2009**, unpublished manuscript.

(33) Dockery C. R., Stefan, A. R., Nieuwland, A. A., Roberson, S. N., Baguley, B.M., Hendrix, J. E., Morgan, S. L. Automated extraction of direct, reactive, and vat dyes from cellulosic fibers for forensic analysis by capillary electrophoresis. *Anal. Bioanal. Chem*. **2009**, *394*, 2095-2103.

(34) Sirén, H.; Sulkava, R. Determination of black dyes from cotton and wool fibers by capillary zone electrophoresis with UV detection: application of marker technique. *J. Chromatogr. A* **1995**, *717*, 149-155.

(35) Xu, X.; Leijenhorst, H.; Van den Hoven, P.; De Koeijer, J.A.; Logtenberg, H. Analysis of single textile fibres by sample-induced isotachophoresis-micellar electrokinetic capillary chromatography. *Sci. Justice* **2001**, *41*, 93-105.

(36) Croft, S.N.; Lewis, D.M. Analysis of reactive dyes and related derivatives using high-performance capillary electrophoresis. *Dyes and Pigm.* **1992**, *18*, 309-317.

(37) Croft, S.N.; Hinks, D. Analysis of dyes by capillary electrophoresis. *Textile Chemist and Colorist* **1993**, *25*, 47-51.

(38) Burkinshaw, S.M.; Hinks, D.; Lewis, D.M. Capillary zone electrophoresis in the analysis of dyes and other compounds employed in the dye-manufacturing and dye-using industries. *J. Chromatogr. A* **1993**, *640*, 413-417.

(39) Burkinshaw, S.M.; Hinks, D.; Lewis, D.M. The use of capillary electrophoresis for the analysis of several dye classes. In: Special Publication - *Royal Society of Chemistry* **1993**,*122*, 93-100.

(40) Croft, S.N.; Hinks, D. Analysis of dyes by capillary electrophoresis. *J. Soc. Dye. Colour* **1992**, *108*, 546-551.

(41) Takeda, S.; Tanaka, Y.; Nishimura, Y.; Yamane, M.; Siroma, Z.; Wakida, S. Analysis of dyestuff degradation products by capillary electrophoresis. *J. Chromatogr. A* **1999**, *853*, 503-509.

(42) Borros, S.; Barbera, G.; Biada, J.; Agullo, N. The use of capillary electrophoresis to study the formation of carcinogenic aryl amines in azo dyes. *Dyes and Pigm.* **1999**, *43*, 189-196.

(43) Burkinshaw, S.M.; Graham, C. Capillary zone electrophoresis analysis of chlorotriazinyl reactive dyes in dyebath effluent. *Dyes and Pigm.* **1997**, *34*, 307-319.

(44) Riu, J.; Schonsee, I.; Barcelo, D. Determination of sulfonated azo dyes in groundwater and industrial effluents by automated solid-phase extraction followed by capillary electrophoresis mass spectrometry. *J. Mass Spectrom*. **1998**, *33*, 653-663.

(45) Riu, J.; Eichhorn, P.; Guerrero, J.A.; Knepper, T.P.; Barcelo, D. Determination of linear alkylbenzenesulfonates in wastewater treatment plants and coastal waters by automated solid-phase extraction followed by capillary electrophoresis-UV detection and confirmation by capillary electrophoresis-mass spectrometry. *J. Chromatogr. A* **2000**, *889*, 221-229.

(46) Riu, J.; Barcelo, D. Determination of linear alkylbenzene sulfonates and their polar carboxylic degradation products in sewage treatment plants by automated solid-phase extraction followed by capillary electrophoresis-mass spectrometry. *Analyst* **2001**, *126*, 825-828.

(47) Robertson, J.; Wells, R.J.; Pailthorpe, M.T.; David, S.; Aumatell, A.; Clark, R. *An assessment of the use of capillary electrophoresis for the analysis of acid dyes in wool fibers.* Advances in Forensic Sciences, Proceedings of the Meeting of the International Association of Forensic Sciences, 13th, Duesseldorf, Aug. 22-28, 1995, 4, 247-249.

(48) Morgan, S. L.; Vann, B. C.; Baguley, B. M.; Stefan, A. R. *Advances in discrimination of dyed textile fibers using capillary electrophoresis/mass spectrometry*. Trace Evidence Symposium, Clearwater, FL, 2007

(49) Wheals, B.B.; White, P.C.; Paterson, M.D. High-performance liquid chromatographic method utilizing single or multi-wavelength detection for the comparison of disperse dyes extracted from polyester fibers. *J. Chromatogr*. **1985**, *350*, 205-215.

(50) Macrae, R.; Smalldon, K.W. The characterization of dyestuffs on wool fibers with special reference to microspectrophotometry. *J .Forensic Sci.* **1979**, *24*, 109-116.

(51) Roux, C.; Margot, P. The population of textile fibres on car seats. *Sci Justice* **1997**, *37*, 25-30.

(52) Watt, R.; Roux, C.; Robertson, "The population of coloured textile fibres in domestic washing machines. *J. Sci Justice* **2005**, *45*,75-83.

(53) Petrick, L.M.; Wilson, T.A.; Fawcett, W.R. High-performance Liquid Chromatography-Ultraviolet-Visible Spectroscopy-Electrospray Ionization Mass Spectrometry Method for Acrylic and Polyester Forensic Fiber Dye Analysis. *J. Forensic Sci*. **2006**, *51*, 771-779

(54) Yinon, J.; Saar, J. Analysis of dyes extracted from textile fibers by thermospray high-performance liquid chromatography-mass spectrometry. *J. Chromatogr. A* **1991**, *586*, 73-84.

(55) Xu, X.; Leijenhorst, H.; Van den Hoven, P.; De Koeijer, J.A.; Logtenberg, H. Analysis of single textile fibres by sample-induced isotachophoresis-micellar eletrokinetic capillary chromatography. *Sci. Justice* **2001**, *41*, 93-105.

(56) Tuinman, A.A.; Lewis, L.A.; Lewis, S.A. Trace-fiber color discrimination by electrospray ionization mass spectrometry: A tool for the analysis of dyes extracted from submillimeter nylon fibers. *Anal. Chem.* **2003**, *75*, 2753-2760.

(57) Huang, M.; Yinon, J.; Sigman, M. E. Forensic identification of dyes extracted from textile fibers by liquid chromatography mass spectrometry (LC-MS). *J. Forensic Sci.* **2004**, *49*, 238-249.

(58) Huang, M.; Russo, R.; Fookes, B. G.; Sigman, M. E. Analysis of Fiber Dyes by Liquid Chromatography Mass Spectrometry (LC-MS) with Electrospray Ionization: Discriminating Between Dyes with Indistinguishable UV-Visible Absorption Spectra. *J. Forensic Sci*. **2005**, *50*, 526-534.

(59) Pawlak, K.; Puchalska, M.; Miszczak, A.; Rosloniec, E.; Jarosz, M. Blue natural organic dyestuffs – from textile dyeing to mural painting. Separation and characterization of coloring matters present in elderberry, longwood and indigo. *J. Mass Spectrom.* **2006**, *41*, 613-622.

(60) Zhang, X.; Laursen, R. Development of Mild Extraction Methods for the Analysis of Natural Dyes in Textiles of Historical Intersest Using LC-Diode Array Detector-MS. *Anal. Chem.* **2005**, *77*, 2022-2025.

(61) Szostek, B.; Orska-Gawrys, J.; Surowiec, I.; Trojanowicz, M. Investigation of natural dyes occurring in historical Coptic textiles by high-performance liquid chromatography with UV-Vis and mass spectrometric detection. *J. Chromatogr. A* **2003**, *1012*, 179-192.

(62) Petroviciu, I.; Albu, F.; Medvedovici, A. LC/MS and LC/MS/MS based protocol for identification of dyes in historic textiles." *Microchemical Journal*, **2010**, *95*, 247-254.

(63) Rafaëlly, L.; Héron, S.; Nowik, W.; Tchapla, A. Optimization of ESI-MS detection for the HPLC of anthraquinone dyes. *Dyes and Pigm.* **2008**, *77*, 191-203.

(64) Laing, D. K.; Gill, R.; Blacklaws, C.; Bickley, H.M. Characterization of acid dyes in forensic fiber analysis by high-performance liquid chromatography using narrow-bore columns and diode array detection. *J. Chromatogr*. **1988**, *442*, 187-208.

(65) Minioti, K.; Sakellariou, C.; Thomaidis, N. Determination of 13 synthetic food colorants in water-soluble foods by reversed-phase high-performance liquid chromatography coupled with diode-array detector. *Anal. Chim. Acta*, **2007**, *583*, 103-110.

(66) Ji, C.; Feng, F.; Chen, Z.; Chu, X. Highly sensitive determination of 10 dyes in food with complex matrices using SPE followed by UPLC-DAD-Tandem mass spectrometry. *J. Liq. Chromatogr. & Relat. Technol.* **2011**, *34*, 93-105.

(67) Andreasen, M. F.; Telving, R.; Birkler, R.I.D.; Schumacher, B.; Johannsen, M. A fatal poisoning involving Bromo-Dragonfly. *Forensic Sci. Int.* **2009**, *183*, 91–96.

(68) Bendroth, P.; Kronstrand, R.; Helander, A.; Greby, J.; Stephanson, N.; Krantz, P. Comparison of ethyl glucuronide in hair with phosphatidylethanol in whole blood as post-mortem markers of alcohol abuse. *Forensic Sci. Int*. **2008**, *176*, 76-81.

(69) Wood, M.; Laloup, M.; Samync, N.; del Mar Ramirez Fernandez, M.; de Bruijn, E. A.; Maes, R A.A.; De Boeck, G. Recent applications of liquid chromatography-mass spectrometry in forensic science. *J. Chromatogr. A* **2006**, *1130*, 3–15.

(70) Fisher, J. *Forensics under Fire: Are Bad Science and Dueling Experts Corrupting Criminal Justice?* Rutgers University Press: New Brunswick, NJ, 2008.

(71) Kelly, J. F.; Wearner, P. K. *Tainting Evidence: Inside the Scandals at the FBI Crime Lab*, The Free Press: New York, 1998.

(72) National Research Council of the National Academies. *Strengthening Forensic Science in the United States: A Path Forward*, The National Academies Press: Washington, DC, 2009.

(73) Houck, M. *Statistics and trace evidence: the tyranny of numbers*, Forensic Science Communications, 1 January 1999.

(74) Stoney. D.A. The assumption of relevance and an application to one-trace and two-Relaxation of trace problem. *J. Forensic Sci. Soc.* **1994**, *34*, 17-21.

Table 1.1. Limits of detection for food dyes determined by HPLC-DAD and UPLC-DAD.

Food dye	HPLC-DAD LOD (pg)[64]	UPLC-DAD LOD (pg)[65]
Amaranth	204	450
Indigo Carmine	161.8	30
Allura Red AC	149.2	120
Brilliant Blue FCF	54.4	150
Patent Blue V	210	390
Sunset Yellow FCF	88.2	30

CHAPTER TWO

COMPREHENSIVE SCREENING OF ACID, BASIC, AND DISPERSE DYES EXTRACTED FROM MILLIMETER-LENGTH TRACE EVIDENCE FIBERS BY ULTRA-PERFORMANCE LIQUID CHROMATOGRAPHY: METHODOLOGY AND FIGURES OF MERIT

ABSTRACT

Methodology for the microextraction of basic dyes on acrylic, acid dyes on nylon, and disperse dyes on polyester textile fibers is reported. A single ultra-performance liquid chromatography method suited for qualitative and semi-quantitative analysis of all three dye types has also been developed. Although our approach is destructive to the fiber evidence, the ability to analyze sub-millimeter fiber lengths of single fibers, coupled with detection limits in the hundred picogram range by both diode array detection (DAD) and tandem mass spectrometry (MS-MS) make routine forensic characterization feasible.

INTRODUCTION

The ubiquitous nature of textile fibers should provide an information-rich evidence source for crime scene investigations, however in cases of similarly dyed fibers current fiber analysis techniques do not provide adequate chemical information for unambiguous match determinations to be made. The standard procedure for analyzing forensic textile fibers involves polymer and morphology determinations, followed by visual color comparisons and UV/visible absorbance spectrum comparisons between known and questioned fibers.[1] These techniques are efficient and non-destructive, however if a match exclusion cannot be made with sufficient confidence using these techniques, the evidence is left in indetermination as there are no established and validated methods for further analysis.

This research seeks to establish methodology that profiles the chemical identity of constituents attached to textile fibers, including dyes, fluorescent brighteners, and finishing agents. By extracting these components from the fibers, separating them, and individually identifying and quantifying them, match exclusions may be made based on

substantially more discriminative information than possible using visual and spectrophotometric microscopic analysis. Microextraction, followed by chromatography and mass spectrometry, enables fiber comparisons to be based on dye formulations, relative amounts of dyes present. The possible presence of contaminants due to environmental exposure and impurities in dye batch formulations also may increase the individuality of a trace evidence fiber.

The challenge of analyzing dye extracts from forensic fibers stems from the need to preserve the evidence. Extraction of dyes is destructive to the fiber, and recovered trace evidence fibers are often as small as 2 mm in length and contain as little as 2 ng of dye[2], thus very sensitive analysis techniques are needed. Previous research into dye extract analysis has used thin layer chromatography (TLC) as a classification technique, however issues of reproducibility and large required sample size plague the conclusions.[3–13] More advanced techniques have been applied such as capillary electrophoresis (CE), and while CE excels at separating ionized dyes, dye classes such as disperse dyes on polyester and vat dyes on cotton are difficult to ionize.[14–16]

High performance liquid chromatography (HPLC) has the added benefit of both stationary phase and mobile phase tuning to achieve a separation. Because many dyes have acid or base character, control of the mobile phase pH permits adjustment of retention for improved resolution and tuning of retention times for faster analysis speed. The numerous combinations of mobile and stationary phases essentially create a universal separation for small organic molecules, and is the state-of-the-art approach for comprehensive dye analysis. HPLC has been used to separate mixtures of acid, basic, and disperse dyes.[17,18,20] Where HPLC-DAD was not sufficient to differentiate between some

similarly colored dyes, Huang, *et al*. point out that discrimination at the molecular level by HPLC-MS is usually successful.[17] Dye extracts not discriminated by UV/visible detection were also analyzed using HPLC-MS, however success was only demonstrated using 5 mm threads and not single fibers.[18]

Ultra-performance liquid chromatography (UPLC) has demonstrated its utility for rapid analysis by using high pressure pumps (<15,000 psi) capable of moving samples and mobile phases through columns packed with increasingly smaller diameter (1.7 μm) stationary phase particles. This allows UPLC to achieve very high resolution separations in very short analysis times (< 5 min). As a consequence, brand broadening is decreased substantially compared to HPLC and the viability of using UV/visible detection for trace analysis increases.

The objective of this study is to establish comprehensive methodology for the extraction and separation of acid, basic, and disperse dyes from nylon, acrylic, and polyester fibers. Our target fiber size is 1 mm to offset the issue of damaging evidence, and we use UPLC to achieve the necessary sensitivity. We validate the chromatographic methods by establishing calibration models and calculating limits of detection and quantitation.

EXPERIMENTAL

Materials

Analytical grade chlorobenzene, glacial acetic acid, pyridine, ammonium hydroxide, ammonium acetate, formic acid, and HPLC/UPLC grade acetonitrile and methanol were purchased from Fisher Scientific (Pittsburg, PA). Dyed fabric and textile dye standards were sampled from our collection of production samples, which were donated by textile

and dyestuff manufacturers from the southeastern United States. The dyes used in this work are listed in Table 2.1 using the Color Index nomenclature (Society of Dyers and Colourists, Bradford, UK). The nine dyes selected for this study included three dyes from each of the acid, basic, and disperse classes.

Fiber sample preparation

Prior to extraction analysis, all samples are cut to prescribed lengths. In previous CE analyses for fiber dyes, percent relative standard deviations (RSDs) for peak areas have varied from 10-20%, of most synthetic fibers to as high as 25-35% for cotton.[14-16] We attribute these high RSDs to the inability to cut small fiber sizes reproducibly. Fibers that have intrinsic curled, crinkly, or helical shapes, such as cotton and acrylic fibers, must be stretched lengthwise while cutting. We have designed and machined a device to facilitate reproducible measurement and cutting of fibers down to 5 mm in length (Figure 2.1). The device has a metal block with a groove within which the fiber can be securely positioned; above the block is a rotating shaft on which multiple razor blades are fixed, spaced in 5 mm distance increments and aligned with cutting slots. Once the fiber is positioned, the operator selects the desired length and can safely rotate the shaft to cut the fiber.

Individual fibers 5-mm in length were cut using the fiber guillotine; 1 mm and 0.5 mm fibers were cut by hand using a table-mounted magnifying glass and scalpel. Each fiber length was cut in triplicate. Cut fibers were then loaded into Waters Total Recovery® vials for extraction. These vials enable extractions to be performed with low solvent volumes (< 50 μL), enabling concentration of dyes in the resulting extract. When typical low volume vial inserts were employed for extractions, solvent often condensed

on the inside vial wall outside the vial insert because of poor sealing between the insert and the top of the vial.

Calibration design

Experimental designs for UPLC-DAD calibration were constructed for all nine dyes based on 5 replicate experiments at 7 levels of dye concentration (0 ppb, 100 ppb, 500 ppb, 1000 ppb, 1500 ppb, 2000 ppb, and 2500 ppb). A blank sample was measured 15 times as a quality control sample interspersed through the runs. A lower concentration design was also performed based on five replicate experiments at using standard mixtures of the 9 dyes at concentrations 10 ppb, 20 ppb, 30 ppb, 40 ppb, 50 ppb, and 18 blank injections to better characterize low limits of detection. For UPLC-MS-MS, calibration designs included standards at 10 ppb, 200 ppb, 400 ppb, 600 ppb, 800 ppb, and 1000 ppb. For each dye peak, QuanLynx™, data management software included with MassLynx™ (Waters Corporation, Milford, MA) was used to integrate peak areas above corrected baselines. For each dye standard at 1000 ppb concentration, the retention time window encompassing the baseline peak width was determined; this window was then employed as the dye peak integration window for all samples, including blanks.

Instrumentation

Dye standards and extracts were separated and detected using a Waters Acquity™ UPLC H-Class equipped with a quaternary solvent pump system and a Waters PDA eλ detector. The column was a 2.1 × 50 mm I.D. 1.7 μm particle size Waters Acquity™ BEH C18 column with a 2.1 × 5 mm I.D. 1.7 μm particle size Waters Acquity UPLC® BEH C18 VanGuard precolumn. The mobile phase gradient was based on mixtures of 50 mM ammonium acetate in water and 0.15% formic acid in methanol (program shown in

Table 2.2). The column temperature was set at 40 °C. The diode array detector scanned the wavelength range from 325 nm to 675 nm at a rate of 40 Hz and 1.2 nm resolution. The sample injection volumes were 10 μL.

Separations using MS characterization were performed using a Waters Acquity UPLC® equipped with a binary solvent system coupled to a Waters Micromass Quattro Premier XE® tandem quadrupole mass spectrometer. For MS compatibility, the mobile phase consisted of 50 mM ammonium acetate in water and 0.15% formic acid (FA) in methanol. The mobile phase gradient, shown in Table 2.2, differs from that for UPLC-UV/visible detection to compensate for the slower flow rate required for MS. The column was at ambient temperature during runs. Sample injection volumes were 5 μL. The MS-MS transitions, cone voltages, and collision voltages are listed in Table 2.3.

Acid dyes on nylon

The optimum solvent conditions for extraction of acid dyes from nylon was previously investigated by Stefan, *et al*., using a mixtures of pyridine, ammonium hydroxide, and water.[14] Because the extraction response was robust over the center of the design, here we used equal proportions (33:33:33) of the three components for extractions. Aliquots (100 μL) of the extractant were added to vials containing fibers, and vials were capped and extracted at 100°C for 1 h. After extraction, the vials were uncapped and heated at 90°C to evaporate solvent (*ca*. 30-45 min). Samples were reconstituted in a 50 μL mixture of 50:50 methanol and 50 mM ammonium acetate buffered at pH 4.5, then vortex-mixed to ensure complete solvation of extracted dye.

Basic dyes on acrylic

Extraction conditions for basic dyes on nylon were also explored by Stefan, *et al.*[15] In the present work, 50:50 mixtures of 88% formic acid and water were employed for all extractions, in agreement with literature-cited values.[6,19,20] Aliquots (100 μL) of extractant were added to the vials containing the fibers and then capped. The extraction was carried out at 100°C for 1 h, then the vials were uncapped and evaporated at 90°C until dry (*ca.* 30-45 min). The samples were reconstituted in a 50 μL mixture of 50:50 methanol and 50 mM ammonium acetate buffered at pH 4.5. Samples were then vortex-mixed to ensure complete solvation of the extracted dye.

Disperse dyes on polyester

Chlorobenzene was previously reported to extract disperse dyes on polyester.[21] As with acid and basic dyes, aliquots of 100 μL of extractant were added to vials containing the fibers and the extractions were carried out at 100 °C for 1 h. The vials were then uncapped and heated to evaporate solvent at 90 °C until dry (*ca.* 30-45 min). The samples were then reconstituted in a 50 μL mixture of 50:50 methanol and 50 mM ammonium acetate buffered at pH 4.5. Samples were then vortex-mixed to ensure complete solvation of the extracted dye.

MS-MS Optimization

Electrospray ionization (ESI) and MS-MS transition parameters were tuned by infusing 1000 ppb of each dye into the source with a 0.300 mL/min mobile phase of a 50:50 mixture of 0.05 M ammonium acetate and methanol with 0.15% formic acid by volume. Desolvation temperature was set at 450 °C. Dye standards were infused at 20 μL/min and the optimum cone voltage for maximum ion count was determined,

characteristic mass fragments were found, and collision voltages were adjusted to maximize fragment ion counts. Table 2.3 summarizes the MS-MS parameters employed.

RESULTS AND DISCUSSION

Chromatographic analysis of dyes

A comprehensive separation of all nine dyes was achieved using the mobile phase gradient shown in Table 2.2. In developing this gradient method, ammonium acetate buffered to pH 4.5 was found to broaden several dye peaks, and caused Basic Yellow 28 and Acid Yellow 49 to coelute. pH-neutral ammonium acetate produced two peaks almost baseline-resolved for these dyes. Further the Basic Violet 16 baseline peak width decreased from 5.4 s to 4.2 s, and peak height and area increased by *ca.* 20%.

Figure 2.2 displays the separation, in under five min, of all nines dyes evaluated for this work. The first (peak 1, Basic Red 46), third (peak 3, Acid Yellow 49), and last dye (peak 9, Disperse Blue 60) produced two peaks. In each case, each pair of peaks exhibited UV/visible spectra identical to those in Table 2.1. For the last pair of peaks, the absorbance is shifted to longer wavelength compared to many of the other dyes.

Figure 2.3 shows the chromatograms of dyes extracted from fibers of lengths 5 mm, 1 mm, and 0.5 mm; these extractions were performed in triplicate. All extractions were successful down to 0.5 mm except those involving Acid Yellow 49 and Disperse Blue 60, which were only successful down to 1 mm lengths. Acid Yellow 49 failed at 0.5 mm due to difficulty handling, and even seeing, a. A 1 mm fiber extract of Acid Yellow 49 dye appears to have sufficient signal for a 0.5 mm extract to be detectable; however, pale yellow-colored fiber are difficult to see regardless of length, which makes handling fibers 0.5 mm long is difficult. Even the stock fabric, from which fibers dyes with Disperse

Blue 60 were sampled, were lightly colored indicative of low dye loading. As seen below, Disperse Blue 60 has the highest limit of detection of all nine dyes, and although LOD values found suggest that a 0.5 mm extract should be detectable, there is increased noise associated with its absorbance peak.

Calibration Models of Dye Standards

Table 2.4 shows UPLC-DAD results for all dyes over in the high and low concentration calibration designs; calibration results are also shown for UPLC-MS-MS over mid-range concentrations. Figures 12-37 display calibration plots for the nine dyes investigated. All first order linear calibration models (with intercept and slope parameters) produced coefficients of determination (R^2) of 0.9993 or higher for the wide range calibrations. Calculated signal-to-noise ratios (SNR) were 100 or higher at 100 ppb in the wide range calibrations (based on integrated baseline root-mean-square variation from the MassLynx®). The second calibration, performed over a range of standards bracketing the estimated dye limits of detection, produced lower R^2 values of 0.9913 or higher, except for one dye. The decrease is expected from data in this region of higher uncertainty—noise and detector linearity have a larger impact on peak shape as concentrations approach the LOD—but these results are still excellent. The single dye whose behavior differed from the other eight dyes was Disperse Yellow 114. The low-range UPLC-DAD results exhibited higher variability about the calibration line than any other dye. Although an R^2 of 0.9687 was achieved, the model also exhibited a statistically significant lack of fit ($p < 0.05$).

Calibration models for MS-MS were constructed using 5 replicate standard injections at concentrations 10 ppb, 200 ppb, 400 ppb, 600 ppb, and 6 blank injections. The MS-MS

models exhibit heteroscedastic behavior and greater variation at higher concentrations, and consequently these models had the least fit ($R^2 > 0.9813$) with Disperse Violet 77 ($R^2=0.9700$) and Basic Red 46 ($R^2=0.9371$) showing wide residual distribution, possibly due to unoptimized MS ionization conditions.

Limits of detection are reported in Table 2.4 based on three different estimation approaches. Each method calculates the LOD or LOQ using

$$LOD = (3.3 \times \sigma_b)/S$$

$$LOQ = (10 \times \sigma_b)/S,$$

where σ_b is the standard deviation of the blank and S is the slope of the calibration line. The three methods used differ with how σ_b is estimated. LOD_1 estimates σ_b using the standard deviation of the integrated blank signals across the width of the actual peak. LOD_2 approximates σ_b using the standard deviation of the lowest non-zero concentration calibrator (at 100 ppb for the high concentration DAD calibration; at 10 ppb for the low concentration DAD and MS calibrations). LOD_3 estimates σ_b based on the standard error of the *y*-intercept of the calibration model; because the standard error of the *y*-intercept is calculated from the standard deviation of residuals, this may be inflated by the presence of lack fit of the model and by heteroscedasticity (non-constant variability at different concentration levels). There are many ways to calculate LODs; we present these three approaches to indicate a range of reasonable values for the LODs. Most LODs calculated using the high concentration calibration design were 10 ppb or lower, suggesting absolute amounts of dye less than 100 pg can be detected by UPLC-DAD.

LODs of the disperse dyes using diode array detection appear to be higher than the other dye types. Disperse Blue 60 had the lowest absorbance response of all dyes

investigated ; the low concentration(10-50 ppb) calibration on UPLC-DAD was not determined because only the 50 ppb standard produced a peak that could be integrated by MassLynx®. LOD_1 and LOD_3 estimated the limit of detection for Disperse Blue 60 to be 13.50 ppb and 16.80 ppb, respectively. This result illustrates an important point: confirming actual detection for a sample concentration at the estimated LOD is required if one plans to operate near the LOD. Conducting the low concentration calibration design achieved this requirement for the present study. MS-MS calibration for Disperse Blue 60 produced LODs ranging from 2.88 to 30.50 ppb, depending on the estimation approach. The calibration in Figure 2.31 exhibits an R^2 of 0.9813; however, the curvature visible in the calibration plot is confirmed by a statistically significant lack of fit ($p < 0.0001$).

Estimated LODs based on the lower concentration calibration designs for all dyes were all less than 4.38 ppb (corresponding to 43.8 pg of dye), except for the Disperse Yellow 114 dye (mentioned above). The calibration for Disperse Yellow 114 had abnormally high variance in the blanks and consequently LOD_1 was 12.60 ppb while LOD_2 and LOD_3 were 1.67 ppb and 2.34 ppb. LODs calculated for ESI-MS-MS by LOD_1 and LOD_2 were evenly distributed between 0.38 ppb and 10.30 ppb. The high LOD_3 values are due to the high amount of variance at 600 ppb for each dye by MS. This may be due to unoptimized dye ionization conditions for higher concentrations.

CONCLUSIONS

A single liquid chromatographic method has been developed, using an ultra high pressure system with columns packed with 1.7 µm diameter stationary phase particles, that is capable of comprehensive analysis for acid, basic, and disperse dyes extracted

from nylon, acrylic, and polyester fibers, respectively. While this method has only been evaluated using three dyes from each class, it not common to find more than 3-5 dyes on a single fiber. If dyes are not resolved by the gradient programs proposed here, further method development for improvement of the resolution of merged peak is easily done. For present set of nine dyes, changes in the gradient start and the rate of change of solvent composition during the gradient were successful in adjusting conditions for complete separation. The limit of detection results across the broad of three dye classes were displayed considerable consistency, notwithstanding the few exceptions. The low concentration range calibration designs for UPLC produced lower LODs that achieved by UPLC-MS-MS. the high concentration range calibrations for UV/visible and MS-MS detection showed lower detection limits than MS-MS in this study. , and more importantly that both methods are sensitive enough to detect and quantify the estimated 2 ng of dye on a 2 mm fiber. UPLC-DAD appears to be more sensitive than UPLC-MS-MS, however more optimized ionization conditions are needed to confirm.

Using UPLC-DAD, extracts from single 1 mm fibers were detected for each dye, with all but two dye extracts being detected from 0.5 mm fibers. Further tuning of our MS-MS system may lead to even smaller fiber length possibilities, however improved handling techniques are needed to prepare for extraction fibers smaller than 1 mm in length. It is clear that trace evidence fibers can be analyzed for dye formulation even when very little sample is present.

ACKNOWLEDGMENTS

Coauthors of this work include Molly R. Burnip, Kaylee R. McDonald, Oscar G. Cabrices, and Stephen L. Morgan (Department of Chemistry and Biochemistry,

University of South Carolina, Columbia, SC 29208). Research in this presentation was supported by award 2010-DN-BX-K245 from the National Institute of Justice, Office of Justice Programs, U. S. Department of Justice. The opinions, findings, and conclusions or recommendations expressed in this publication are those of the author(s) and do not necessarily reflect those of the Department of Justice. Mention of commercial products does not imply endorsement on the part of the National Institute of Justice or the University of South Carolina.

RFERENCES

(1) Robertson, J.; Grieve, M. *Forensic Examination of Fibres*; 2nd ed.; Taylor & Francis: London, 1999.

(2) Macrae, R.; Smalldon, K. The Extraction of Dyestuffs from Single Wool Fibers. *J. Forensic Sci*. **1979**, *24*, 109–116.

(3) Macrae, R.; Dudley, R.; Smalldon, K. The characterization of dyestuffs on wool fibers with special reference to microspectrophotometry. *J. Forensic Sci*. **1979**, *74*, 117–129.

(4) Shaw, I. C. Micro-scale thin-layer chromatographic method for the comparison of dyes stripped from wool fibres. *The Analyst* **1980**, *105*, 729.

(5) Home, J.; Dudley, R. Thin-layer chromatography of dyes extracted from cellulosic fibres. *Forensic Sci.Int*. **1981**, *17*, 71–78.

(6) Beattie, I.; Roberts, H.; Dudley, R. Thin-layer chromatography of dyes extracted from polyester, nylon and polyacrylonitrile fibres. *Forensic Sci.Int*. **1981**, *17*, 57–69.

(7) Hartshorne, A. W.; Laing, D. K. The dye classification and discrimination of coloured polypropylene fibres. *Forensic Sci.Int*. **1984**, *25*, 133–141.

(8) Wiggins, K.; Crabtree, S.; March, B. The importance of thin layer chromatography in the analysis of reactive dyes released from wool fibers. *J. Forensic Sci*. **1996**, *41*, 1042–1045.

(9) Laing, D.; Boughey, L.; Hartshorne, A. The standardisation of thin layer chromatographic systems for comparison of fibre dyes. *J. Forensic Sci. Soc*. **1990**, *30*, 299–307.

(10) Laing, D.; Hartshorne, A.; Bennet, D. Thin layer chromatography of azoic dyes extracted from cotton fibres. *J. Forensic Sci. Soc*. **1990**, *30*, 309–315.

(11) Rendle, D. F.; Wiggins, K. G. Forensic analysis of textile fibre dyes. *Review of Progress in Coloration and Related Topics* **1995**, *25*, 29–34.

(12) Rendle, D. F.; Crabtree, S. R.; Wiggins, K. G.; Salter, M. T. Cellulase digestion of cotton dyed with reactive dyes and analysis of the products by thin layer chromatography. *Journal of the Society of Dyers and Colourists* **1994**, *110*, 338–341.

(13) Crabtree, S. R.; Rendle, D. F.; Wiggins, K. G.; Salter, M. T. The release of reactive dyes from wool fibres by alkaline hydrolysis and their analysis by thin layer chromatography. *Journal of the Society of Dyers and Colourists* **1995**, *111*, 100–102.

(14) Stefan, A. R.; Dockery, C. R.; Nieuwland, A. a; Roberson, S. N.; Baguley, B. M.; Hendrix, J. E.; Morgan, S. L. Forensic analysis of anthraquinone, azo, and metal complex acid dyes from nylon fibers by micro-extraction and capillary electrophoresis. *Anal. Bioanal. Chem* **2009**, *394*, 2077–85.

(15) Stefan, A. R.; Dockery, C. R.; Baguley, B. M.; Vann, B. C.; Nieuwland, A. a; Hendrix, J. E.; Morgan, S. L. Microextraction, capillary electrophoresis, and mass spectrometry for forensic analysis of azo and methine basic dyes from acrylic fibers. *Anal. Bioanal. Chem* **2009**, *394*, 2087–94.

(16) Dockery, C. R.; Stefan, a R.; Nieuwland, a a; Roberson, S. N.; Baguley, B. M.; Hendrix, J. E.; Morgan, S. L. Automated extraction of direct, reactive, and vat dyes from cellulosic fibers for forensic analysis by capillary electrophoresis. *Anal. Bioanal. Chem* **2009**, *394*, 2095–103.

(17) Huang, M.; Russo, R.; Fookes, B. G.; Sigman, M. E. Analysis of Fiber Dyes By Liquid Chromatography Mass Spectrometry (LC-MS) with Electrospray Ionization: Discriminating Between Dyes with Indistinguishable UV-Visible Absorption Spectra. *J. Forensic Sci* **2005**, *50*, 1–9.

(18) Huang, M.; Yinon, J.; Sigman, M. E. Forensic identification of dyes extracted from textile fibers by liquid chromatography mass spectrometry (LC-MS). *J. Forensic Sci* **2004**, *49*, 238–49.

(19) Beattie, I. B.; Dudley, R. J.; Smalldon, K. W. The Extraction and Classification of Dyes on Single Nylon, Polyacrylonitrile and Polyester Fibres. *Journal of the Society of Dyers and Colourists* **1979**, *95*, 295–302.

(20) Petrick, L. M.; Wilson, T. a; Ronald Fawcett, W. High-performance liquid chromatography-ultraviolet-visible spectroscopy-electrospray ionization mass spectrometry method for acrylic and polyester forensic fiber dye analysis. *J. Forensic Sci* **2006**, *51*, 771–9.

(21) West, J. C. Extraction and analysis of disperse dyes on polyester textiles. *J. Chromatogr. A* **1981**, *208*, 47–54.

Table 2.1. List of textile dyes, molecular structures, and UV/visible absorbance spectra.

C.I. Name Formula Mol. Wt. (g/mol)	Structure	Absorbance Spectrum
Basic Red 46 $C_{18}H_{21}BrN_6$ 401.30	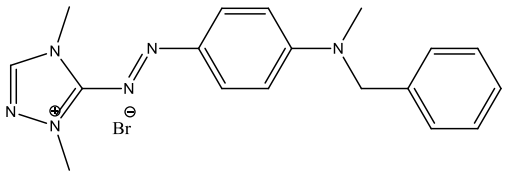	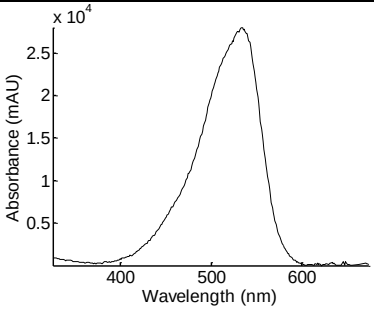
Basic Violet 16 $C_{23}H_{29}N_2^+$ 333.49	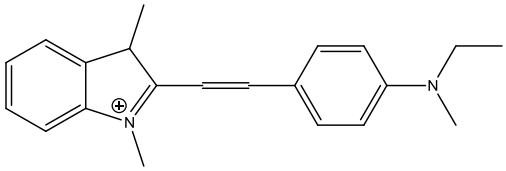	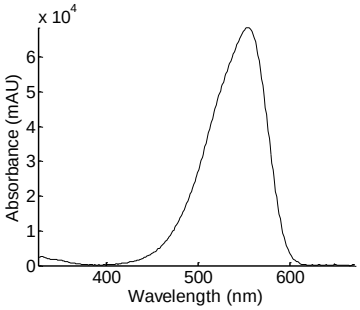
Basic Yellow 28 $C_{20}H_{24}N_3O^+$ 322.42	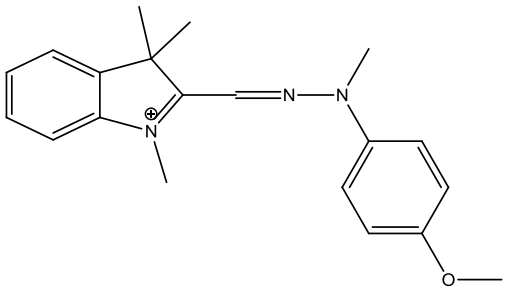	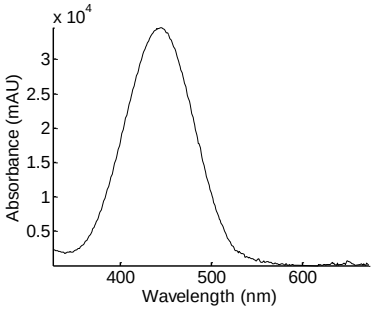
Acid Red 337 $C_{17}H_{12}F_3N_3O_4S$ 411.36	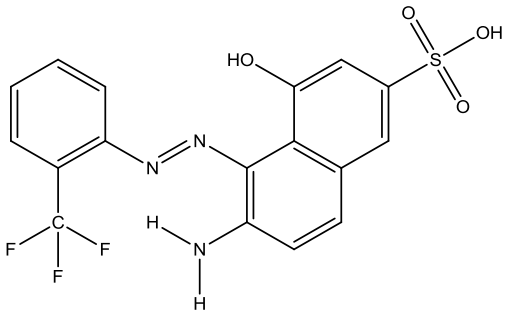	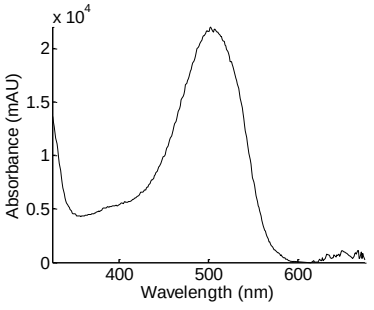

Table 2.1. Continued

Acid Yellow 49 $C_{16}H_{13}Cl_2N_5O_3S$ 426.28	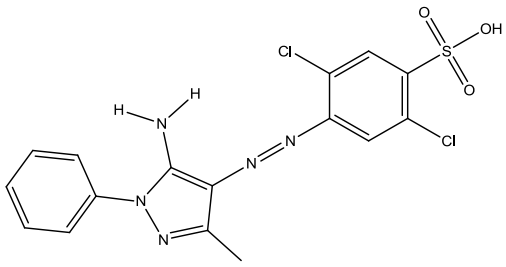	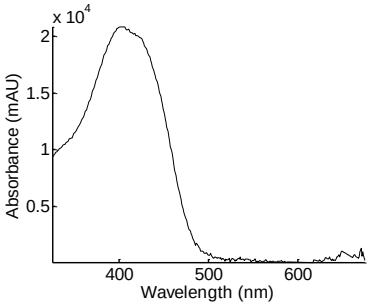
Acid Blue 281 $C_{27}H_{20}N_2O_8S_2$ 564.59	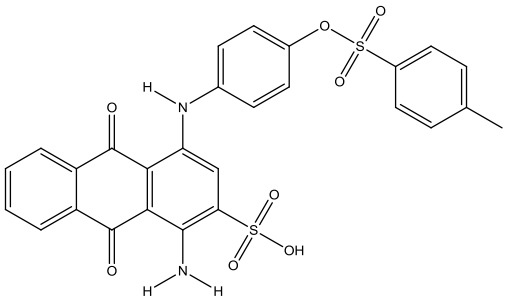	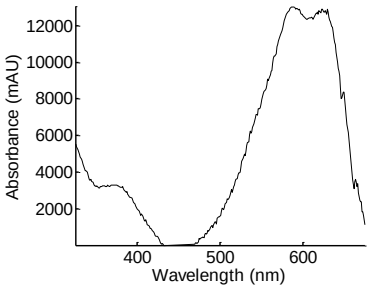
Disperse Violet 77 $C_{21}H_{24}N_6O_5$ 440.45	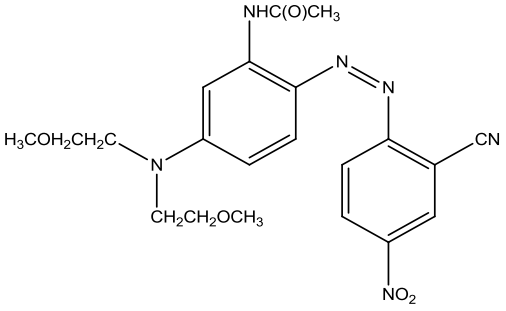	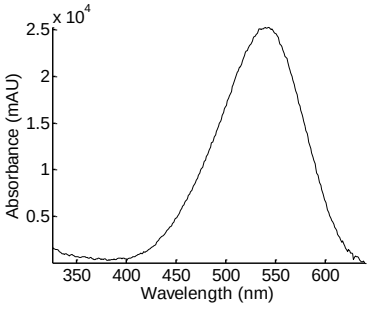
Disperse Blue 60 $C_{22}H_{21}N_3O_6$ 423.42	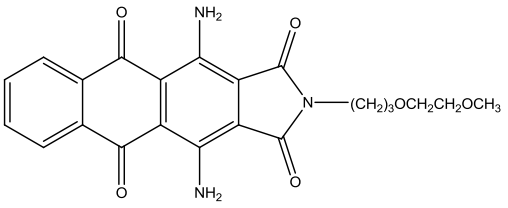	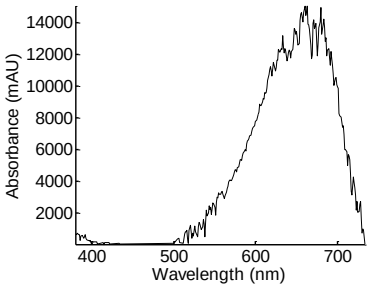
Disperse Yellow 114 $C_{20}H_{16}N_4O_5S$ 424.43	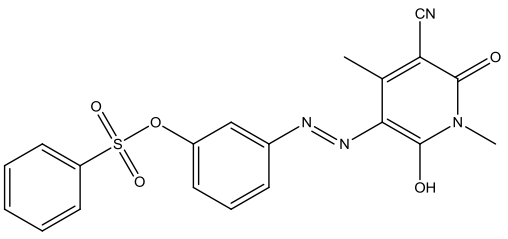	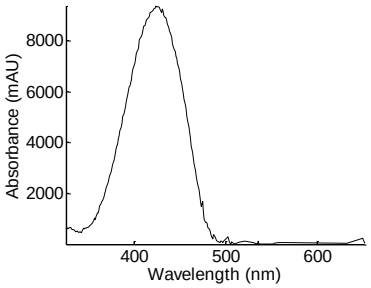

Table 2.2. Mobile phase gradient profiles.

UPLC mobile phase gradient for UV/visible detection

Time (min)	Flow Rate (mL/min)	Methanol 0.15 % FA (%)	50 mM Ammonium Acetate (%)
0.0	0.6	10	90
0.5	0.6	10	90
4.0	0.6	90	10
4.5	0.6	90	10
4.6	0.6	10	90
6.5	0.6	10	90

UPLC mobile phase gradient for MS-MS detection

Time (min)	Flow Rate (mL/min)	Methanol 0.15% FA (%)	50 mM Ammonium Acetate (%)
0.0	0.3	20	80
0.5	0.3	20	80
4.0	0.3	90	10
4.5	0.3	90	10
4.6	0.3	20	80
6.5	0.3	20	80

Table 2.3. MS-MS transitions and voltage settings.

Dye	Transition (m/z)	Cone Voltage (V)	Collision Voltage (V)
Basic Red 46	321-196	30	16
Basic Violet 16	333-319	39	29
Basic Yellow 28	322-136	33	30
Acid Red 337	412-161	45	33
Acid Yellow 49	426-144	40	35
Acid Blue 281	565-409	40	30
Disperse Violet 77	441-221	36	21
Disperse Blue 60	424-348	32	18
Disperse Yellow 114	425-178	47	30

Table 2.4. Summary of the calibration and LOD results. LOD_1, LOD_2, and LOD_3 are calculated from the standard deviation of the blanks, from the standard deviation of the lowest non-zero concentration replicates, and from the standard deviation of the y-intercept of the calibration line respectively. DAD-HIGH, DAD-LOW, and MS represent data from the high concentration diode array models, the low concentration diode array models, and the tandem mass spectrometry models respectively.

Dye	$R^2_{DAD-HIGH}$	$R^2_{DAD-LOW}$	R^2_{MS}	$LOD_{1\ DAD-HIGH}$ (ppb)	$LOD_{2\ DAD-HIGH}$ (ppb)	$LOD_{3\ DAD-HIGH}$ (ppb)	$LOD_{1\ DAD-LOW}$ (ppb)	$LOD_{2\ DAD-LOW}$ (ppb)	$LOD_{3\ DAD-LOW}$ (ppb)	$LOD_{1\ MS}$ (ppb)	$LOD_{2\ MS}$ (ppb)	$LOD_{3\ MS}$ (ppb)
Basic Red 46	0.9996	0.9914	0.9371	4.77	5.41	11.80	2.37	3.12	1.21	1.70	6.44	57.30
Basic Violet 16	0.9999	0.9952	0.9970	3.62	1.69	6.32	1.84	2.09	0.91	0.38	2.55	12.00
Basic Yellow 28	0.9995	0.9965	0.9840	6.97	1.07	14.10	2.69	0.93	0.77	2.34	3.87	28.10
Acid Red 337	0.9998	0.9957	0.9953	9.50	2.17	8.90	3.07	1.89	0.86	10.30	8.08	15.20
Acid Yellow 49	0.9997	0.9940	0.9858	3.22	1.96	10.40	4.26	2.59	1.01	6.41	4.76	26.50
Acid Blue 281	0.9999	0.9913	0.9879	4.87	1.56	6.79	4.38	0.41	1.22	7.09	4.67	27.40
Disperse Violet 77	0.9998	0.9942	0.9700	10.10	0.37	9.42	2.23	1.28	0.99	0.62	1.46	38.80
Disperse Blue 60	0.9993	–	0.9813	37.00	13.50	16.80	–	–	–	4.67	2.88	30.50
Disperse Yellow 114	0.9999	0.9687	0.9833	11.30	4.68	7.60	12.60	1.67	2.34	2.89	7.62	28.80

Table 2.5. Summary of the calibration and LOQ results. LOQ_1, LOQ_2, and LOQ_3 are calculated from the standard deviation of the blanks, from the standard deviation of the lowest non-zero concentration replicates, and from the standard deviation of the y-intercept of the calibration line respectively. DAD-HIGH, DAD-LOW, and MS represent data from the high concentration diode array models, the low concentration diode array models, and the tandem mass spectrometry models respectively.

Dye	$R^2_{DAD-HIGH}$	$R^2_{DAD-LOW}$	R^2_{MS}	$LOQ_{1\ DAD-HIGH}$ (ppb)	$LOQ_{2\ DAD-HIGH}$ (ppb)	$LOQ_{3\ DAD-HIGH}$ (ppb)	$LOQ_{1\ DAD-LOW}$ (ppb)	$LOQ_{2\ DAD-LOW}$ (ppb)	$LOQ_{3\ DAD-LOW}$ (ppb)	$LOQ_{1\ MS}$ (ppb)	$LOQ_{2\ MS}$ (ppb)	$LOQ_{3\ MS}$ (ppb)
Basic Red 46	0.9996	0.9914	0.9371	14.5	16.4	35.8	7.2	9.5	3.7	5.2	19.5	173.6
Basic Violet 16	0.9999	0.9952	0.9970	11.0	5.1	19.2	5.6	6.3	2.8	1.2	7.7	36.4
Basic Yellow 28	0.9995	0.9965	0.9840	21.1	3.2	42.7	8.2	2.8	2.3	7.1	11.7	85.2
Acid Red 337	0.9998	0.9957	0.9953	28.8	6.6	27.0	9.3	5.7	2.6	31.2	24.5	46.1
Acid Yellow 49	0.9997	0.9940	0.9858	9.8	5.9	31.5	12.9	7.8	3.1	19.4	14.4	80.3
Acid Blue 281	0.9999	0.9913	0.9879	14.8	4.7	20.6	13.3	1.2	3.7	21.5	14.2	83.0
Disperse Violet 77	0.9998	0.9942	0.9700	30.6	1.1	28.5	6.8	3.9	3.0	1.9	4.4	117.6
Disperse Blue 60	0.9993	–	0.9813	112.1	40.9	50.9	–	–	–	14.2	8.7	92.4
Disperse Yellow 114	0.9999	0.9687	0.9833	34.2	14.2	23.0	38.2	5.1	7.1	8.8	23.1	87.3

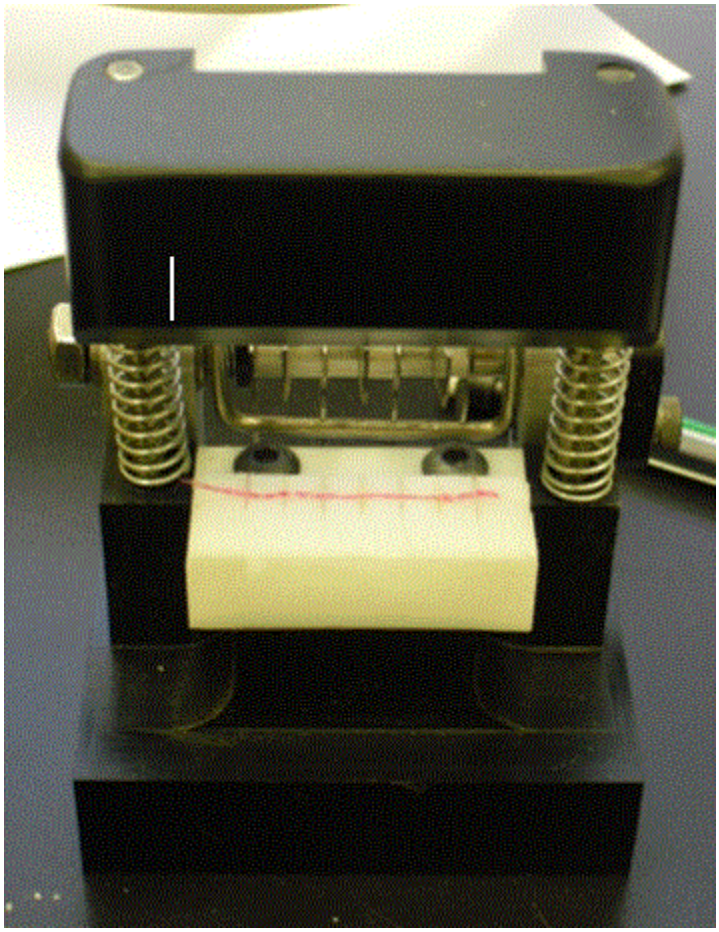

Figure 2.1. Fiber guillotine for cutting fibers down to 5 mm in length,

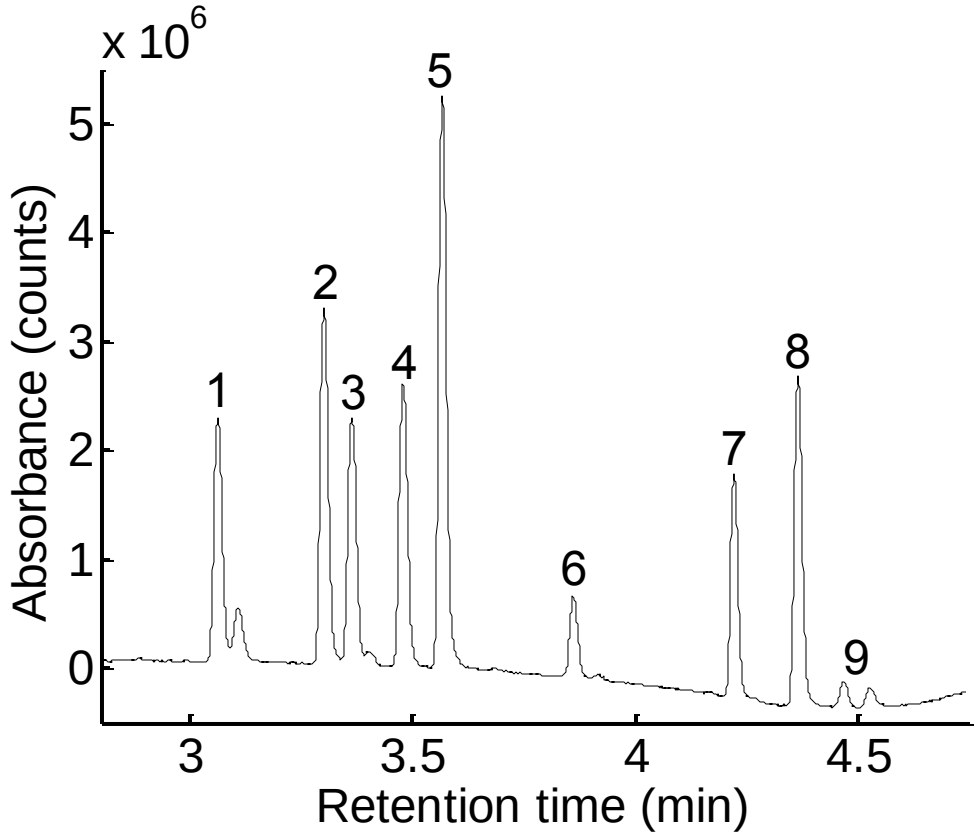

Figure 2.2. Separation of acid, basic, and disperse dyes at 1 ppm concentration. Peak identification: (1) Basic Red 46 (two peaks); (2) Basic Yellow 28; (3) Acid Yellow 49 (two peaks); (4) Acid Red 337; (5) Basic Violet 16; (6) Disperse Yellow 114; (7) Acid Blue 281; (8) Disperse Violet 77; (9) Disperse Blue 60 (two peaks).

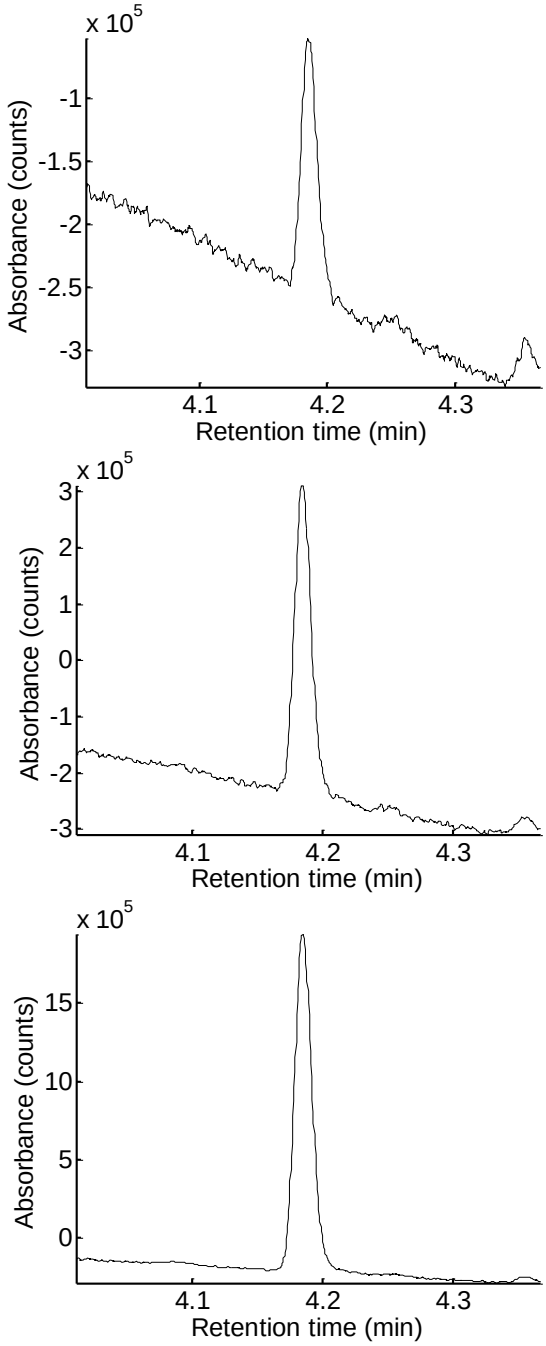

Figure 2.3. UPLC-DAD chromatograms for Acid Blue 281 extracted from a 0.5 mm fiber (top), 1 mm fiber (middle), and 5 mm fiber (bottom).

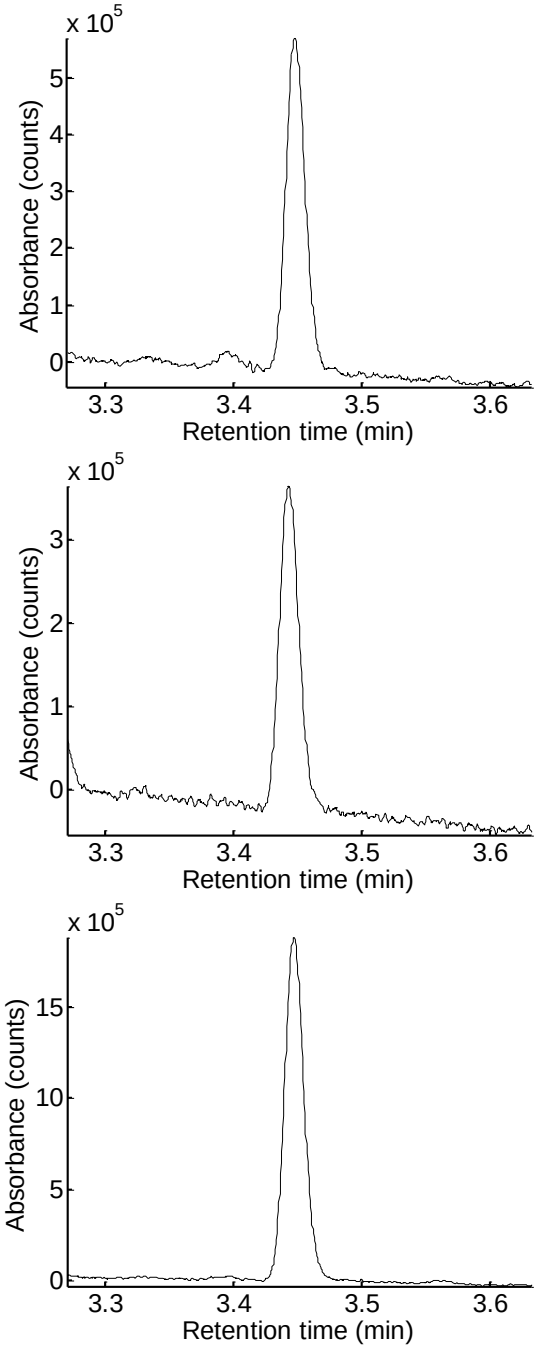

Figure 2.4. UPLC-DAD chromatograms for Acid Red 337 extracted from a 0.5 mm fiber (top), 1 mm fiber (middle), and 5 mm fiber (bottom).

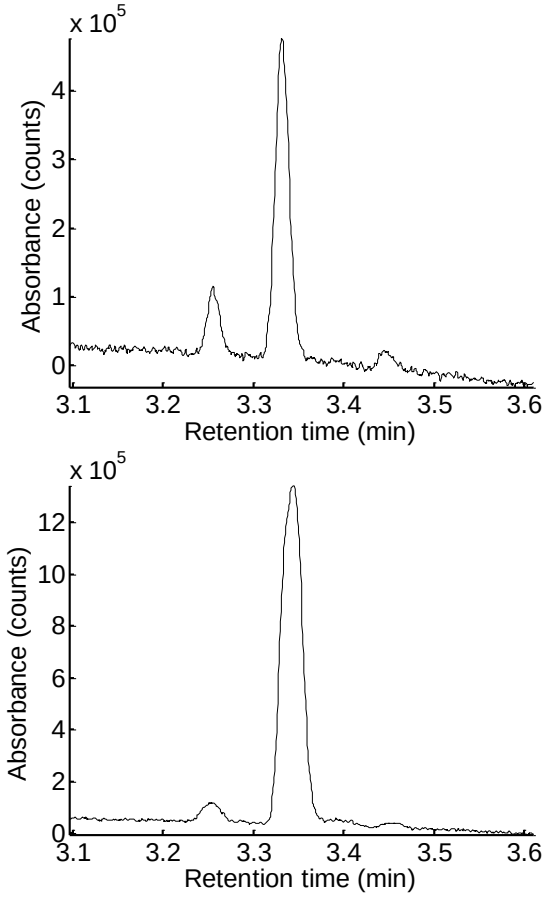

Figure 2.5. UPLC-DAD chromatograms for Acid Yellow 49 extracted from a 1 mm fiber (top) and a 5 mm fiber (bottom).

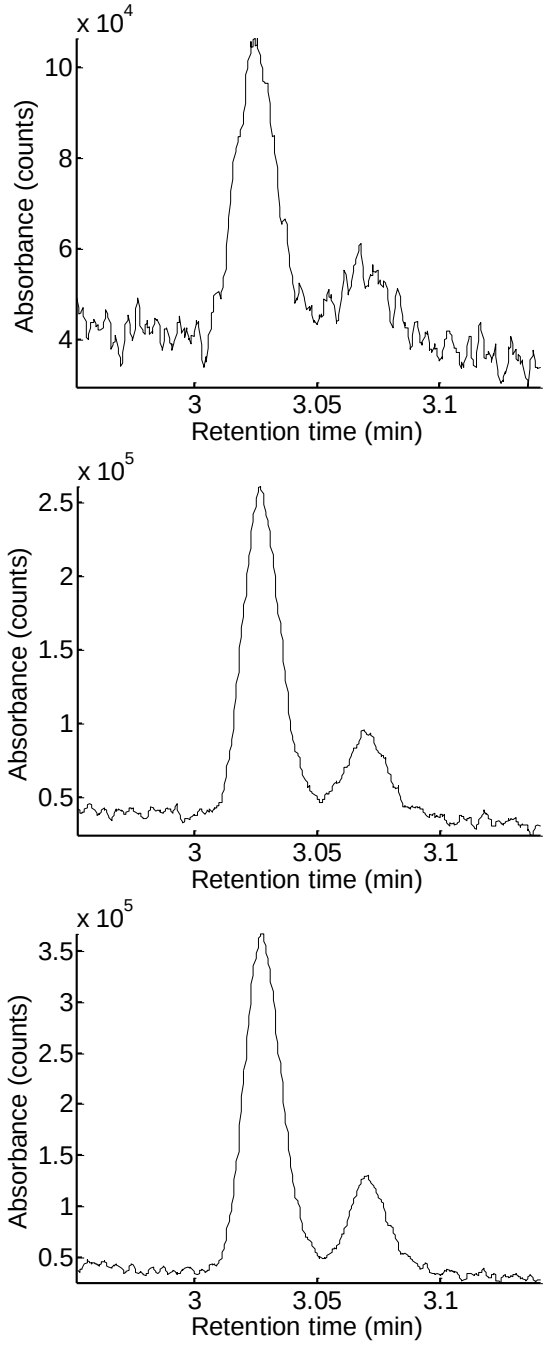

Figure 2.6. UPLC-DAD chromatograms for Basic Red 46 extracted from a 0.5 mm fiber (top), 1 mm fiber (middle), and 5 mm fiber (bottom).

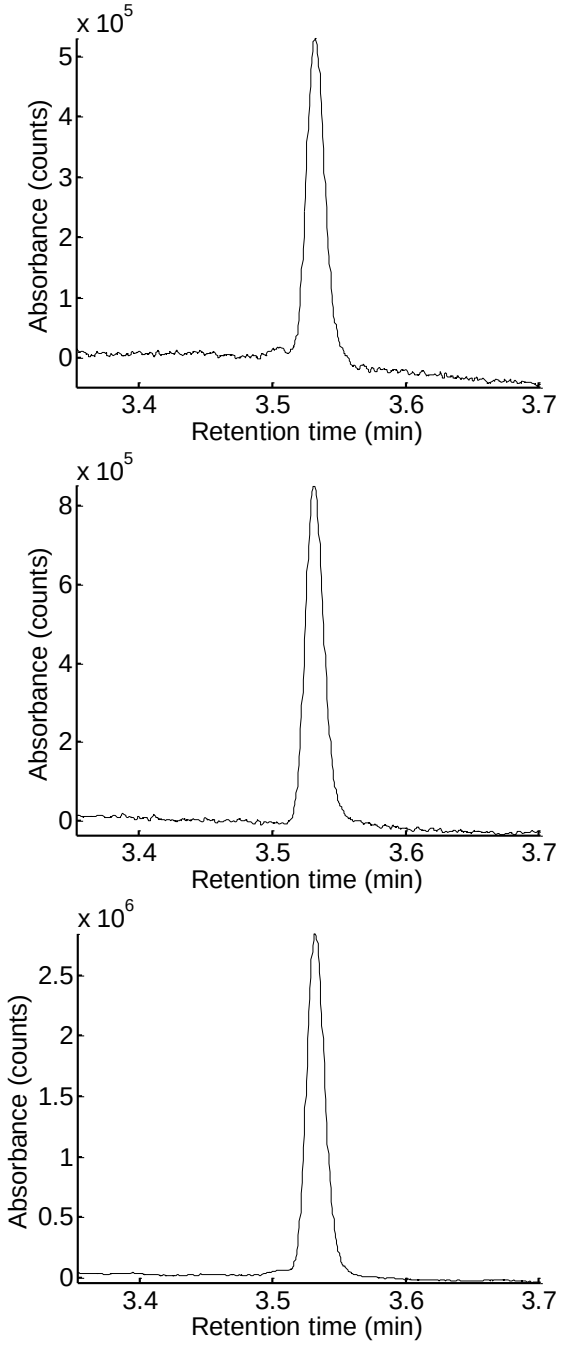

Figure 2.7. UPLC-DAD chromatograms for Basic Violet 16 extracted from a 0.5 mm fiber (top), 1 mm fiber (middle), and 5 mm fiber (bottom).

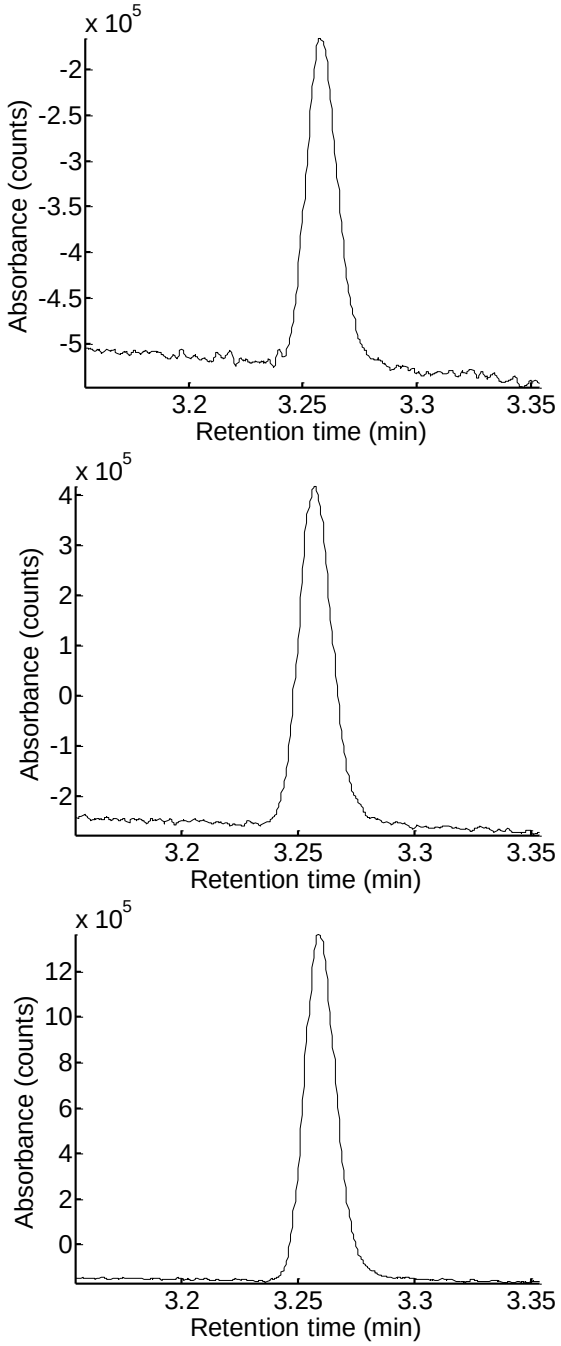

Figure 2.8. UPLC-DAD chromatograms for Basic Yellow 28 extracted from a 0.5 mm fiber (top), 1 mm fiber (middle), and 5 mm fiber (bottom).

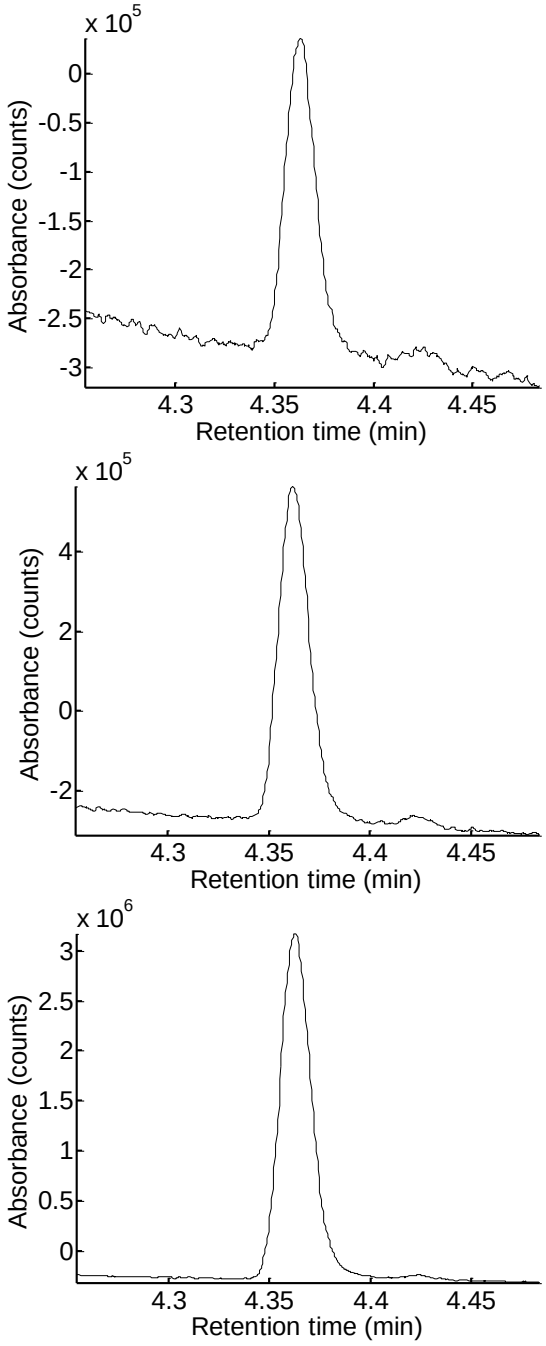

Figure 2.9. UPLC-DAD chromatograms for Disperse Violet 77 extracted from a 0.5 mm fiber (top), 1 mm fiber (middle), and 5 mm fiber (bottom).

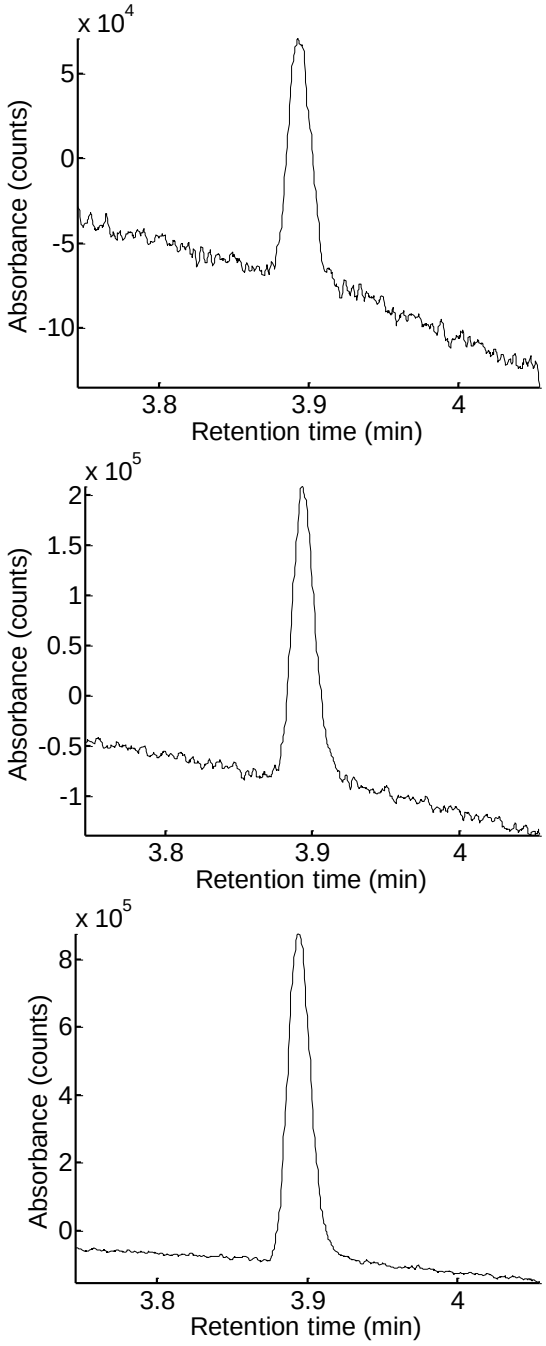

Figure 2.10. UPLC-DAD chromatograms for Disperse Yellow 114 extracted from a 0.5 mm fiber (top), 1 mm fiber (middle), and 5 mm fiber (bottom).

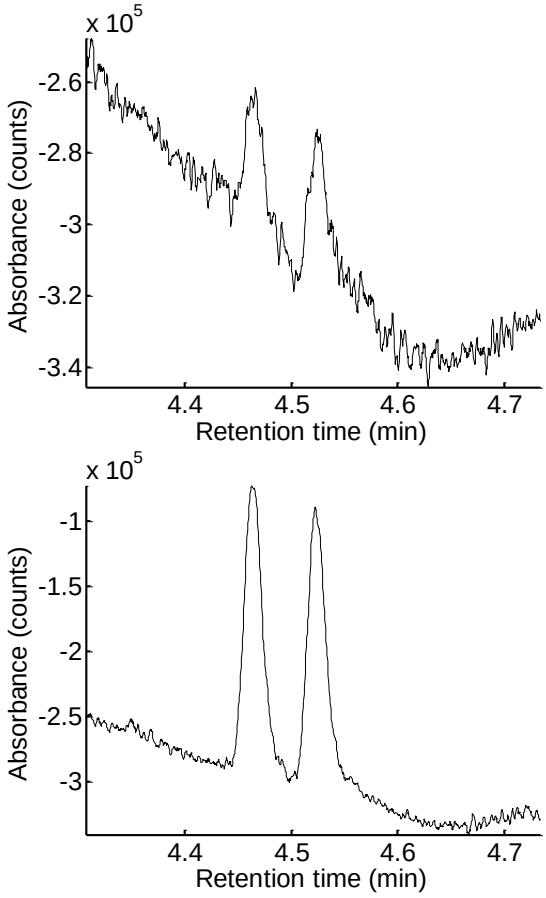

Figure 2.11. UPLC-DAD chromatograms for Disperse Blue 60 extracted from a 0.5 mm fiber (top), 1 mm fiber (middle), and 5 mm fiber (bottom).

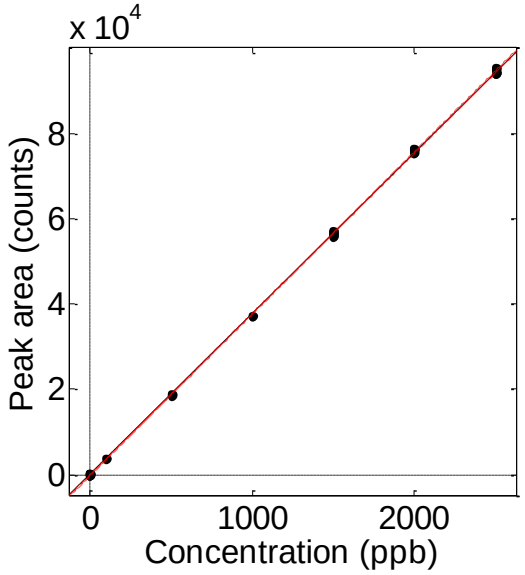

Figure 2.12. High concentration UPLC-DAD calibration plot for Acid Blue 281.

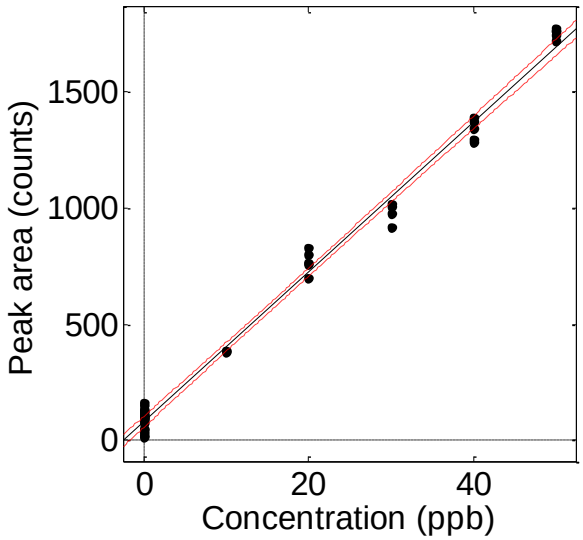

Figure 2.13. Low concentration UPLC-DAD calibration plot for Acid Blue 281.

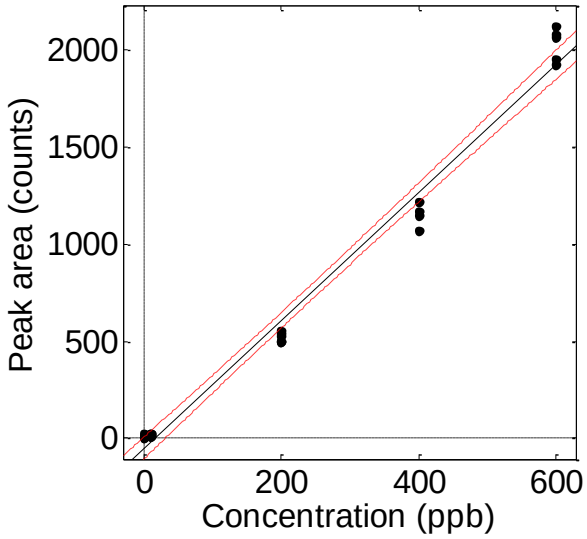

Figure 2.14. UPLC-MS-MS Calibration plot for Acid Blue 281.

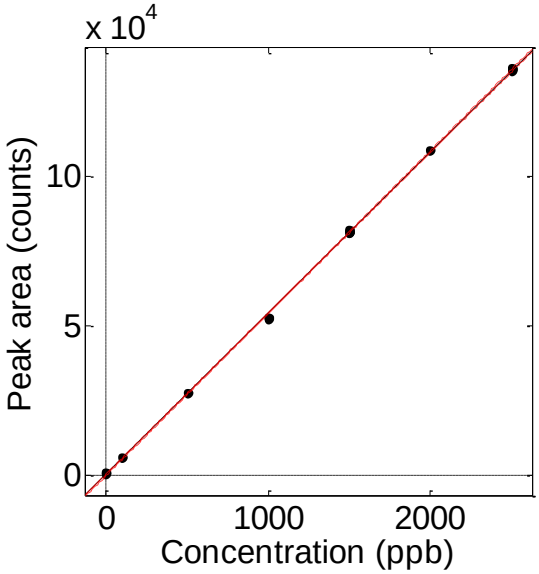

Figure 2.15. High concentration UPLC-DAD calibration plot for Acid Red 337.

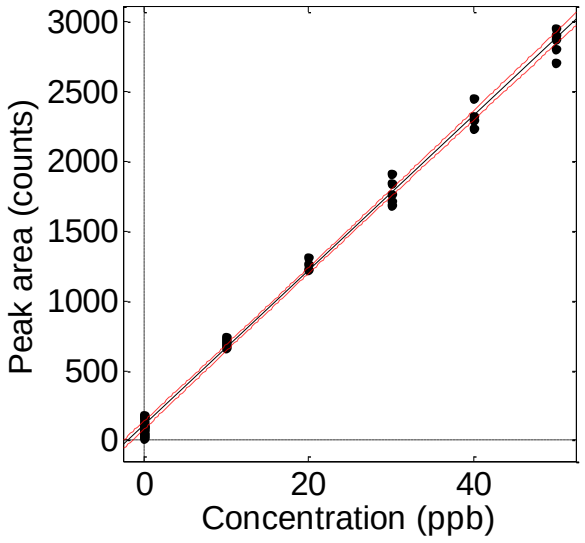

Figure 2.16. Low concentration UPLC-DAD calibration plot for Acid Red 337.

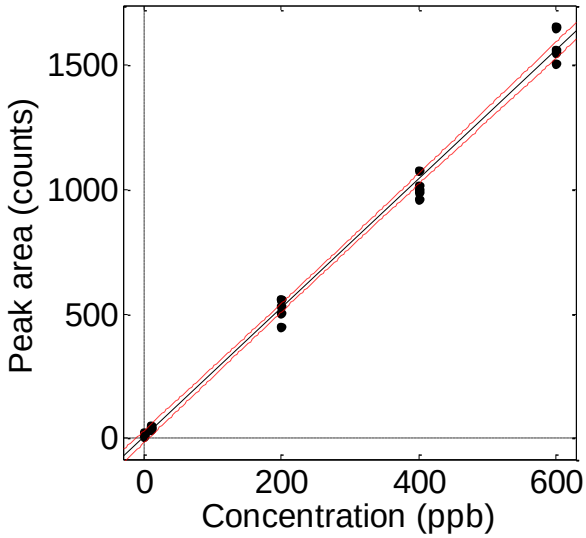

Figure 2.17. UPLC-MS-MS Calibration plot for Acid Red 337.

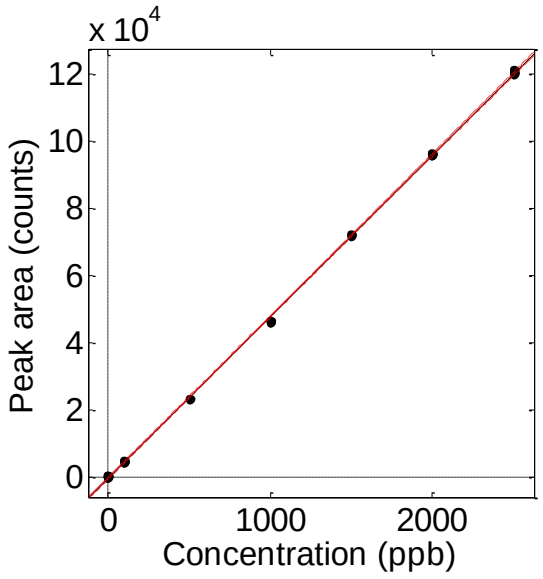

Figure 2.18. High concentration UPLC-DAD calibration plot for Acid Yellow 49.

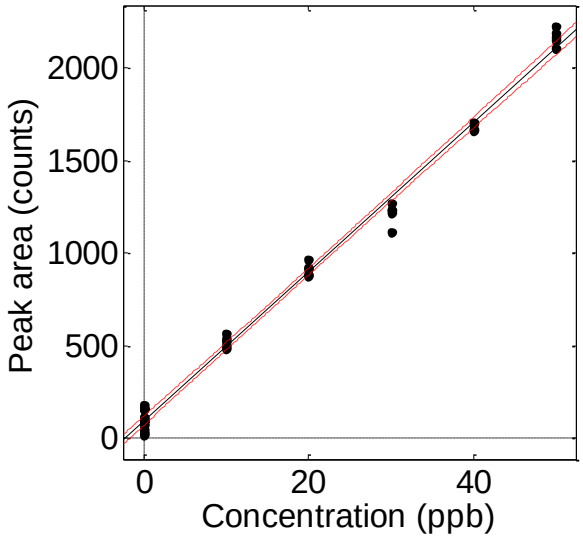

Figure 2.19. Low concentration UPLC-DAD calibration plot for Acid Yellow 49.

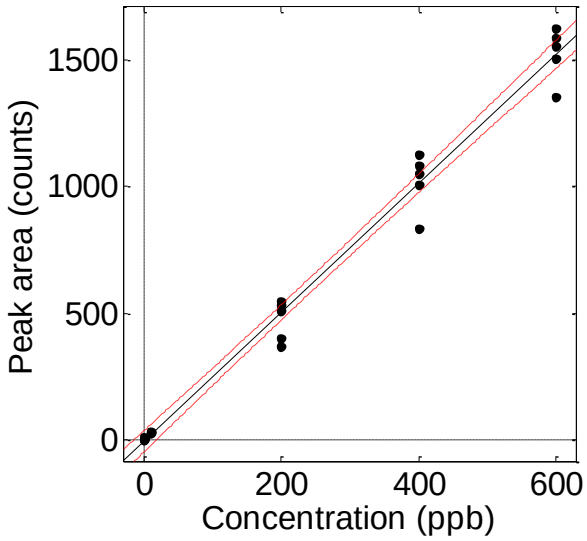

Figure 2.20. UPLC-MS-MS Calibration plot for Acid Yellow 49.

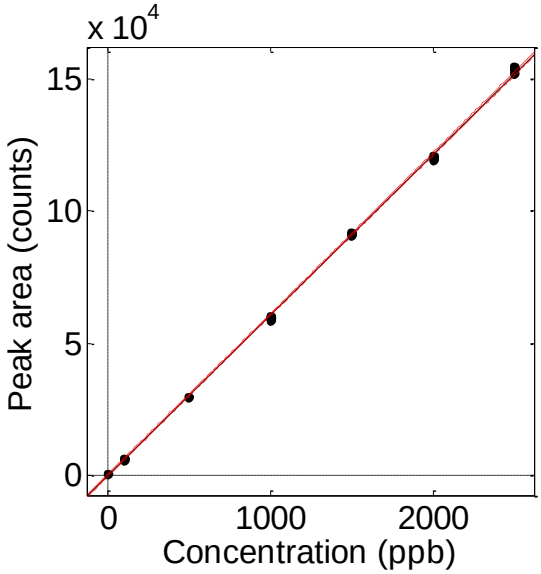

Figure 2.21. High concentration UPLC-DAD calibration plot for Basic Red 46.

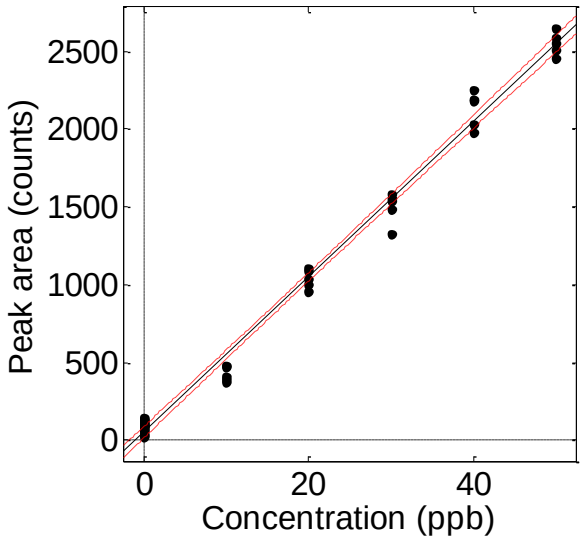

Figure 2.22. Low concentration UPLC-DAD calibration plot for Basic Red 46.

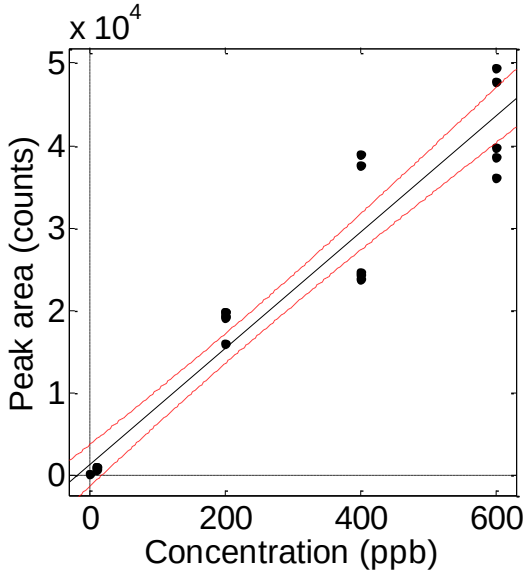

Figure 2.23. UPLC-MS-MS Calibration plot for Basic Red 46.

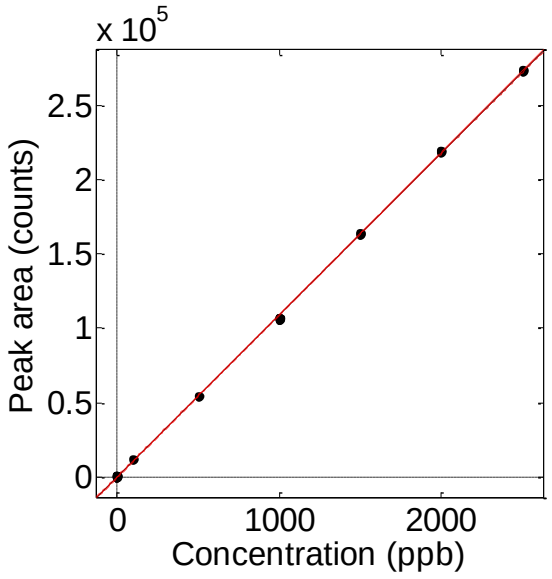

Figure 2.24. High concentration UPLC-DAD calibration plot for Basic Violet 16.

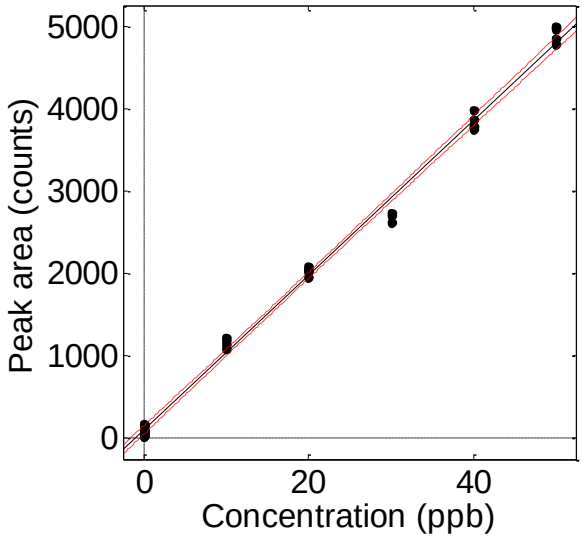

Figure 2.25. Low concentration UPLC-DAD calibration plot for Basic Violet 16.

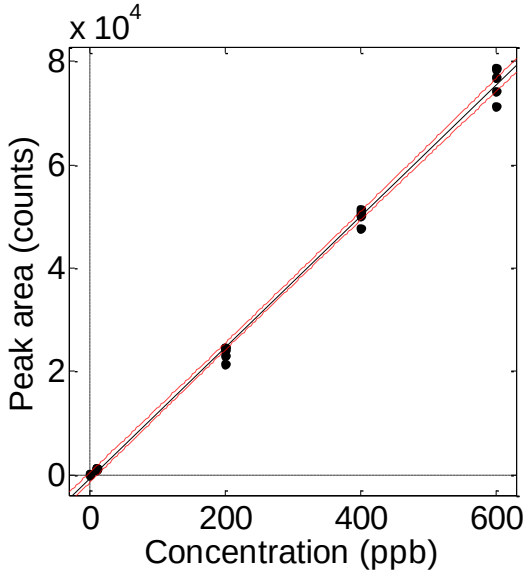

Figure 2.26. UPLC-MS-MS calibration plot for Basic Violet 16.

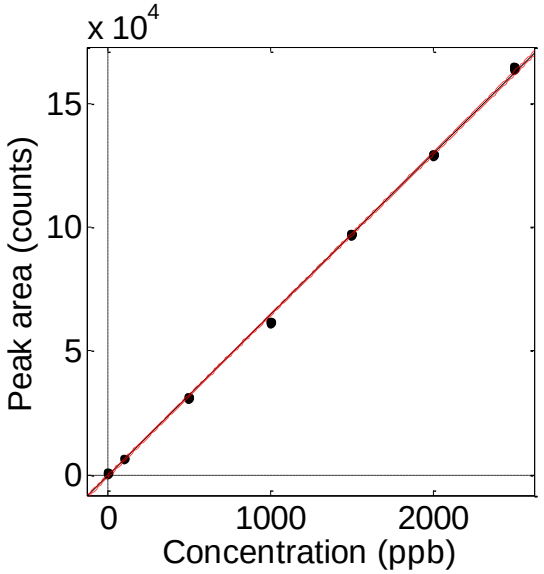

Figure 2.27. High concentration UPLC-DAD calibration plot for Basic Yellow 28.

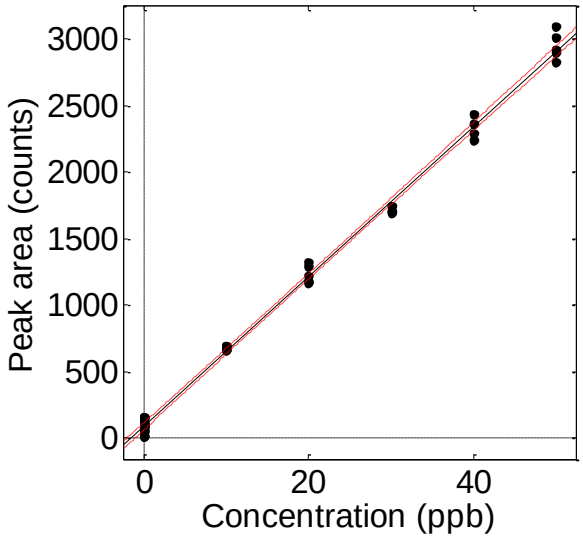

Figure 2.28. Low concentration UPLC-DAD calibration plot for Basic Yellow 28.

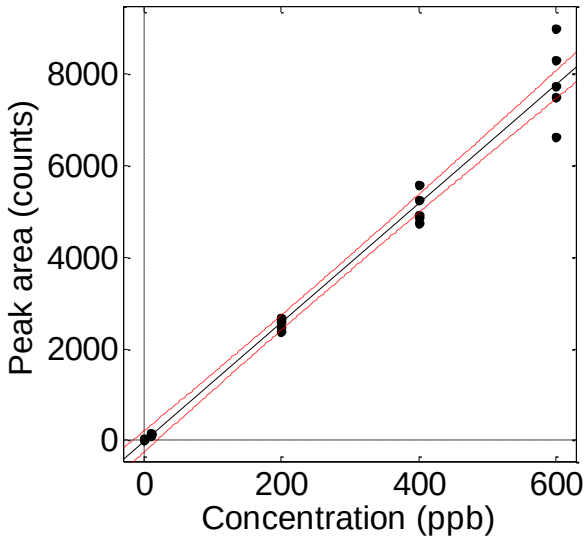

Figure 2.29. UPLC-MS-MS Calibration plot for Basic Yellow 28.

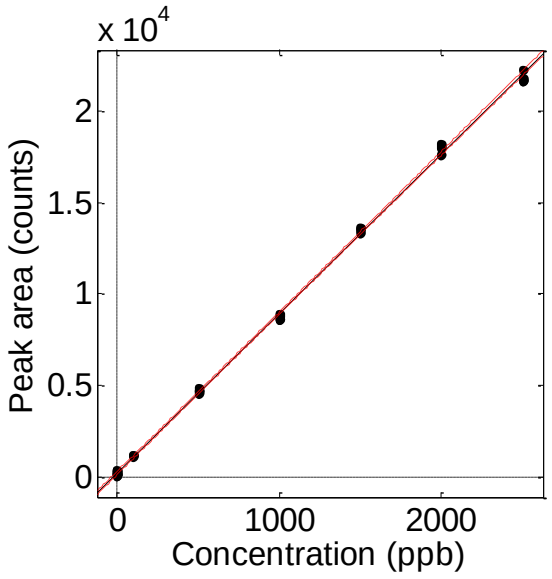

Figure 2.30. High concentration UPLC-DAD calibration plot for Disperse Blue 60.

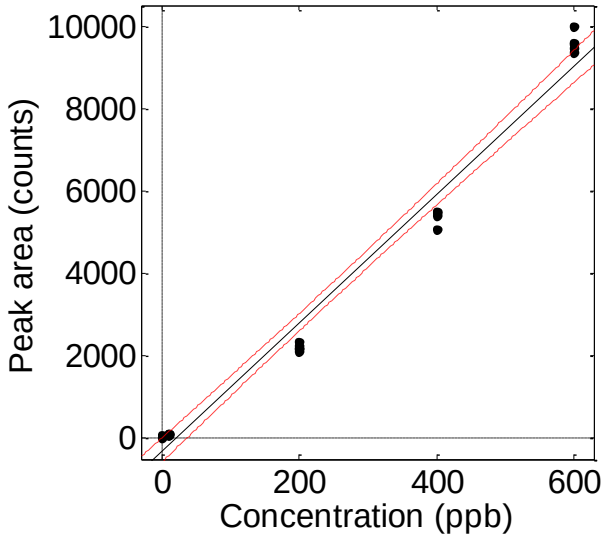

Figure 2.31. UPLC-MS-MS Calibration plot for Disperse Blue 60.

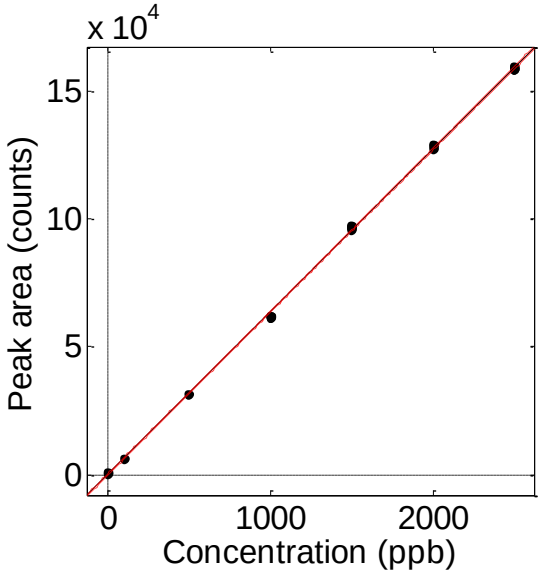

Figure 2.32. High concentration UPLC-DAD calibration plot for Disperse Violet 77.

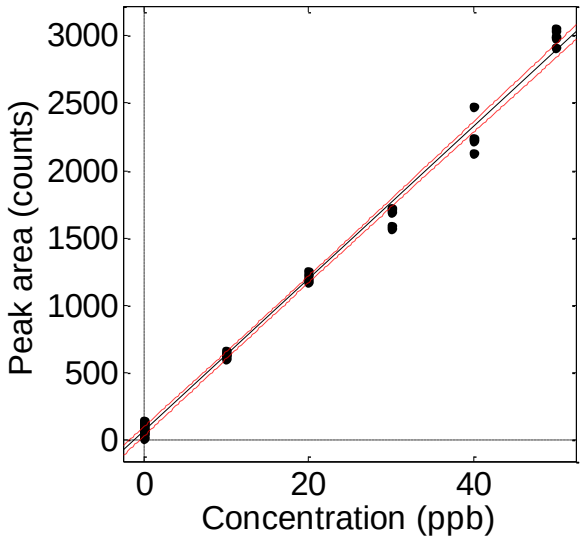

Figure 2.33. Low concentration UPLC-DAD calibration plot for Disperse Violet 77.

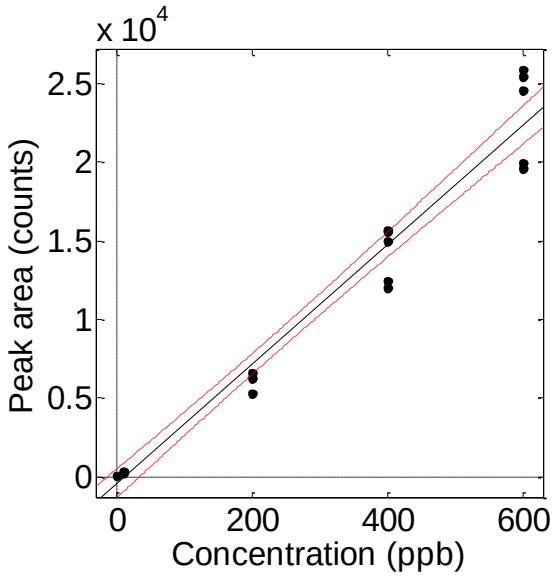

Figure 2.34. UPLC-MS-MS Calibration plot for Disperse Violet 77.

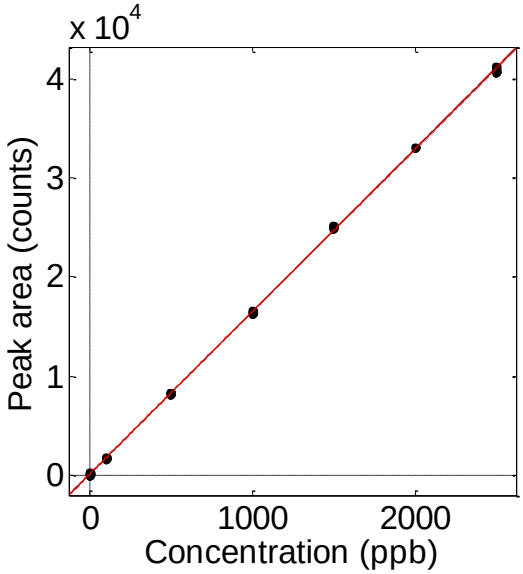

Figure 2.35. High concentration UPLC-DAD calibration plot for Disperse Yellow 114.

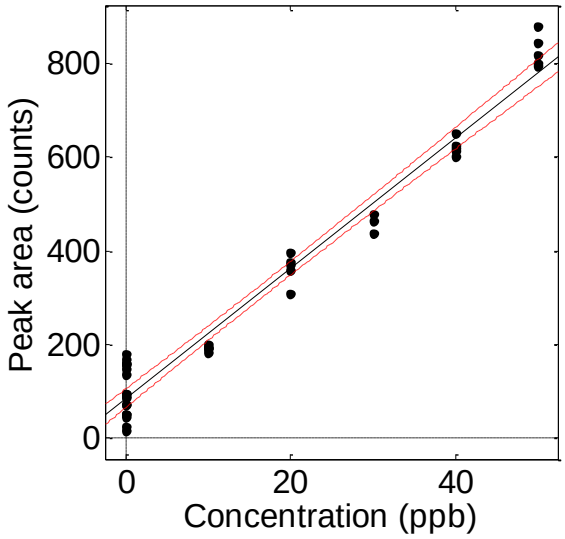

Figure 2.36. Low concentration UPLC-DAD calibration plot for Disperse Yellow 114.

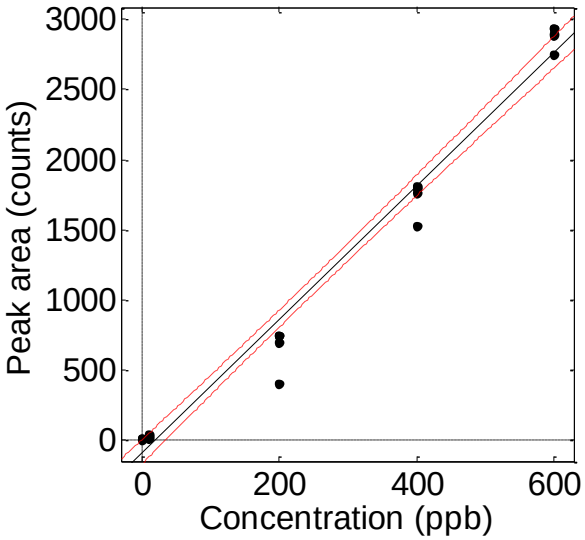

Figure 2.37. UPLC-MS-MS calibration plot for Disperse Yellow 114.

CHAPTER THREE

EXTRACTION OF DIRECT AND INDIGO DYES FROM TRACE COTTON FIBERS FOR FORENSIC CHARACTERIZATION BY ULTRA-PERFORMANCE LIQUID CHROMATOGRAPHY

ABSTRACT

Microextraction, followed by ultra-performance liquid chromatography, can often distinguish similar fibers containing different, but similar, dyes with the combination of retention time matching, UV/visible spectral comparison, and structural analysis by mass spectrometry. The analysis of cotton fibers is challenging because they can be dyed with three different classes of dye, each requiring a different method for extraction and analysis. This work focuses on the chemistries of direct dyes and indigo and their optimum extraction conditions and chromatographic methods. Cotton fibers as small as 1 mm in length have been successfully extracted and characterized. Analytical figures of merit and validation statistics, including extraction reproducibility, linearity, limits of detection and quantitation, and UPLC precision, are reported.

INTRODUCTION

The classic example of forensic fiber analysis involves the comparison of "known" and "questioned" fibers using various microscopic techniques in an attempt to establish associations between crime scenes, suspects, and victims. Cotton is an extremely abundant fiber material and cotton fibers are easily identified using polarized light microscopy by their refractive index and visually based on their unique morphology.[1] Additional discriminative information can be obtained from fibers using techniques such as infrared spectroscopy and UV-visible microspectrophotometry.[2] These techniques are preferred due to them being non-destructive to the fiber sample; however they provide limited information on the identity and amount of chemical constituents on the fibers.

Though many different types of fibrous textiles are commonly manufactured, 80% of all fibers found as criminal evidence are made of cotton, nylon, polyester, or acrylic.[1–4]

Cotton is of high interest due to its popularity in clothing. Cotton is a natural fiber made of cellulose, a polysaccharide containing hydroxyl groups and acetal linkages. The absence of ionic sites on the polymer backbone necessitates the use of direct dyes that are attached through hydrogen bonding, and reactive dyes that are covalently bound to the hydroxyl groups of the polymer. An additional dyeing technique involves water-insoluble vat dyes which migrate into the cellulose in their reduced form and are then oxidized and "locked" into the cellulose polymer. Direct, reactive, and vat dyes account for approximately 82% of all dyes used in the dyeing of cotton.[5]

Direct dyes are soluble in water due to the abundance of sulfonic acid, amine, and hydroxyl groups in their structures. The anionic dyes coat the fiber during the dying process and are held in place through hydrogen bonding. The removal of these dyes requires the disruption of the hydrogen bonds using alkaline solvents. A 4:3 (v/v) mixture of pyridine and water has been widely reported to extract direct dyes from cotton efficiently.[6,7]

Vat dyes are water-insoluble pigments used to dye cotton and account for approximately 15-25% of all cotton dyes consumed in the last 20 years.[8,9] This usage is due largely to indigo, an historically important and the oldest discovered vat dye, which is used today as the primary color of blue jeans. Due to their water-insoluble nature, vat dyes must first be chemically reduced to their water-soluble leuco form before application to cotton. Figure 3.1 shows this process for indigo. This process is commonly referred to as “vatting” in the textile industry as it is usually performed in a large vat. Vatting is typically conducted using sodium dithionite at very high pH conditions. Once the leuco form of the dye has been formed, the dye can migrate into the hydrophilic

cellulose backbone of cotton. After the dye permeates into the cotton, it is reoxidized back to its original water-insoluble form, mechanically trapping the dye within the cellulose lattice. This leads to exceptionally high fastness to cotton, comparable to reactive dyes.

Indigo and its derivatives are unique vat dyes in that they require a weaker reducing agent than anthraquinone vat dyes to convert into their leuco forms. Additionally, indigo can be extracted from plants and textiles without being reduced. Several methods have been reported for indigo extraction including acidified methanol [10], chloroform and pyridine in water [6], and DMSO [11]. For UPLC analysis techniques, these extraction methods are desirable over reduction because they eliminate the possibility of over reduction and degradation of the dye, as well as injection of strong reducing agents that can damage the stationary phase.

This study focuses on the extraction of direct dyes and indigo, and the analysis of the resulting extracts by ultra-performance liquid chromatography (UPLC). Because the extraction process is destructive to the fiber and because forensic fiber examiners wish to preserve as much of the actual fiber evidence as possible, only a small segment of an original evidence fiber can be subjected to analysis. In many cases, fibers of 2 mm size of less may be all that is found at a crime scene. Fibers of lengths of 1-10 mm can contain between 2-200 ng of dye.[4] Various cotton dyes and dyestuffs have a large polarity range and varying solubility conditions which necessitates a widely compatible analysis technique. UPLC instruments employ a higher pressure pump system compared to HPLC, which enables the use of smaller particle stationary phases of exquisite efficiency. UPLC columns are packed tighter and are shorter than typical HPLC columns, which

allows for significantly faster chromatographic analyses, sharper peaks, and higher signal-to-noise measurements. As in other forms of liquid chromatography, both the column and mobile phase systems can be tuned to analyze samples of varying chemical makeup.

EXPERIMENTAL

Materials and Instrumentation

Analytical grade water, acetone, pyridine, ammonium acetate, dimethyl sulfoxide (DMSO), chloroform, formic acid, glacial acetic acid, and HPLC/UPLC grade acetonitrile and methanol were purchased from Fisher Scientific (Pittsburg, PA).

Dye standards and extracts were separated and detected using a Waters Acquity™ UPLC H-Class equipped with a quaternary solvent pump system and a Waters PDA eλ detector. The column was a 2.1 × 50 mm I.D. 1.7 μm particle size Waters Acquity™ BEH C18 column with a 2.1 × 5 mm I.D. 1.7 μm particle size Waters Acquity UPLC® BEH C18 VanGuard precolumn. Mobile phase gradients are shown in Table 3.3 and Table 3.4. The column temperature was set at 40 °C. The diode array detector scanned at a rate of 40 Hz and 1.2 nm resolution. The sample injection volumes were 10 μL.

All dyed fabrics and matching dye standards were current production samples donated by dyestuff manufacturers in the southeastern United States. Dye names follow the Color Index nomenclature. All fibers were dyed at levels consistent with commercial use (2–4% by weight). All dye standards were solid in phase and stored in a dark room to avoid photodegradation. Photographs of cotton fibers were made with a Nikon (Melville, NY) model SMZ1500 microscope with a DS-Fi1 camera at 11.25x magnification.

Direct Dye Extraction Optimization

Direct Blue 71 (structure in Table 3.1) was selected as a representative direct dye for cotton fibers. Fibers dyed with this single dye were extracted under the solvent combinations shown in Table 3.2, generated using a three-component mixture design with Design Expert 7 (Milwaukee, WI). For each of the ten design points, four replicate 1 cm threads dyed with Direct Blue 71 were individually subjected to microextraction.

Extractions at each design point were performed on four replicate fibers of the same length, for a total of 40 extractions. Extractions were conducted in Waters Total Recovery Vials because the narrow diameter of the vial allows the entire fiber sample to be submerged in less solvent than that of a typical conical vial, concentrating the extract. The threads were extracted by adding 1 mL of solvent, capped, and heated in an oven at 100°C for 60 min. Following extraction, the vials were uncapped and the solvents were evaporated at 95°C and then reconstituted in 1 mL of water for UPLC analysis. A Waters (Milford, MA) Acquity H-Class Quaternary Solvent UPLC coupled to a Waters PDA eλ diode array detector for UV-visible analysis and equipped with a Waters Acquity BEH C_{18} column (1.7 um particle size, 2.1 mm ID x 50 mm length) was used for all analysis. The diode array detector measured absorbance from 400-700 nm at 40 Hz and 1.2 nm resolution. Dye peak areas were used as the response, and ternary response surface models were generated using Design Expert, v. 7 (StatEase Corp., Inc., Minneapolis, MN, USA). The mobile phase gradient conditions are given in Table 3.3.

Indigo Dye Extraction Optimization

A second ternary component mixture containing chloroform, pyridine, and DMSO was studied for the extraction of indigo. As with the direct dye optimization study, five replicate fibers were extracted at each design point and then quantified by UPLC. The

solvents used were DMSO, chloroform, and pyridine. Extractions were carried out at 100°C for 60 min in 1 mL of solvent. The solvent was then boiled off and samples were reconstituted in 1 mL of 50:50 methanol and water. UPLC gradient conditions for indigo analysis are listed in Table 3.4.

Limits of Detection and Extract Quantitation

Standard mixtures of direct dyes were made 1-10 ppm concentrations. The direct dye mixtures contained Direct Blue 80, Direct Blue 71, and Direct Orange 39 in 90:10 (v/v) 0.2 M ammonium acetate and acetonitrile. The dye mixtures were analyzed (five replicates) using UPLC. A calibration plot was generated for each dye and limits of detection were determined.

Direct Dye Extraction

For the extraction of direct dyes, fibers 1 cm in length, dyed with Direct Orange 39, Direct Blue 71, or Direct Blue 80 from Dystar (structures shown in Table 3.1), were cut using a fiber guillotine and loaded into total recovery vials. 100 μL of optimal extraction solvent mixture (50% DI H_2O, 25% pyridine, 25% Acetone) was dispensed into the vial. The vials were sealed with screw tops to minimize solvent evaporation and were placed in a laboratory oven at 100°C for 60 min. The vials were uncapped and allowed to completely evaporate in the oven at 95°C. Dye residues were reconstituted with 50 uL 90% 0.2 M ammonium acetate and 10% acetonitrile and vortex-mixed to ensure solvation. The dyes were then analyzed by UPLC-DAD using the same chromatographic conditions as the extraction study.

Indigo Extraction

It was determined from the indigo extraction optimization that the optimum extraction solvent was 100% DMSO. Extractions were carried out by adding 100 μL of DMSO to the fibers in the vials which were then capped and heated to 100°C for 60 min. After extraction, the extractant was allowed to cool to room temperature and then injected.

Dye samples were analyzed using a diode array detector measuring absorbance from 400-700 nm. The area of the peak on the chromatogram was acquired for each dye using the corresponding maximum wavelength (for Direct Orange 39, Direct Blue 80, and Direct Blue 71 at 420, 571, and 586 nm, respectively), and compared to standard mixtures of dyes to quantify the amount of dye on each fiber.

RESULTS AND DISCUSSION

Extraction optimization for direct dyes

Figure 3.2 displays a three dimensional fitted surface and contour plot for the absorbance of direct dye extracts as a function of solvent conditions. Optimum absorbance is predicted at 51.5% A (water), 20.6% B (pyridine), and 27.9% C (acetone). Because the region around this optimum is relatively flat, this outcome is relatively robust: slight variations in solvent conditions do not diminish significantly the amount of dye extracted. For ease of use, 50% water, 25% pyridine, and 25% acetone was employed for direct dye extractions.

Table 3.5 shows variability of UPLC peak retention and area for extracts of Direct Blue 80 for ten replicate dyed cotton fibers taken from the same 1 cm thread Variability in amounts of dye extracted from single fibers originates from several sources. The Q test

rejected the data from Fiber 4 as an outlier at the 99% level of confidence. The percent relative standard deviation (%RSD) for the fiber extractions, if the datum from Fiber 4 is retained, was 47.4%.; after deleting the outlier, the RSD drops to 35.4%. These results are typical for cotton. Unlike synthetic fibers (e.g., nylon), natural cotton fibers exhibit biological variety and differ in morphology among fibers and even along the length of the same fiber. Physical parameters that may differ include diameter, cross section shape, degree of fiber convolutions, and surface area. Many of these characteristics are affected by the processes to which cotton is subjected prior to dyeing, such as desizing, bleaching, or mercerization. Although mercerization (treatment with sodium hydroxide) commonly makes cotton cross section more rounded and decreases convolutions, process variations may impart variations in fiber shape.[12]

Figure 3.3 shows an optical microscopy photograph of several cotton fibers. Because cotton fiber morphology exhibits variability, dye amounts on an individual fiber can vary significantly from the other 80-100 fibers taken from the same segment of thread. Additionally, fibers on the inside of the thread can also be "shielded" by those on the outside during the dyeing process, also affecting dye uptake.

Extraction optimization for indigo

Design Expert 8 (Statease Corp., Minneapolis, MN) was used for construction of experimental designs and response surface modeling. Figure 3.4 shows the fitted response surface for the indigo extraction optimization study. The calculated model-F value indicated that a linear model best fit the data. According to the model, the optimum extraction solvent mixture is pure DMSO. This result is favorable because mixtures of DMSO, chloroform, and pyridine when heated evolved pungent fumes that smelled

characteristic of hydrogen sulfide. DMSO is also compatible with C18 stationary phase, thus the reconstitution step after dye extraction can be skipped and the extract injected after cooling to room temperature, minimizing potential sample loss during evaporation.

UPLC of dye standards

Separation of the direct dye standards shows that some of the dyes have multiple components. In Figure 3.5, Direct Orange 39 is clearly comprised of two dye components. Many smaller peaks are also obvious in the expanded view of Figure 3.6. These peaks can be attributed to various "dyestuffs" that are added during the dyeing process such as compounds that aid in the dye-uptake by the fibers, finishing agents, and fluorescent brighteners. Indigo did not contain any miscellaneous peaks and its chromatogram is shown in Figure 3.7. UV/visible spectra for the main dye peaks are shown in Table 3.1.

Limit of Detection

The limits of detection and quantification for each dye can be determined from the calibration models by:

$$LOD = 3.3\sigma_b/S$$

$$LOQ = 10\sigma_b/S$$

where σ_b is the standard deviation of the blank and S is the slope of the calibration model. LOD and LOQ values are reported in Table 3.6 using three different methods that differ in how σ_b is estimated. $LOD_1$and LOQ_1 estimate σ_b using the standard deviation of the integrated noise signal across the width of the actual peak. LOD_2 and LOQ_2 estimate σ_b by calculating the standard deviation of the lowest concentration calibrator and requires this concentration to be near the actual LOD to be considered accurate. LOD_3 and LOQ_3

estimate σ_b using the standard deviation of the y-intercept of the calibration line. Variance in the high concentration calibrators will increase the variance of the y-intercept leading LOD_3 to provide a high estimate for LOD and LOQ.

Calibration models had generally good fit with coefficients of determination of 0.9997 for Direct Orange 39 and Direct Blue 71, 0.9946 for Direct Blue 80, and 0.9986 for Indigo. The calibration plot for Direct Blue 80 is shown in Figure 3.8. Detection limits were below 1 ppb for three of the dyes according to LOD_1 due to low and reproducible noise. LOD_2 showed values in the 25-60 ppb range for the direct dyes and 6.07 ppb for Indigo. LOD_2 for Indigo is lower due to the addition of a 500 ppb calibrator not present for the direct dyes. Direct Blue 80 has the lowest LOD_2 value despite having higher LOD_1 and LOD_3 values because it has the lowest detector response of all the dyes, resulting in a lower standard deviation for the lowest calibrator. The LOD_3 values are the highest overall due to the number of high concentration calibrators. Variance in the high concentration region of a calibration model can lead to high variance of the y-intercept. Together, LOD_1, LOD_2, and LOD_3 present a possible range for the true limit of detection to reside. With exception to LOD_3, all calculated detection limits indicate that detection of 2 ng of dye from a 1 mm fiber is possible.

Trace fiber extractions

Direct dyes were extracted and detected from fibers of lengths down to 1 mm. Because of their non-uniform morphology, cotton fibers do not lay flat. Cutting cotton fibers reproducibly to small lengths is difficult. We found that cutting an entire thread to the desired length and then unweaving the fibers from that thread produced many fibers of lengths very close to the desired length. These fibers can then be examined under a

magnifying glass using a ruler and similar length fibers can be selected. As fiber length decreases down to 1 mm, handling of the fibers becomes extremely difficult. It is very important to ensure that the fiber is deposited on the bottom of the inside of the vial, and that extractant covers the entire fiber. Additionally, during the extractant evaporation stage, care must be taken to not let the extractant boil. Otherwise extracted dye will be deposited all over the inside of the vial and lower the amount that is successfully reconstituted.

A batch of three 1 mm fibers that were cut from a thread dyed with Direct Blue 71 were analyzed. Of the three samples, only one was extracted successfully. This was due entirely to the difficulty of handling 1 mm fibers. The chromatogram for the 1 mm fiber extract is shown in Figure 3.9. The dye peak is located at 1.85 min. The RMS signal-to-noise for the dye peak of interest is 118.05. The negative response and sloping baseline is due to the mobile phase gradient response on the UV/visible detector.

Another extraction study was conducted on 5 mm fibers to compare their extraction success to the 1 mm extraction study. Five samples were taken from the same 5 mm thread and similar length fibers were chosen for extraction. Of the five samples, four were extracted successfully and the data is presented in Table 3.7. The %RSD for the four successful 5 mm extractions was 38.73% and is comparable to the 35.42% RSD for the 1 cm reproducibility study.

Indigo was successfully extracted from a 1 mm fiber and detected by UPLC-DAD. A set of five 1 mm indigo-dyed cotton fibers were extracted using DMSO. Because DMSO has such a high boiling point and is compatible with the C18 stationary phase, the boil-off and reconstitute step of the extraction process was skipped, and the extract was injected

directly into the UPLC after cooling to room temperature. The extract chromatogram had a RMS signal-to-noise of 62.80 and is shown in Figure 3.10.

CONCLUSIONS

Solvent conditions were optimized for the extraction of direct and indigo dyes from cotton. UPLC separation methods were also devised that, together with the optimized extraction conditions, was successful in detecting extracts from single 1 mm length fibers with RMS signal-to-noise ratios of 118.05 and 62.80 for Direct Blue 71 and Indigo respectively. Calibration models yielded limits of detection and quantification as low as 2.1pg and 6.2 pg respectively, suggesting the possibility of analyzing sub-millimeter length fibers. Handling fibers of millimeter and sub-millimeter lengths continues to be a challenge and new fiber handling techniques need to be developed. Future work will involve mass spectrometry characterization of the various dye stuffs present in the dye standards as well as characterizing finishing agents from fiber extracts.

ACKNOWLEDGMENTS

Coauthors of this work include Molly R. Burnip, Kaylee R. McDonald, and Stephen L. Morgan (Department of Chemistry and Biochemistry, University of South Carolina, Columbia, SC 29208). Research in this presentation was supported by award 2010-DN-BX-K245 from the National Institute of Justice, Office of Justice Programs, U. S. Department of Justice. The opinions, findings, and conclusions or recommendations expressed in this publication are those of the author(s) and do not necessarily reflect those of the Department of Justice. Mention of commercial products does not imply endorsement on the part of the National Institute of Justice or the University of South Carolina.

References

(1) Robertson, J.; Grieve, M. *Forensic Examination of Fibres*; 2nd ed.; Taylor & Francis: London, 1999.

(2) Rendle, D. F.; Wiggins, K. G. Forensic analysis of textile fibre dyes. *Review of Progress in Coloration and Related Topics* **1995**, *25*, 29–34.

(3) Gaudette, B. D. The forensic aspects of textile fiber examination. Chapter 5 in: *Forensic Science Handbook*, vol. 2, R. Saferstein, Ed.; Prentice Hall: Englewood Cliffs, NJ, 1988.

(4) Macrae, R.; Smalldon, K. The Extraction of Dyestuffs from Single Wool Fibers. *J. Forensic Sci*. **1979**, *24*, 109–116.

(5) Shore, J.; Colourists, S. of D. and *Colorants and Auxiliaries: Colorants*; Society of Dyers and Colourists, 2002.

(6) Laing, D.; Dudley, R.; Hartshorn, A.; Home, J.; Rickard, R.; Bennet, D. The extraction and classification of dyes from cotton and viscose fibres. *Forensic Sci.Int*. **1991**, *50*, 23–35.

(7) Cheng, J.; Wanogho, S. O.; Watson, N. D.; Caddy, B. The extraction and classification of dyes from cotton fibres using different solvent systems. *J. Forensic Sci. Soc*. **1991**, *31*, 31–40.

(8) Meksi, N.; Ben Ticha, M.; Kechida, M.; Mhenni, M. F. Using of ecofriendly α-hydroxycarbonyls as reducing agents to replace sodium dithionite in indigo dyeing processes. *Journal of Cleaner Production* **2012**, *24*, 149–158.

(9) Hunger, K. *Industrial dyes: Chemistry, Properties, Applications*; Wiley-VCH, 2003.

(10) Surowiec, I.; Quye, A.; Trojanowicz, M. Liquid chromatography determination of natural dyes in extracts from historical Scottish textiles excavated from peat bogs. *J. Chromatogr. A* **2006**, *1112*, 209–17.

(11) Michel, R. H.; Lazar, J.; McGovern, P. E. The chemical composition of the indigoid dyes derived from the hypobranchial glandular secretions of Murex molluscs. *Journal of the Society of Dyers and Colourists* **1992**, *108*, 145–150.

(12) Incorporated, C.; Staff, C. I. *Cotton Dyeing and Finishing: A Technical Guide*; Cotton, Incorporated, 1997.

Table 3.1. Structures and spectra of the direct dyes and indigo.

Structure	Absorbance Spectra
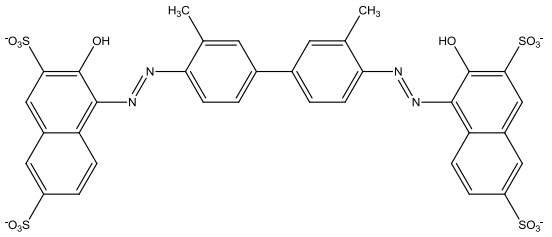 Direct Blue 80	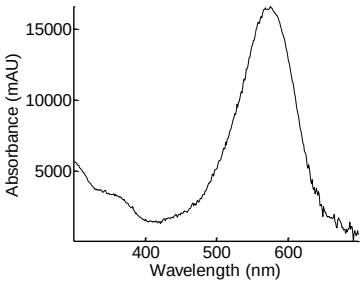
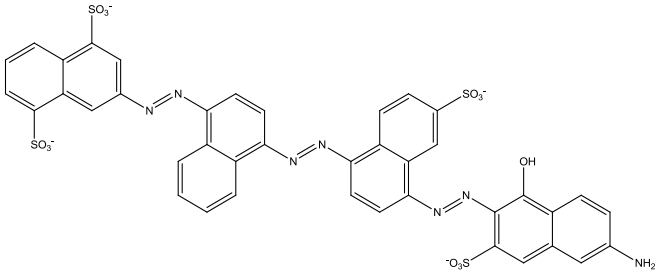 Direct Blue 71	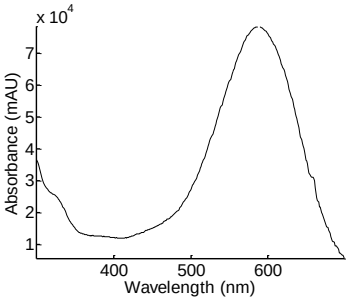
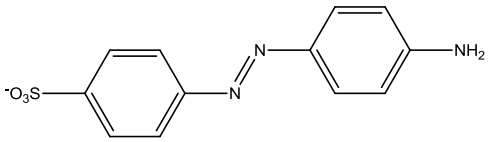 Direct Orange 39	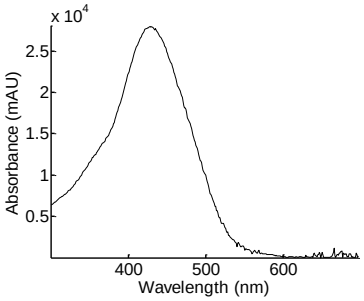
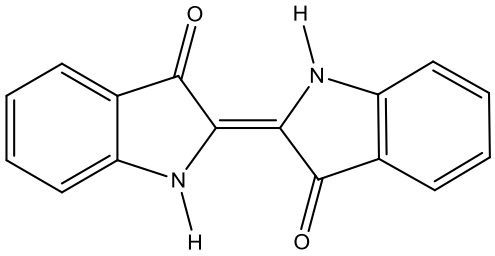 Indigo	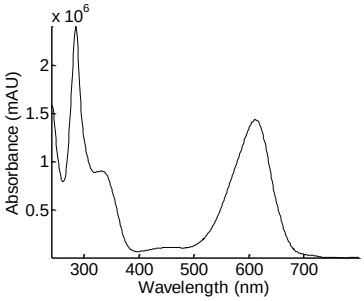

Table 3.2. Solvent compositions for each design point for the extraction optimization for direct-dyed cotton fibers.

Design Point	A: Water (%)	B: Pyridine (%)	C: Acetone (%)
1	100	0	0
2	0	100	0
3	0	0	100
4	50	50	0
5	50	0	50
6	0	50	50
7	33.33	33.33	33.33
8	66.66	16.66	16.66
9	16.66	66.66	16.66
10	16.66	16.66	66.66

Table 3.3. Mobile phase conditions for the analysis of direct dyes by UPLC.

Time (min)	Flow Rate (mL/min)	% Methanol	% 0.2 M Ammonium Acetate	% Acetonitrile
Initial	0.45	5	90	5
5	0.45	5	5	90
6	0.45	5	90	5
8	0.45	5	90	5

Table 3.4. Mobile phase conditions for the analysis of indigo by UPLC.

Time (min)	Flow Rate (mL/min)	% Water (0.15% Formic Acid)	% Methanol
0	0.5	70	30
0.25	0.5	70	30
2	0.5	0	100
3	0.5	0	100
3.1	0.5	70	30
5.5	0.5	70	30

Table 3.5. Peak retention time and area reproducibility for 1 cm fibers dyed with Direct Blue 80.

Fiber	Retention time (min)	Area (counts)
1	1.34	28667.68
2	1.35	14122.29
3	1.34	25609.83
4	1.33	68574.72
5	1.34	34615.79
6	1.34	21941.95
7	1.34	37175.18
8	1.33	49014.68
9	1.34	33480.44
10	1.34	20549.12

Table 3.6. Limits of detection and quantitation of the direct and indigo dyes. Calculations based on the standard deviation of the blanks (LOD/LOQ_1), the standard deviation of the lowest concentration calibrator (LOD/LOQ_2), and the standard deviation of the y-intercept of the calibration plot (LOD/LOQ_3).

Dye	R^2	LOD_1 (ppb)	LOD_2 (ppb)	LOD_3 (ppb)	LOQ_1 (ppb)	LOQ_2 (ppb)	LOQ_3 (ppb)
Direct Blue 80	0.9946	1.39	26.3	166	4.21	79.7	503.03
Direct Orange 39	0.9997	0.83	59.3	39.6	2.5	179.7	120
Direct Blue 71	0.9997	0.21	44.2	39.5	0.63	133.94	119.7
Indigo	0.9986	0.74	6.07	79.9	2.23	18.39	242.12

Table 3.7. Peak areas for four 5 mm fiber extracts for Direct Blue 71.

Fiber	Peak Area
1	19319.44
2	25204.23
3	28823.84
4	10275.35
%RSD	38.73

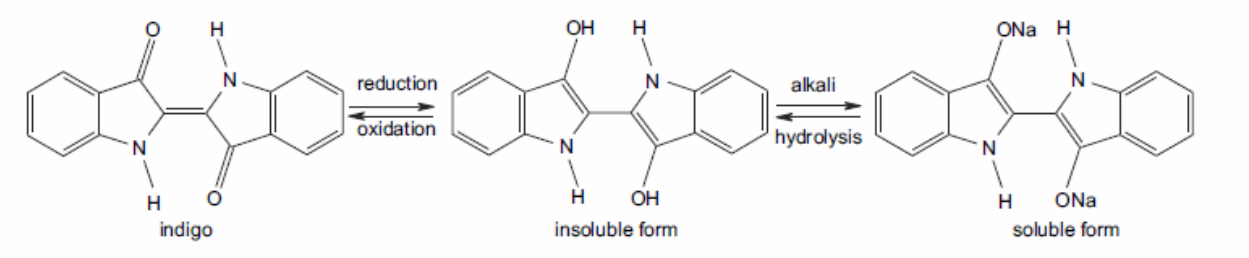

Figure 3.1. Reduction of indigo to its water-soluble leuco form.

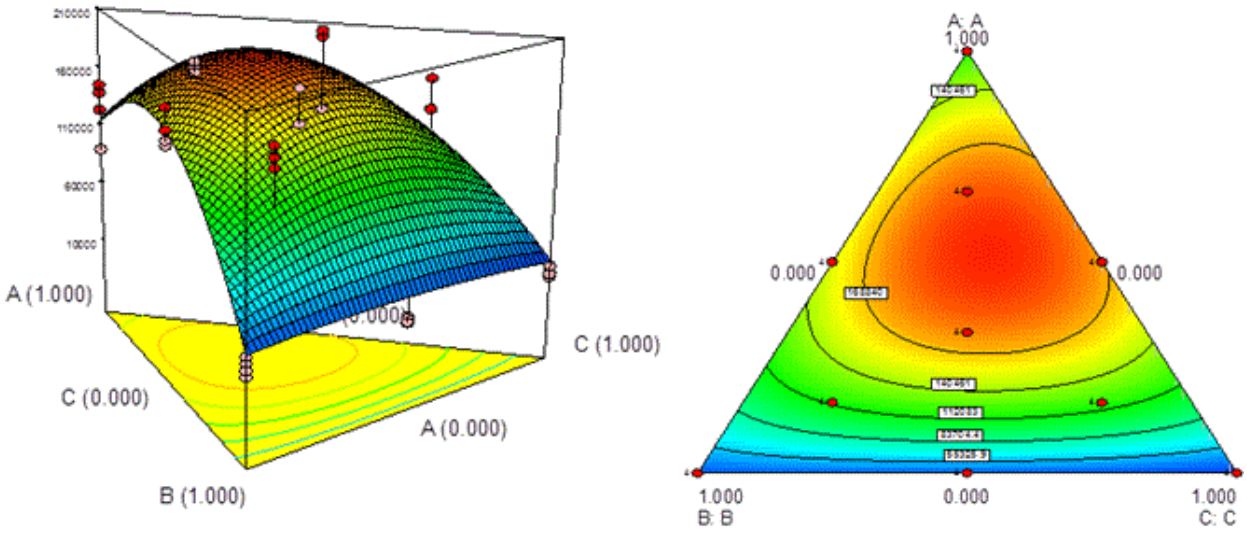

Figure 3.2. Perspective view (left) and contour plot (right) of fitted absorbance response surface for direct dye extraction as a function of solvent conditions. Design points from Table 3.2 are indicated by solid dots. A, Water; B, Pyridine; C, Acetone.

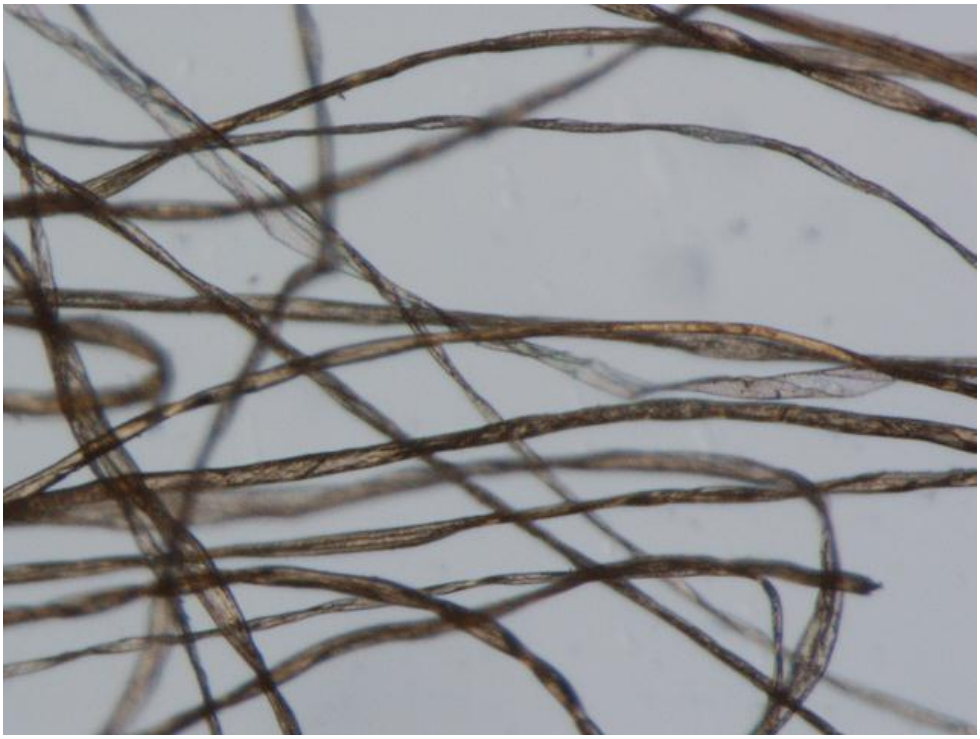

Figure 3.3. Optical microscope image (magnification12.5×) of cotton fibers dyed with Direct Orange 39.

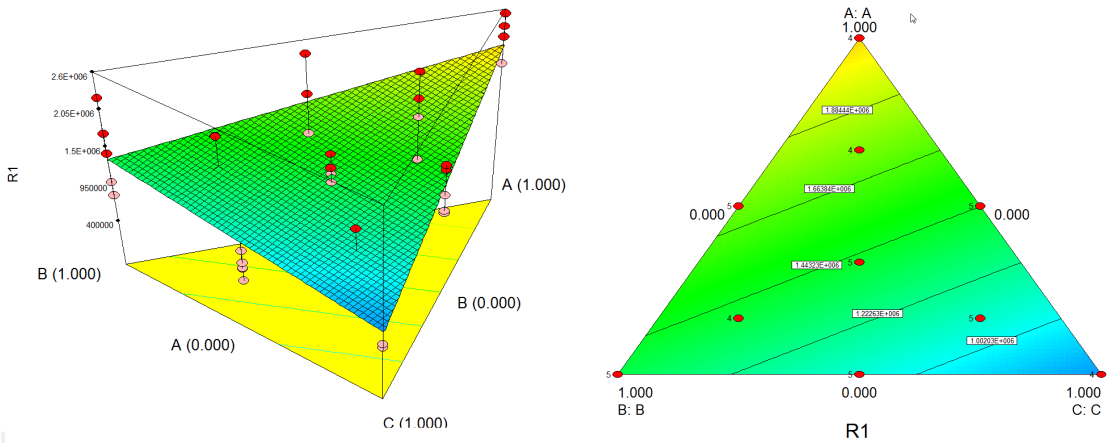

Figure 3.4. Fitted linear absorbance response surface for Indigo extraction as a function of solvent conditions Design points follow those from Table 4.2 and are indicated by solid dots. A, DMSO; B, Chloroform; C, Pyridine.

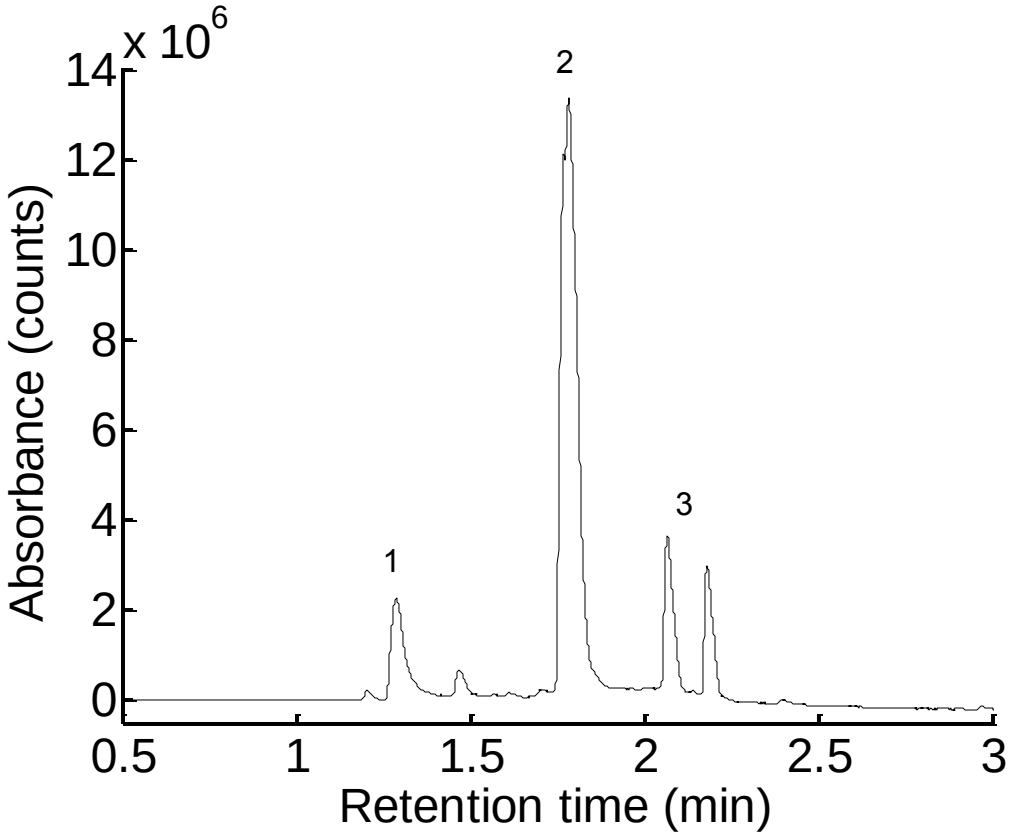

Figure 3.5. Chromatogram showing the separation of all three direct dyes. Some dyes have multiple components. Peak 1 is Direct Blue 80, peak 2 is Direct Blue 71, and peak 3 is Direct Orange 39.

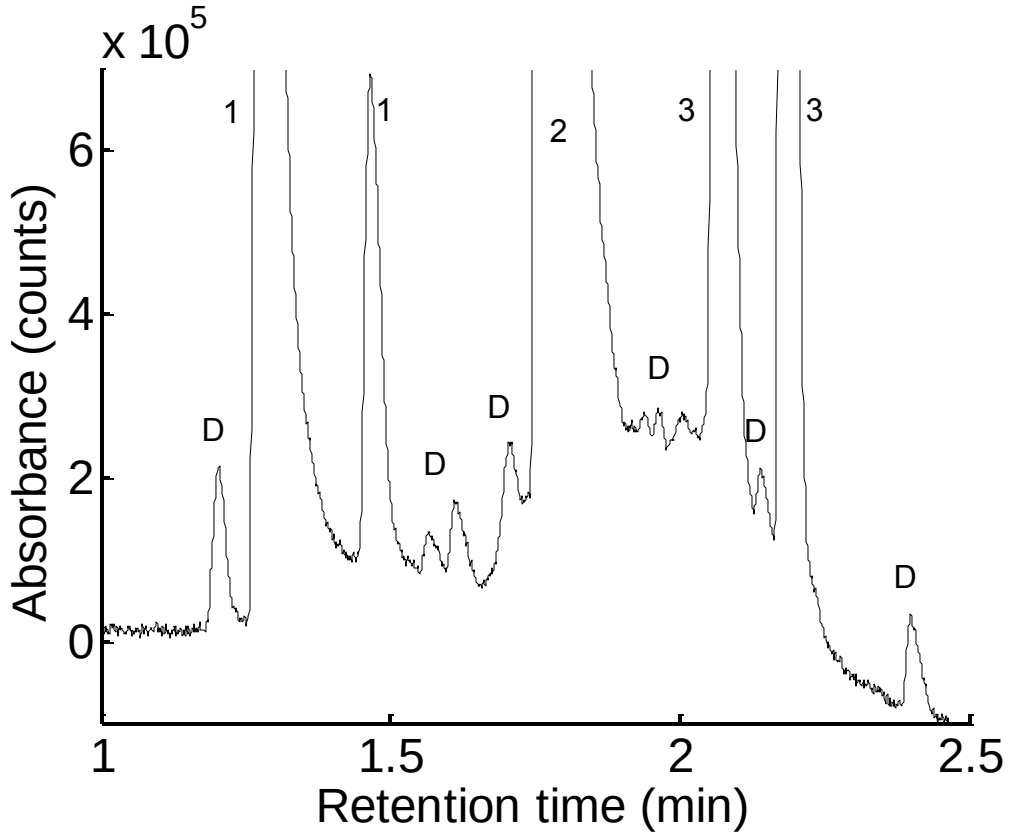

Figure 3.6. Multiple direct dye component in the chromatographic region of 1 to 2,5 min from Figure 3.5. Peak 1 is Direct Blue 80, peak 2 is Direct Blue 71, peak 3 is Direct Orange 39, and peaks labeled "D" are miscellaneous dye stuff.

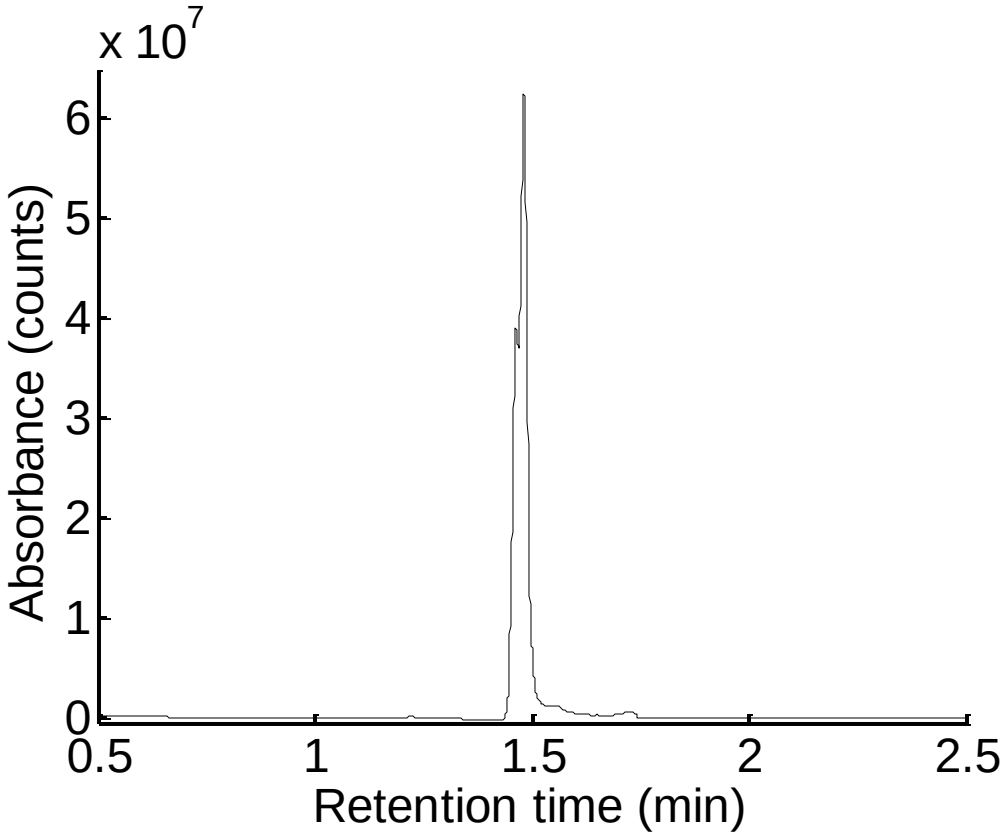

Figure 3.7. UPLC-DAD chromatogram of Indigo.

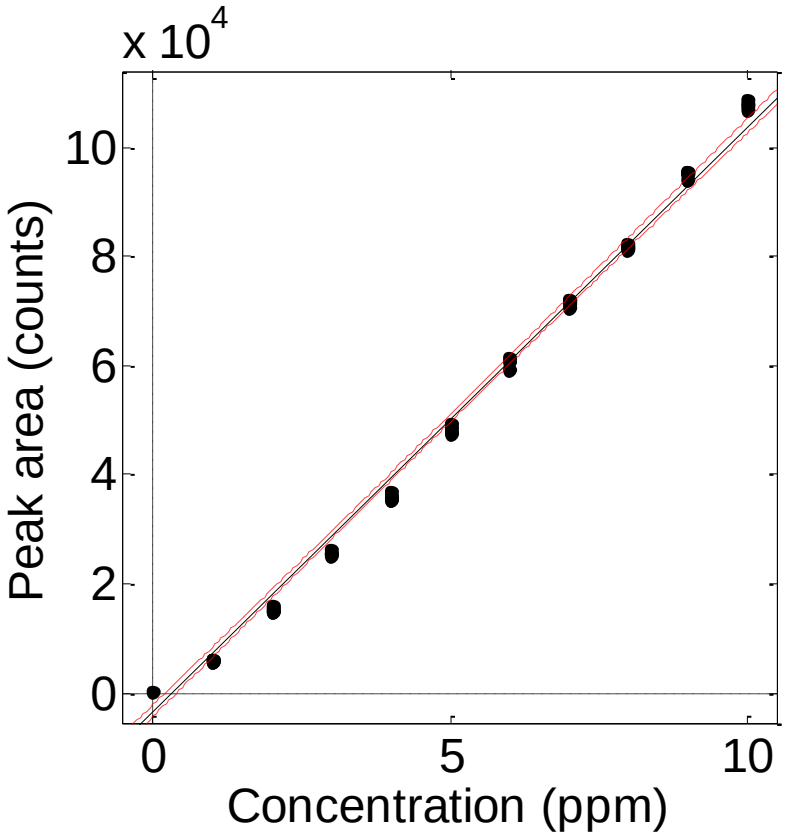

Figure 3.8. Calibration relationship for Direct Blue 80.

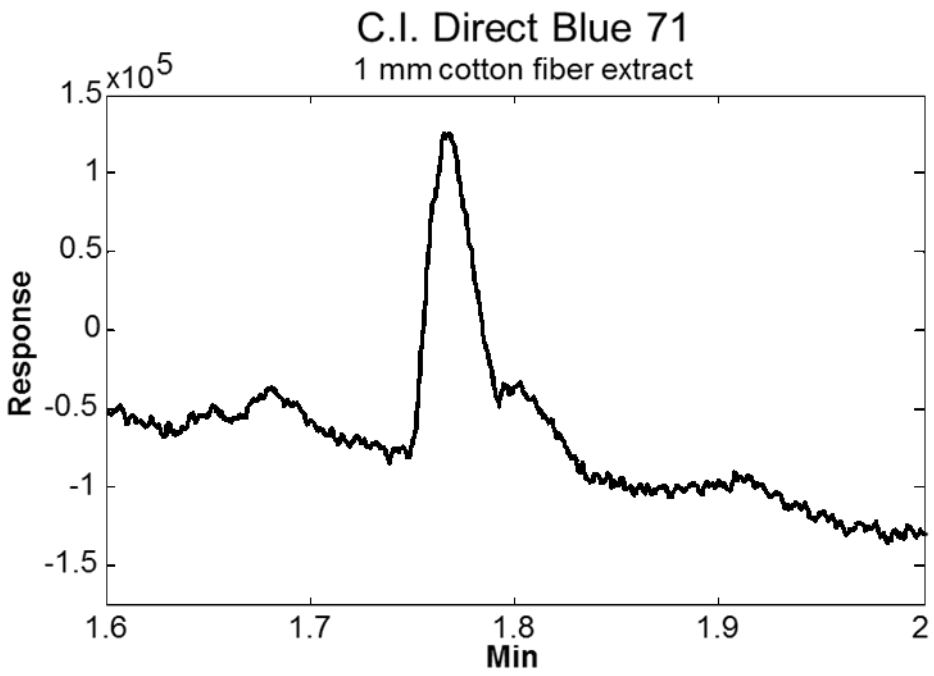

Figure 3.9. Chromatogram of 1 mm Direct Blue 71 dye peak from 1.6-2 min.

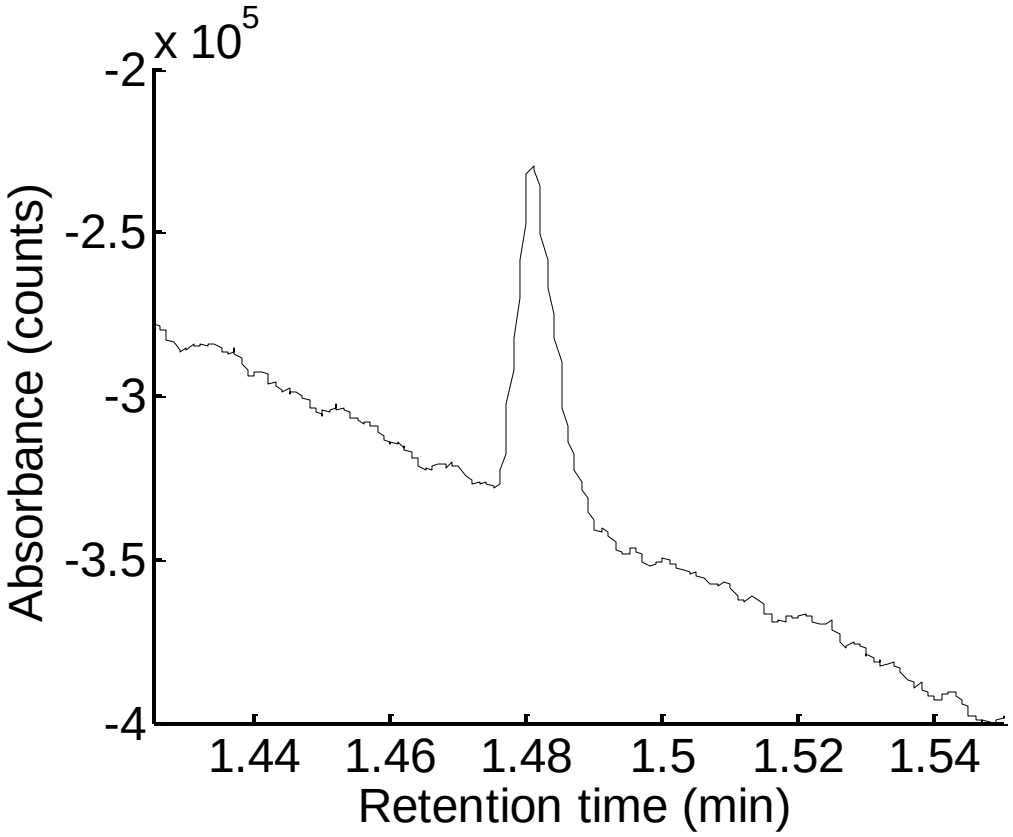

Figure 3.10. Chromatogram of the extraction of Indigo from a 1 mm cotton fiber.

CHAPTER FOUR

EXTRACTION AND CHARACTERIZATION OF REACTIVE DYES AND THEIR HYDROLYSIS PRODUCTS FROM TRACE COTTON FIBERS BY ULTRA-PERFORMANCE LIQUID CHROMATOGRAPHY

ABSTRACT

Microextraction and ultra-performance liquid chromatography methods have been developed for reactive dyes on cotton. Reactive dyes are chemically bound to the cellulose structure of the fiber and present an analytical challenge to the forensic fiber examiner because release of these dyes requires breaking of the covalent bond using hot sodium hydroxide. The resulting hydrolysis reactions can also cleave amide bonds and possibly other chemical bonds in the dye molecule. The various structural changes that can take place leads, in many cases, to production of multiple reaction products from a single dye molecule. We demonstrate successful extraction of reactive dyes from single 1 mm cotton fibers with detection limits as low as 3.3 pg. Systematic experiments at varying reaction conditions, with product analysis by mass spectrometry, were also performed to characterize the degradation of reactive dyes under hydrolysis, and to facilitate interpretation of reactive dye extractions.

INTRODUCTION

Cotton fibers are unique in the textile industry because they can be dyed with three different classes of dyes: direct, vat, and reactive. Reactive dyes differ from most other dye classes in that they are covalently bound to the fiber. This makes reactive dyes the most substantive of dyes used on cotton because the covalent bonding of the dye to the fiber provides excellent fastness to laundering. As a result, reactive dyes are the most popular dye class used to color cotton textiles. Figure 4.1 summarizes worldwide consumption of cotton dyes in 2003, showing that reactive dyes constitute 50% of all dyes on cotton textiles.[1]

The reactive dyeing process typically involves the reaction of a haloheterocycle such as a chlorotriazine on the dye with a hydroxyl group on the fiber.[2,3] Reactive dyes can also attach to cotton via vinylsulphone groups that form activated alkenes when treated with sodium hydroxide, as shown in Figure 4.2. The extraction of reactive dyes from cotton requires the hydrolysis of the covalent bond using sodium hydroxide at elevated temperatures via the mechanism shown in Figure 3.[5]

This study focuses on the extraction of reactive dyes from cotton followed by separation and detection using ultra-performance liquid chromatography (UPLC). This chemical extraction process is destructive to the fiber and the dyes itself because sodium hydroxide and heat are used to break the covalent fiber-dye bond. Our research hypothesis is that, despite chemical degradation of the original dye to various products, separation of the resulting product mixture and (ultimately, identification of components by mass spectrometry) can provide forensic profiling to discriminate reactive dyes from one another. Improved understanding of reactive dye degradation can also assist interpretation of extracted components and potentially enable identification of the parent reactive dye. Trace evidence fibers can often be as short as 10 mm and contain between 2-200 ng of dye.[6] Emphasis will be placed on optimizing extraction and UPLC conditions to facilitate extracting from 1 mm fibers.

EXPERIMENTAL

Analytical grade water, sodium hydroxide, ammonium acetate, ammonium hydroxide, and HPLC/UPLC grade acetonitrile were purchased from Fisher Scientific (Pittsburg, PA).

Dyed fabrics and matching dyes standards were current production samples donated by dyestuff manufacturers in the southeastern United States. Dye names reported here follow the Color Index nomenclature (Society of Dyers and Colourists, Bradford, UK). All fibers were dyed at levels consistent with commercial use (2–4% by weight). All dye standards were solid in phase and stored in a dark room to avoid photodegradation.

Literature has suggested that 1.5% NaOH and heat should be used to facilitate the extraction of reactive dyes from cotton.[6-9] Previous reactive dye extraction work in our laboratory has also employed these conditions.[2] Hydrolysis presents a number of potential issues. The dye to be extracted may change its chemical form under hydrolysis conditions. Strongly alkaline solutions are also not compatible with many stationary phases for liquid chromatography. In the present work, reactive dye standards were treated with 1.5% sodium hydroxide and heated at 100 °C for 60 min. The resulting solution was then treated with equimolar hydrochloric acid to neutralize any excess sodium hydroxide remaining prior to liquid chromatography.

Fibers of lengths 10 mm, 5 mm, and 1 mm dyed with Reactive Yellow 160, Reactive Blue 220, or Reactive Orange 72 (structures shown in Table 4.1) were cut with a fiber guillotine (as described in chapter 2) and placed into 200 µL conical Total Recovery Vials. A 50 µL aliquot of 0.1875 M sodium hydroxide was dispensed into the vial and sealed to prevent evaporation. Extraction was carried out in the laboratory oven at 100°C for 60 min. The dyes were reconstituted by addition in sequence of 25 µL of 0.375 M hydrochloric acid (equimolar with the sodium hydroxide), 25 µL of 10 mM ammonium acetate adjusted to pH 9.3. Dyes were separated using a Waters Acquity UPLC system coupled to a diode array detector (DAD). The system was equipped with a room

temperature sample manager and a Waters Acquity BEH C18 column (1.7 um particle size, 2.1 mm ID × 50 mm length) heated to 40 °C. The mobile phase solvent gradient conditions employed for all runs is listed in Table 4.2. The sample injection volumes were 10 μL.

Dyes samples were detected using a UV/visible diode array detector scanning absorbance from 300-700 nm. The peak area on the chromatogram was acquired for each dye using the corresponding maximum wavelength (for Reactive Yellow 160, Reactive Blue 220, and Reactive Orange 72 at 405 nm, 610 nm, and 478 nm, respectively), and was used for comparison to standard dye mixtures to determine the amount of dye on each fiber.

Limits of detection and quantitation were determined from calibration models based on the UPLC-DAD analysis of reactive dye standards at varying concentrations. Calibration solutions were made for each dye in water at concentrations 100 ppb, 200 ppb, 400 ppb, 600 ppb, 800 ppb, and 1000 ppb. Five replicates samples were prepared at each concentration level and analyzed by UPLC-DAD.

RESULTS AND DISCUSSION

A chromatogram showing the separation of the mixture of three reactive dyes is shown in Figure 4.4. Figure 4.5 shows a magnified view of the retention time window for 0.75 to 2.75 min within which multiple additional components are present. As indicated, most of these peaks have UV/visible absorbance spectra that match those of the one of three primary reactive dyes. We initially assumed that these peaks are secondary degradation products derived from the corresponding primary dyes, or represent other contaminants introduced during the dye manufacturing process. UV/visible absorbance

spectra of the main dye peaks are shown in Table 4.1. During method development, the first eluting peak, Reactive Blue 220, displayed poor chromatographic peak shape and lower peak height than the other dyes. The addition of 10 mm ammonium acetate adjusted to pH 9.3 resulted in sharpening this peak.

UPLC-DAD analysis of extracted reactive dyes

UPLC-DAD analysis of reactive dyes treated with 1.5% NaOH confirmed that additional reactions occur during the extraction process. Figure 4.6 shows the chromatograms for Reactive Orange 72 standard and "extracted" (treated with NaOH). The standard chromatogram shows a single peak corresponding to the dye with an absorbance maximum of 478 nm. The extracted chromatogram shows two peaks, both of which increased in retention, and the main peak having an absorbance maximum of 473 nm. Because the second peak showed a similar absorbance maximum, we hypothesized that both peaks were "dye" and that one of the peaks was due to the incomplete base-hydrolysis of the dye standard.

To test this hypothesis, a nominal starting ratio of NaOH to dye was first established. Assuming that a single 1 cm cotton fiber contained 20 ng of dye, using 50 μL of 1.5% NaOH to extract the dye from the fiber gives a ratio of 9.375×10^{-7} moles of NaOH to 1 ng of dye. For the purposes of later comparisons, other ratios were expressed as a percentage of this value. Several 1 ppm standards of Reactive Orange 72 were then treated with amounts of NaOH varying 10%-150% of that amount, neutralized with equimolar HCl, and analyzed by UPLC-DAD. Figure 4.7 displays the dependence of the resulting peak areas peaks on NaOH amount. Approximately 50% of the nominal amount of NaOH is required to completely hydrolyze the dye molecule. Due to the variability of

the amount of dye on cotton fibers, 75% of the nominal amount was selected as a compromise between ensuring complete extraction and hydrolysis of the dye and maintaining a low amount of NaOH in solution. Thus, a 1 cm length of a single cotton fiber requires 50 µL of 0.28125 M NaOH for the extraction of a reactive dyes. The amount of NaOH can then be adjusted depending on the length of the cotton fiber of interest.

HPLC-MS of reactive dyes

HPLC-MS confirms that reactive dyes undergo additional reactions during NaOH extraction from cotton. Both C. I. Reactive Orange 72 and Reactive Yellow 160 were analyzed using negative-ion electrospray ionization (ESI-) mass spectrometry. C. I. Reactive Blue 220 did not did not appear in HPLC-MS due to the requirements of using an acidic buffer for the MS analysis (basic buffer is required to maintain a proper chromatographic peak shape for Reactive Blue 220).

Analysis of the C. I. Reactive Yellow 160 standard by HPLC-MS shows at least four derivatives of the dye molecule (Figure 4.8)**.** The molecular mass of Reactive Yellow 160 is 653 g/mol and elutes at a retention time of 16.61 min with a characteristic ion of m/z 652 due to deprotonation of the dye in solution. Derivatives of this molecule appearing at m/z 572 and 554 are probably due to the loss of a sulfonic acid and a sulfate functional group, respectively. The longer retention time for these products can be attributed to the decrease in their mobile phase solubility on losing these functional groups, and their increased affinity for the non-polar C_{18} stationary phase. Additional fragments of mass m/z 572 m/z and 554 appear in the mass spectra of Reactive Yellow 160 peak at 16.61 min. The structure of the component of m/z 614 is unknown, however it has an almost

identical absorbance spectra to that of the dye molecule and its other derivatives (Figure 4.9), suggesting that it also is a derivative of the dye.

Treatment of Reactive Yellow 160 dye standard with NaOH to simulate the extraction conditions yielded two products observable by HPLC-MS (ESI-), as shown in Figure 4.10. The combination of NaOH and heat (100°C) hydrolyzes the amide bond and removes the sulfate group, as seen in the second product at 18.66 min. This compound fragments further with the cleavage of the azo group. Because this compound is a beta-keto acid, it undergoes decarboxylation under basic conditions and heat, with loss of carbon dioxide, resulting in the product eluting at 15.07 min.

Analysis of the Reactive Orange 72 dye standard by HPLC-MS also shows multiple derivatives of the dye. The total ion chromatogram shows only a single chromatographic peak with a mass spectrum containing a spectral peak at 474 m/z, as seen in Figure 4.11. This result is unexpected because the reported mass for Reactive Orange 72 is 572 g/mol. Isolation of 572 m/z from the chromatogram yields a broad chromatographic peak, and the combined spectra for this peak shows what appears at first glance to be a fragmentation pattern for the dye molecule. However, ESI should not yield much, if any, fragmentation as it is a “soft” ionization technique. Extraction of the prominent masses 572 m/z, 492 m/z, 474 m/z, and 417 m/z from the TIC yields four separated chromatographic peaks, shown in Figure 4.12, suggesting that our Reactive Orange 72 dye standard is actually a mixture of multiple compounds. The combination of this result for Reactive Orange 72with the multiple derivatives of Reactive Yellow 160 suggests mixtures of multiple compounds may be common for all reactive dyes.

Reactive Orange 72 was also treated with NaOH to simulate an extraction. The resulting chromatogram, shown in Figure 4.13, as expected only contained one peak of interest. Unlike Reactive Yellow 160, Reactive Orange 72 has an "external" amide bond which upon hydrolysis leaves the bulk of the dye molecule unchanged.

Limits of Detection

The limits of detection and quantification for each dye can be determined from the calibration models by:

$$LOD = 3.3\sigma_b/S$$

$$LOQ = 10\sigma_b/S$$

where σ_b is the standard deviation of the blank and S is the slope of the calibration model. LOD and LOQ values are reported in Table 4.6 using three different methods that differ in how σ_b is estimated. $LOD_1$and LOQ_1 estimate σ_b using the standard deviation of the integrated noise signal across the width of the actual peak. LOD_2 and LOQ_2 estimate σ_b by calculating the standard deviation of the lowest concentration calibrator and requires this concentration to be near the actual LOD to be considered accurate. LOD_3 and LOQ_3 estimate σ_b using the standard deviation of the y-intercept of the calibration line. Variance in the high concentration calibrators will increase the variance of the y-intercept leading LOD_3 to provide a high estimate for LOD and LOQ.

The calibration models produced high coefficients of determination of 0.9987 for Reactive Yellow 160, 0.9989 for Reactive Blue 220, and 0.9993 for Reactive Orange 72. All three LOD estimates yield detection limits in the 3 pg to 83 pg range (based 10 μL injections) which is low enough to detect extracts from 1 mm fibers. LOQ values range

from 10 pg and 252 pg and suggests the possibility of conducting quantitative comparisons between 1 mm fiber extracts.

Trace fiber extractions

All three reactive dyes were extracted and detected from fibers of lengths down to 1 mm. Because of their non-uniform morphology, cotton fibers do not lay flat. Cutting cotton fibers reproducibly to small lengths is difficult. As fiber length decreases down to 1 mm, handling of the fibers becomes extremely difficult. The reactive extractions showed the same amount of variance in the amount extracted from equal length fibers from the same thread. This variance is explained by the biological nature of cotton which produces fibers of different diameters and shapes capable of containing different amounts of dye. Analysis of this variability was conducted in Chapter 3. Figure 4.17 shows successful extraction and detection of a 10 mm, 5 mm, and 1 mm cotton fiber dyed with Reactive Yellow 160. Close inspection of the 1 mm extraction chromatogram suggests that 1 mm fibers dyed with Reactive Yellow 160 are near the fiber length limit of this method. The calibration model for Reactive Yellow 160 returns concentrations of 135 ppb, 35 ppb, and 12 ppb for the 10 mm, 5 mm, and 1 mm extractions respectively. Comparing these values to those in Table 4.3 confirms that the 1 mm extract of Reactive Yellow 160 is detected and is arguably quantifiable.

CONCLUSIONS

Methods for the extraction of reactive dyes from cotton using sodium hydroxide have been reported. Extraction using hot sodium hydroxide results in hydrolysis of the dye-cellulose bond as well as hydrolysis of the amide bonds in the dye molecule. The reported UPLC-DAD method gave detection limits as low as 0.33-1.42 ppb and quantitation limits

as low as 1.00-4.30 ppb, and detection and quantification of 1-10 mm extracts of Reactive Yellow 160 were confirmed. Future work on this project will require the construction of calibration models based on the simulated extraction of the dye standards by addition of sodium hydroxide and heat. Additional extractions are also needed to solidify the validity of the method.

ACKNOWLEDGMENTS

Coauthors of this work include Molly R. Burnip and Stephen L. Morgan (Department of Chemistry and Biochemistry, University of South Carolina, Columbia, SC 29208). Research in this presentation was supported by award 2010-DN-BX-K245 from the National Institute of Justice, Office of Justice Programs, U. S. Department of Justice. The opinions, findings, and conclusions or recommendations expressed in this publication are those of the author(s) and do not necessarily reflect those of the Department of Justice. Mention of commercial products does not imply endorsement on the part of the National Institute of Justice or the University of South Carolina.

REFERENCES

(1) Bozic, M.; Kokol, V. Ecological alternatives to the reduction and oxidation processes in dyeing with vat and sulphur dyes. *Dyes and Pigments*, **2008**, *76*, 299-309.

(2) Dockery, C. R.; Stefan, a R.; Nieuwland, a a; Roberson, S. N.; Baguley, B. M.; Hendrix, J. E.; Morgan, S. L. Automated extraction of direct, reactive, and vat dyes from cellulosic fibers for forensic analysis by capillary electrophoresis. *Anal. Bioanal. Chem* **2009**, *394*, 2095–103.

(3) Christie, R. *Colour Chemistry*. RSC Paperbacks: Cambridge, England, 2001.

(4) Christie, R. *Colour Chemistry*. RSC Paperbacks: Cambridge, England, 2001.

(5) Shore, J. *Colorants and Auxiliaries*, vol. 1, 2nd edition. Society of Dyers and Colourists, West Yorkshire: England, 2002; pp. 18–23.

(6) Gaudette, B. D. The forensic aspects of textile fiber examination. Chapter 5 in: *Forensic Science Handbook*, vol. 2, R. Saferstein, Ed.; Prentice Hall: Englewood Cliffs, NJ, 1988.

(7) Home, J.; Dudley, R. Thin-layer chromatography of dyes extracted from cellulosic fibres. *Forensic Sci.Int*. **1981**, *17*, 71–78.

(8) Sirén, H.; Sulkava, R. Determination of black dyes from cotton and wool fibers by capillary zone electrophoresis with UV detection: application of marker technique. J. Chromatogr. A **1995**, 717, 149-155.

(9) Xu, X.; Leijenhorst, H.; Van den Hoven, P.; De Koeijer, J.A.; Logtenberg, H. Analysis of single textile fibres by sample-induced isotachophoresis-micellar electrokinetic capillary chromatography. *Sci. Justice* **2001**, *41*, 93-105.

Table 4.1. Structures and absorbance spectra for the reactive dyes.

Structure	Absorbance Spectrum
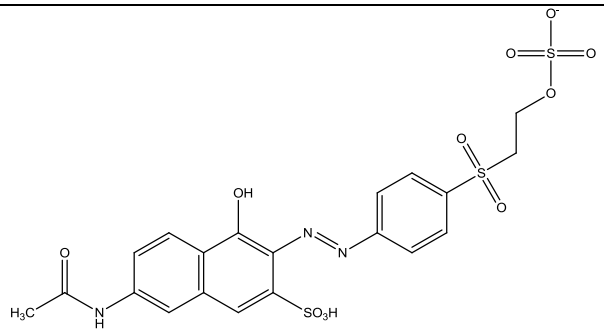 Reactive Orange 72	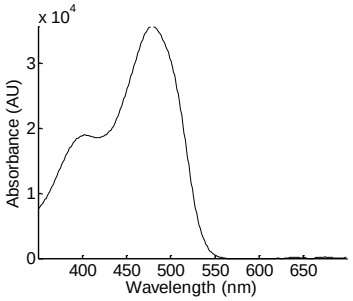
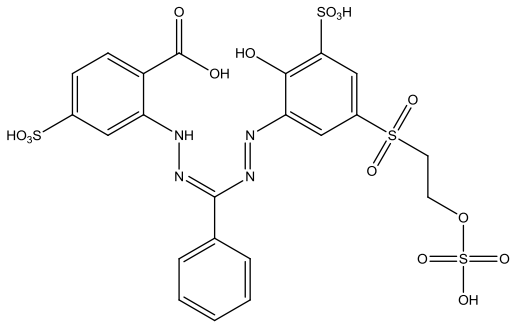 Reactive Blue 220	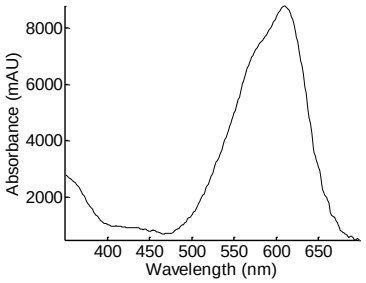
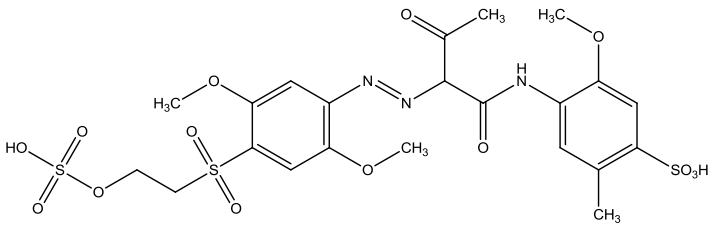 Reactive Yellow 160	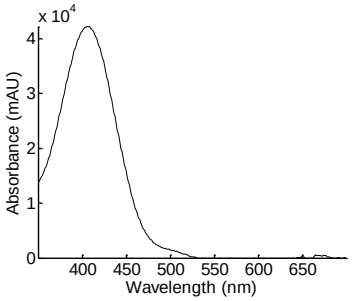

Table 4.2. Mobile phase conditions for the analysis of reactive dyes by UPLC.

Time (min)	Flow rate (mL/min)	% 10 mM Ammonium acetate (pH 9.3)	% Acetonitrile
Initial	0.400	95	5
2	0.400	50	50
3	0.400	95	5
5	0.400	95	5

Table 4.3. Limits of detection and quantitation of the reactive dyes. Calculated based on the standard deviation of the blanks (LOD/LOQ_1), the standard deviation of the lowest concentration calibrator (LOD/LOQ_2), and the standard deviation of the y-intercept of the calibration plot (LOD/LOQ_3).

Dye	R^2	LOD_1 (ppb)	LOD_2 (ppb)	LOD_3 (ppb)	LOQ_1 (ppb)	LOQ_2 (ppb)	LOQ_3 (ppb)
Reactive Yellow 160	0.9987	0.33	2.68	8.31	1.00	8.12	25.18
Reactive Blue 220	0.9989	1.42	6.81	8.09	4.30	20.64	24.52
Reactive Orange 72	0.9993	1.05	1.50	6.31	3.18	4.55	19.12

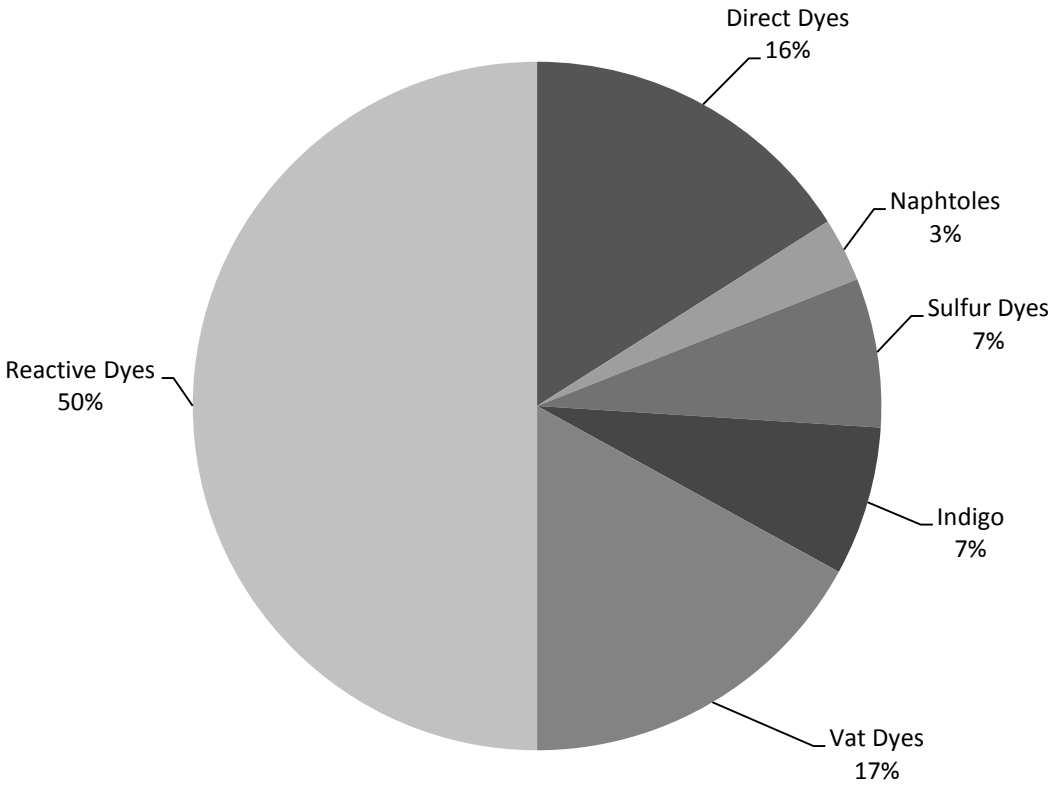

Figure 4.1. Worldwide consumption of cotton dyes.

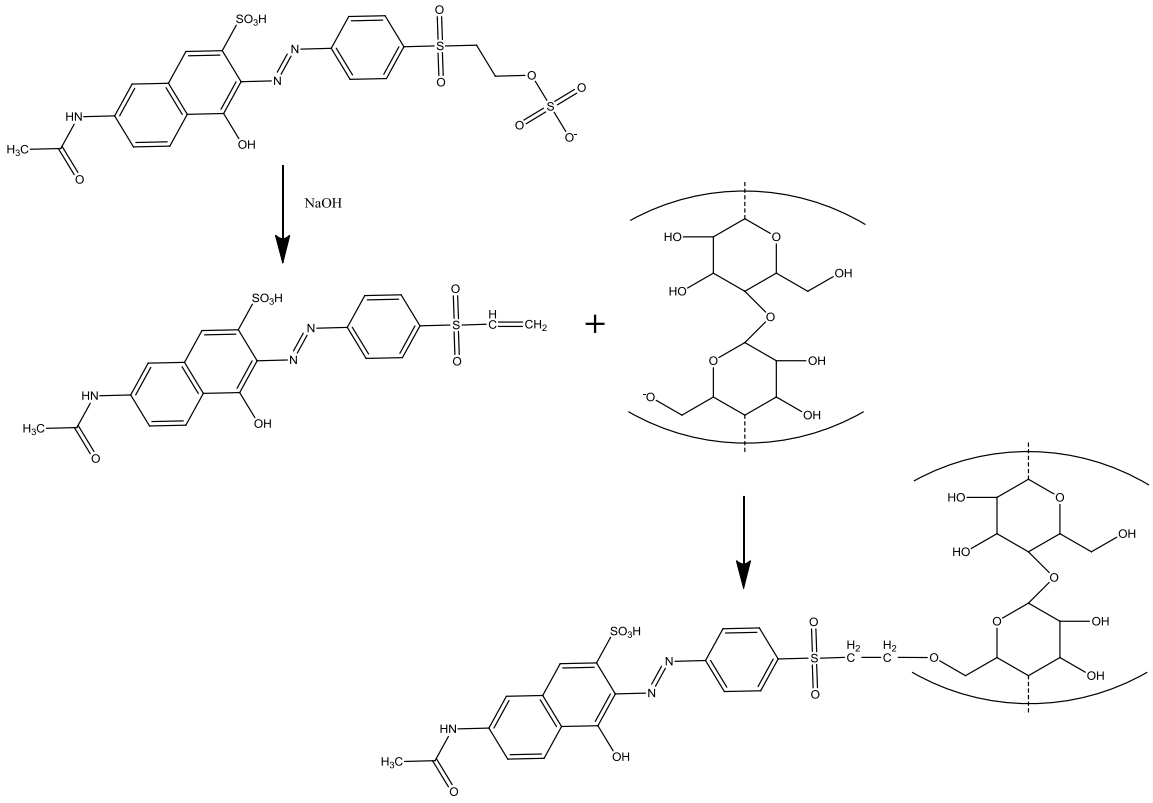

Figure 4.2. Mechanism for the dyeing of cellulose by Reactive Orange 72.[5]

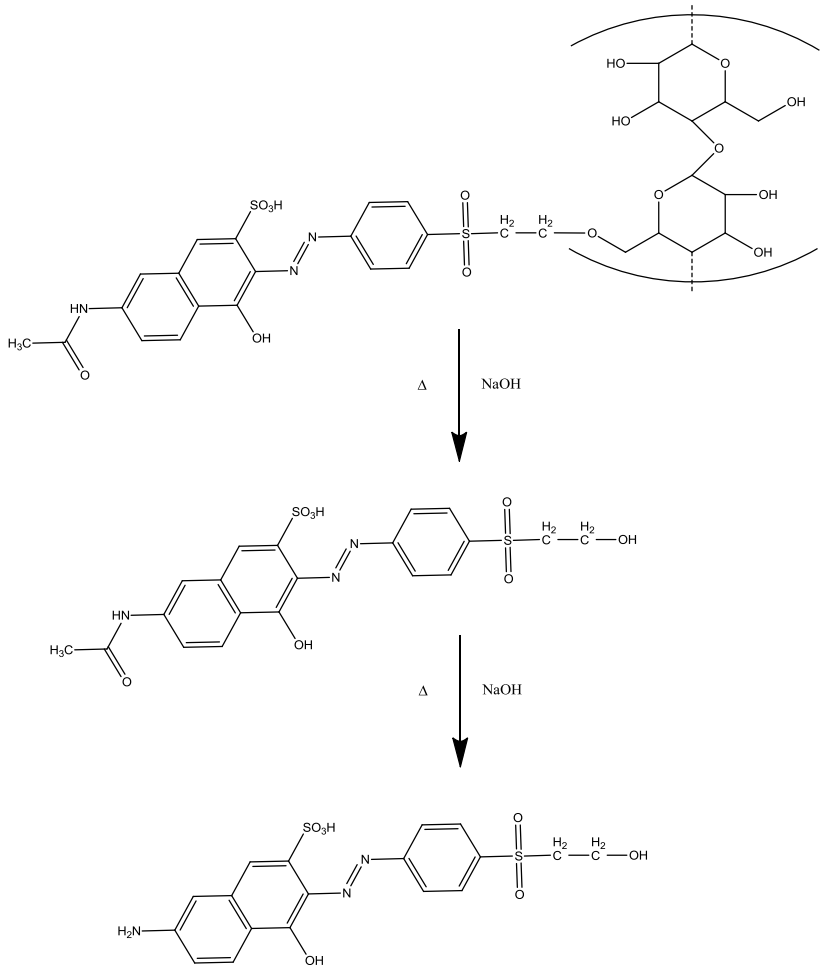

Figure 4.3. Mechanism showing the extraction of Reactive Orange 72 from cellulose, and further dye hydrolysis due to excess NaOH.

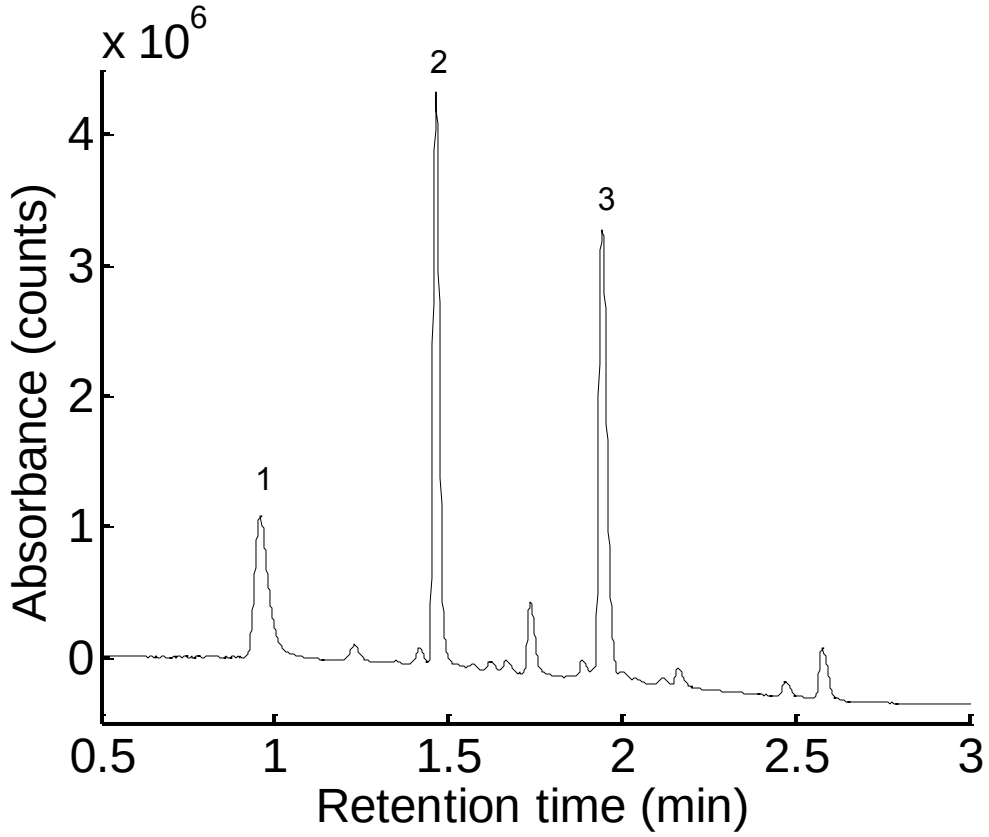

Figure 4.4. Chromatogram showing the separation of all three reactive dyes. Some dyes have multiple components. Peak 1 is Reactive Blue 220, peak 2 is Reactive Orange 72, and peak 3 is Reactive Yellow 160.

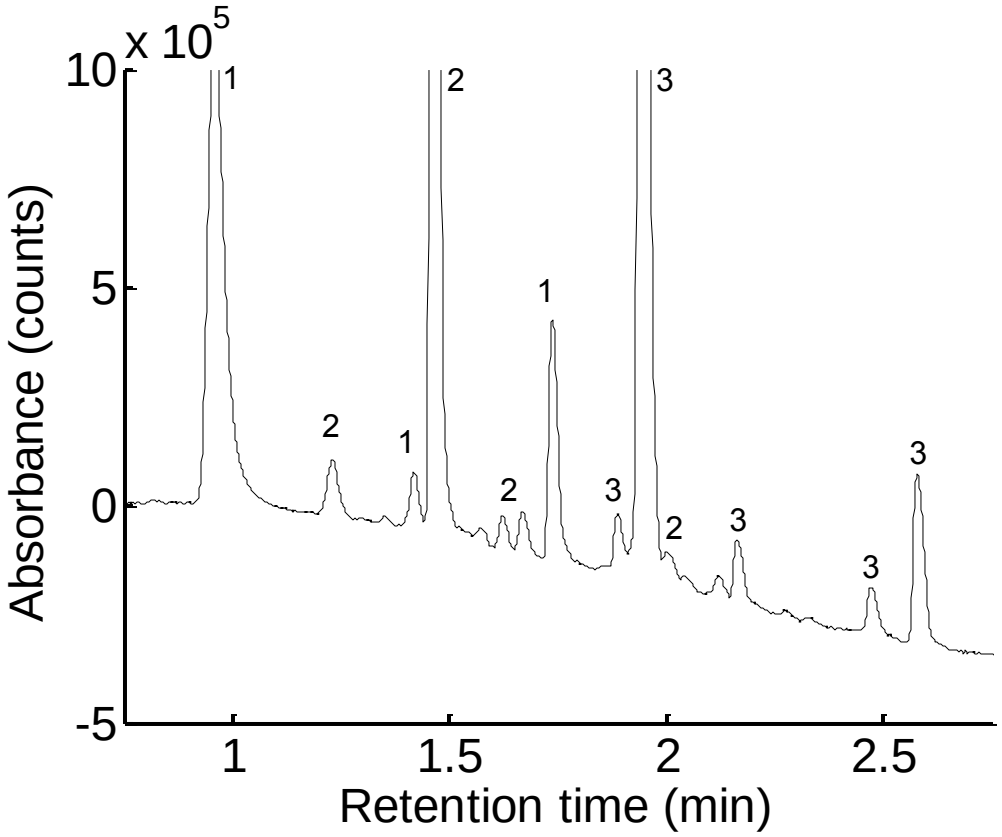

Figure 4.5. Multiple reactive dye components in the chromatographic region of 0.8 to 2.6 min from Figure 4. Peaks labeled with a 1 are Reactive Blue 220, peaks labeled with a 2 are Reactive Orange 72, and peaks labeled with a 3 are Reactive Yellow 160.

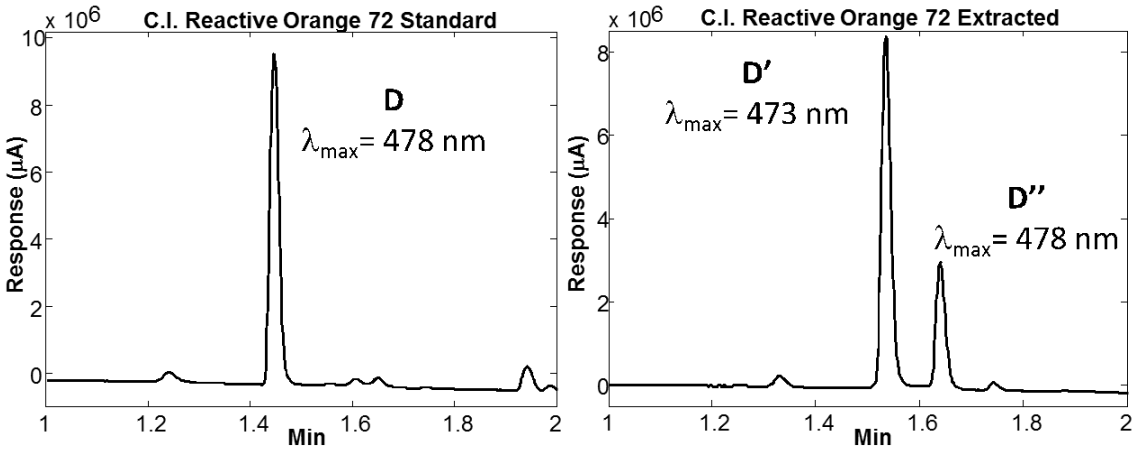

Figure 4.6. (Left) UPLC chromatograms for Reactive Orange 72 standard and (right) extracted (standard treated with NaOH and heat).

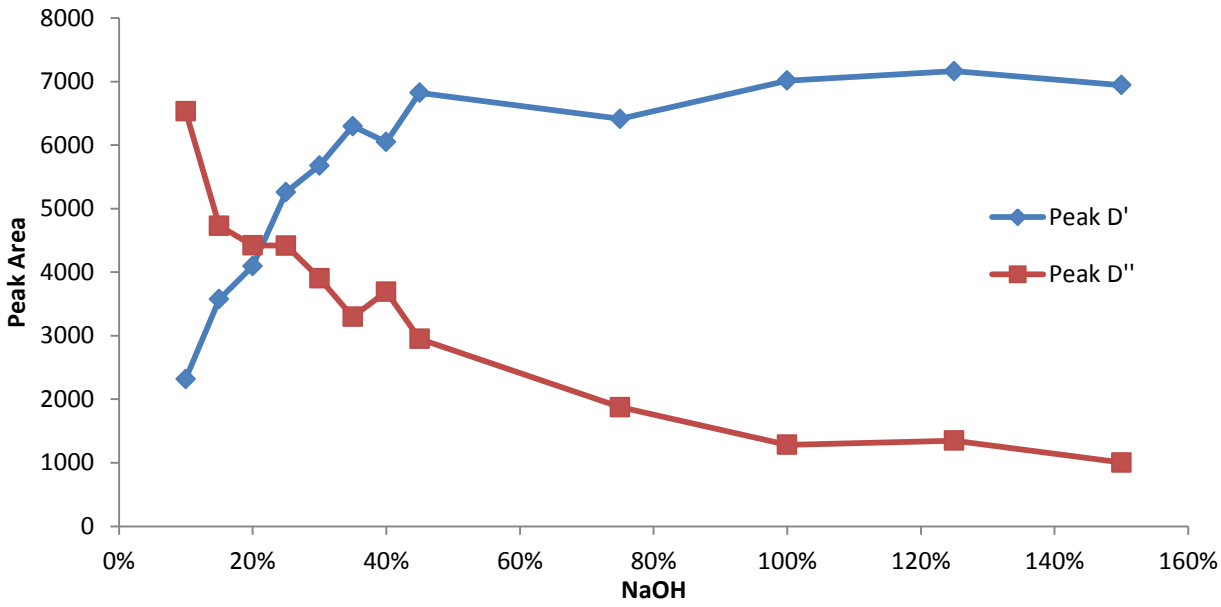

Figure 4.7. Areas of both peaks observed after treatment of Reactive Orange 72 with varying amounts of NaOH. 100% represents 9.375E-7 moles of NaOH to 1 ng of dye.

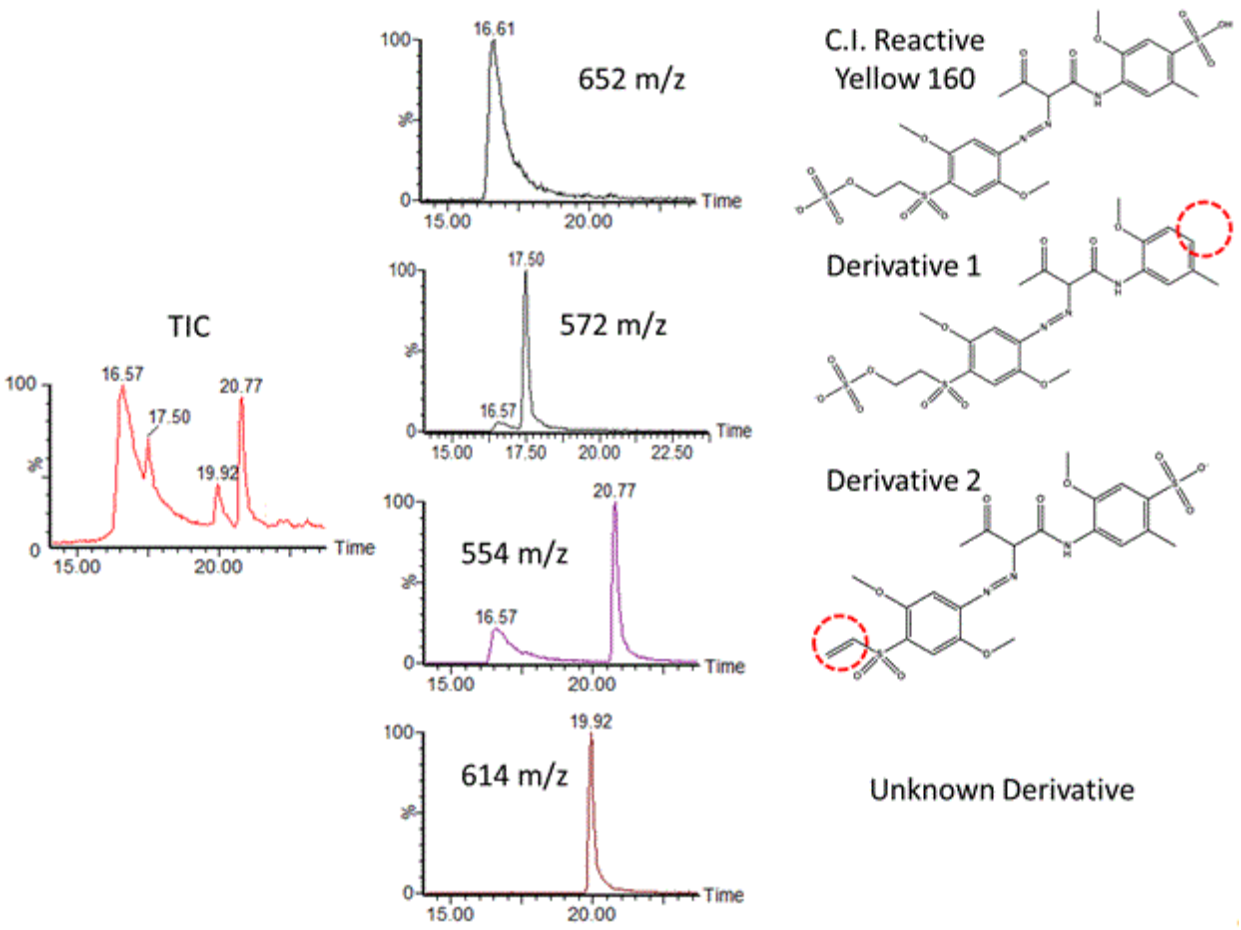

Figure 4.8. Total ion chromatogram of Reactive Yellow 160 standard and isolated molecular ions of four dye derivatives.

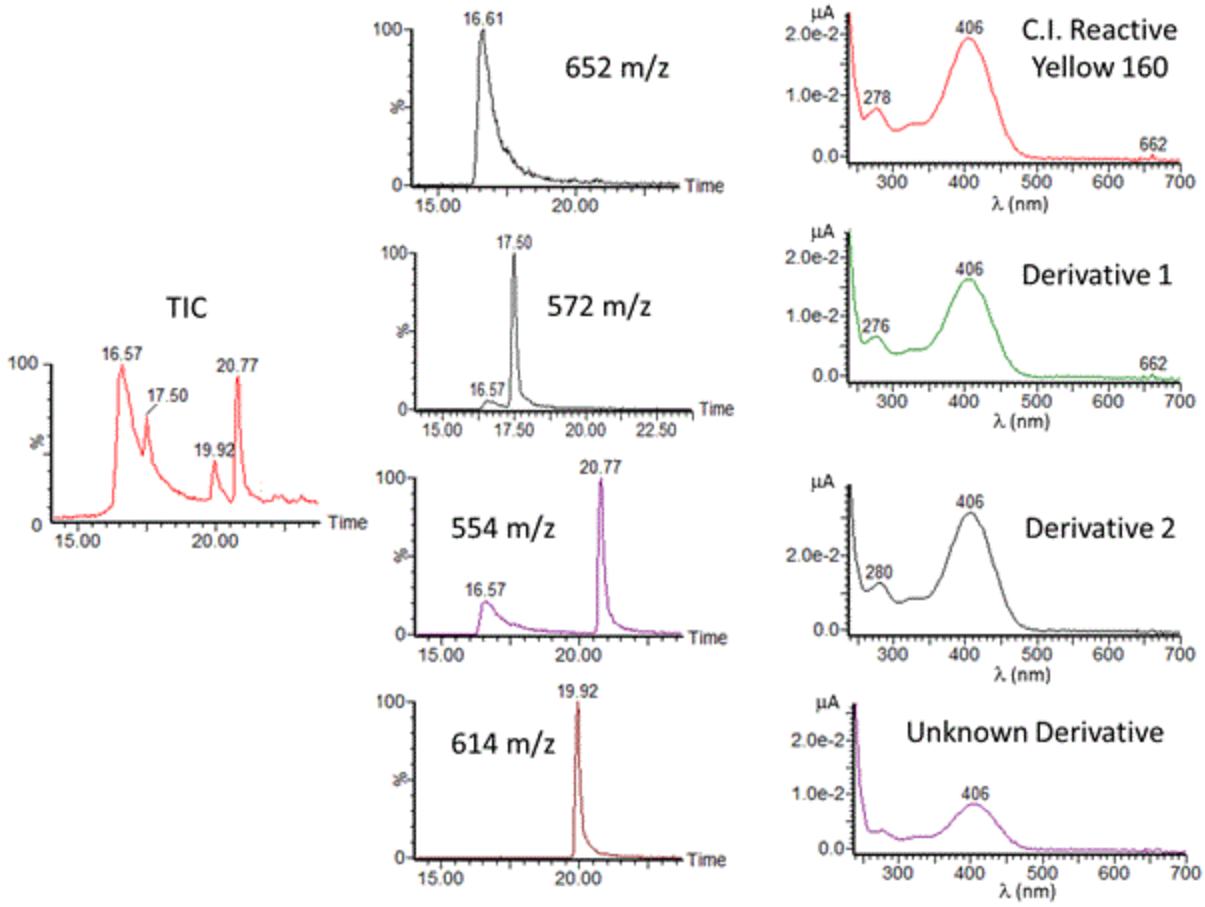

Figure 4.9. Total ion chromatogram of the Reactive Yellow 160 standard, isolated molecular ions of the potential dye derivatives, and their corresponding UV/visible absorbance spectra.

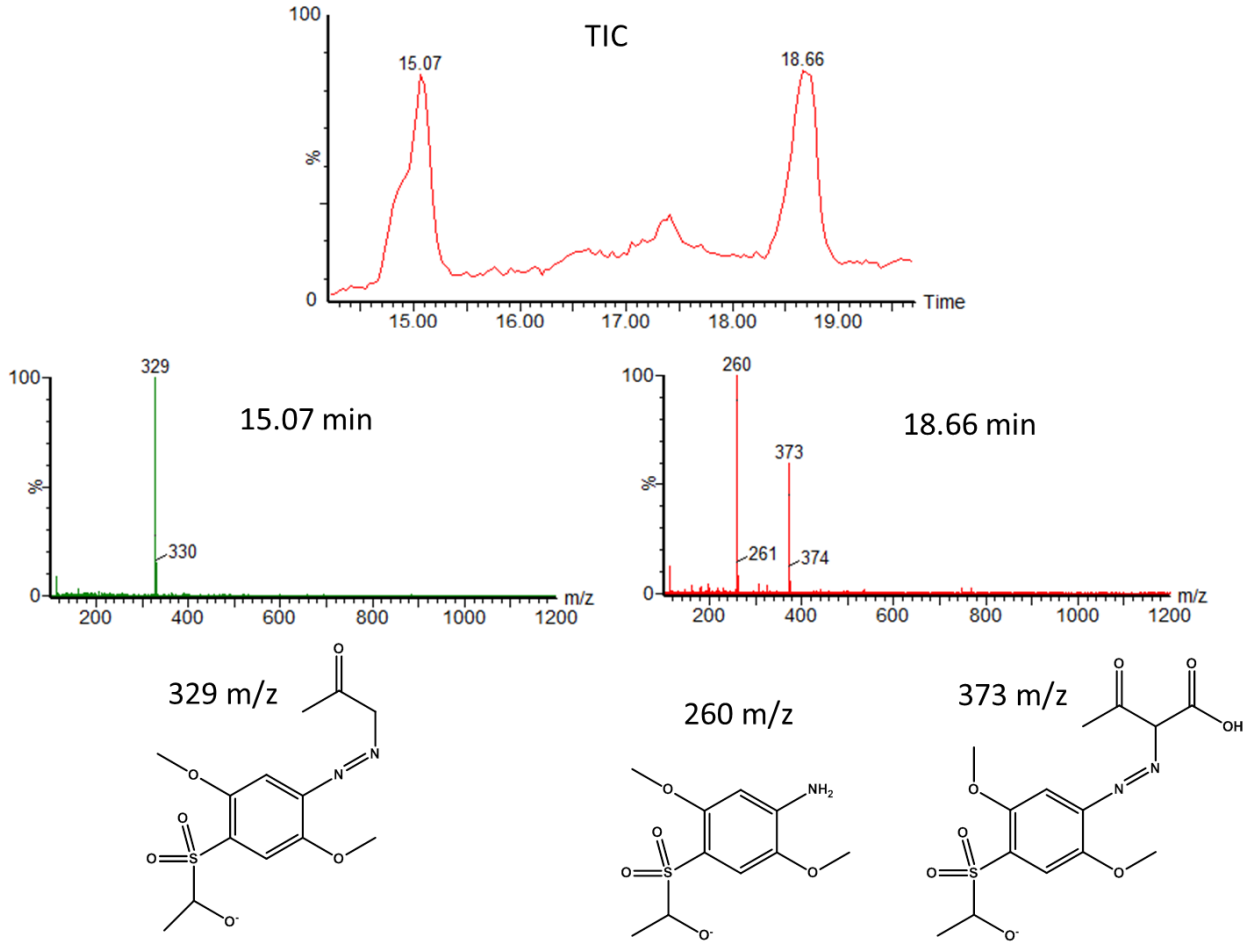

Figure 4.10. TIC of Reactive Yellow 160 after being treated with NaOH and heat (100°C). Two products were visible by HPLC-MS.

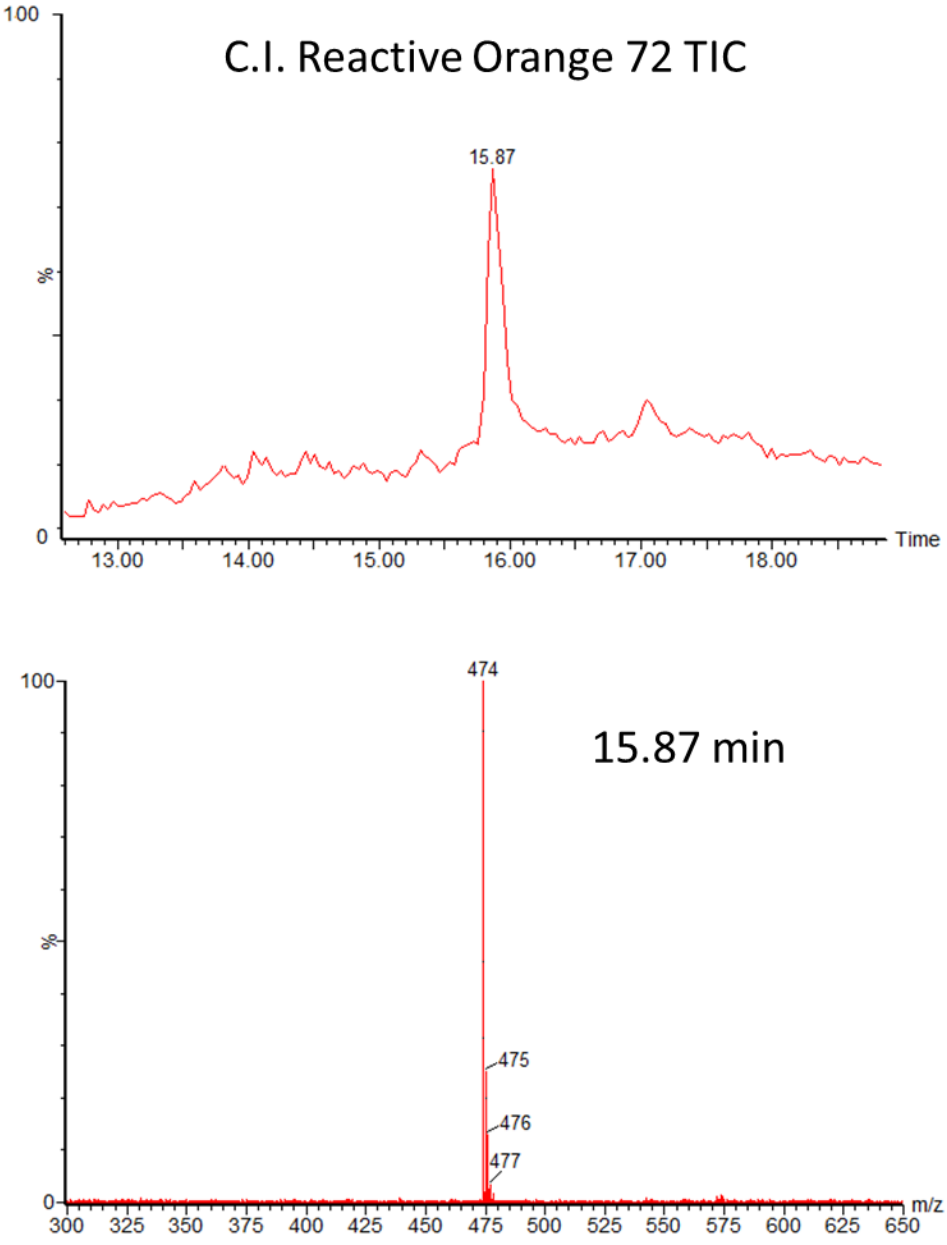

Figure 4.11. TIC of Reactive Orange 72 showing the only visible chromatographic peak and its mass spectra.

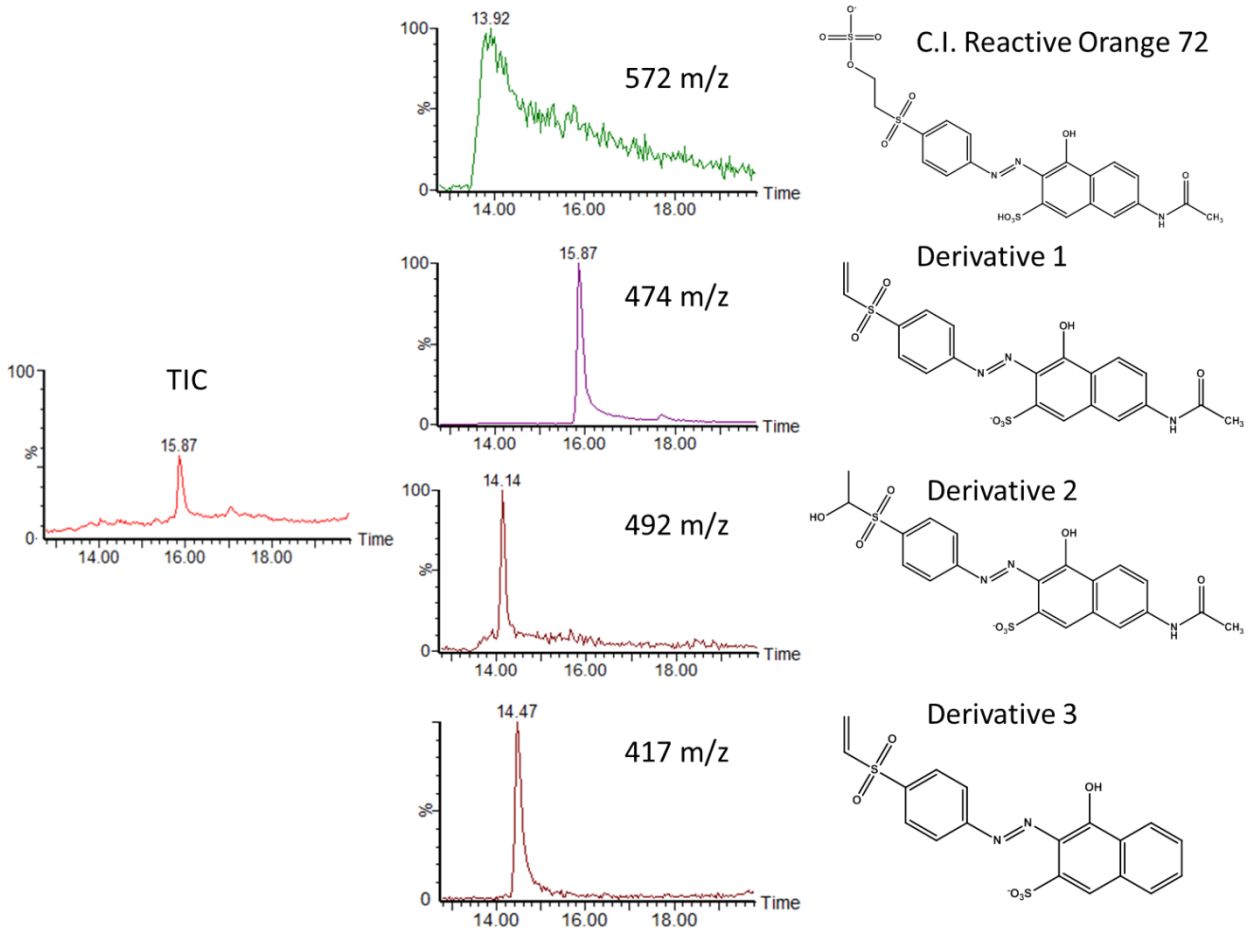

Figure 4.12. Extracted ion chromatograms for m/z 572, 474, 492, and 417 from the analysis of Reactive Orange 72. Individual chromatographic peaks for each mass suggest multiple compounds present in the standard.

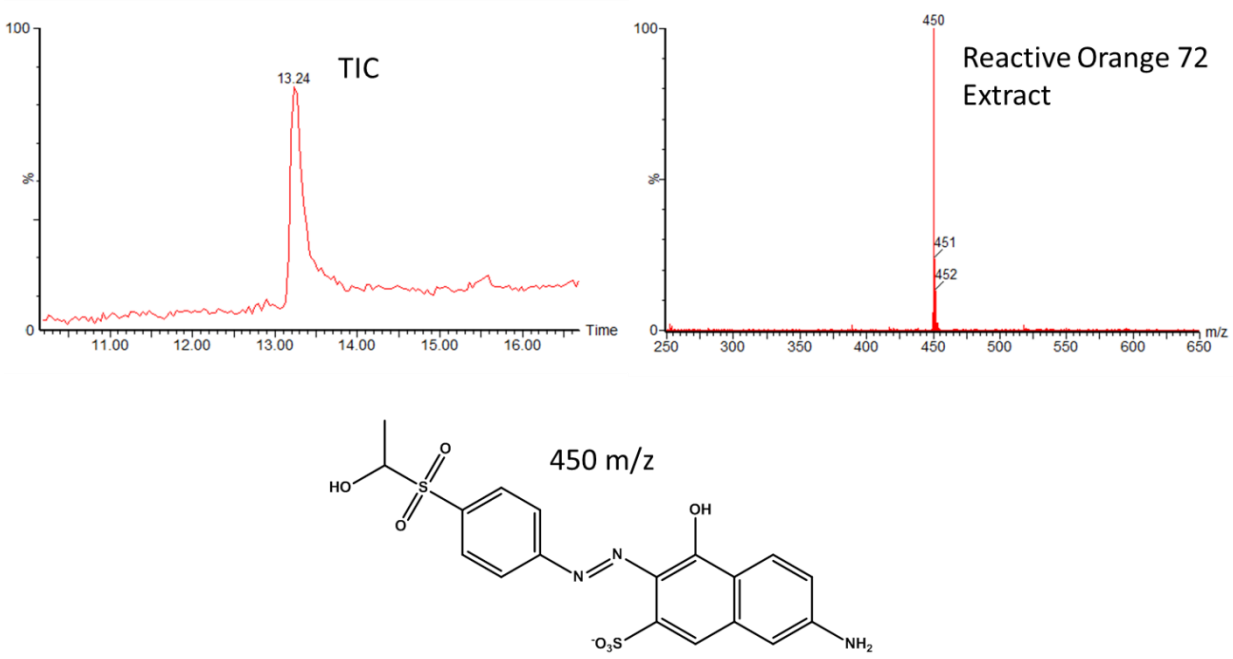

Figure 4.13. TIC and mass spectra of Reactive Orange 72 after treatment with NaOH and heat (100°C).

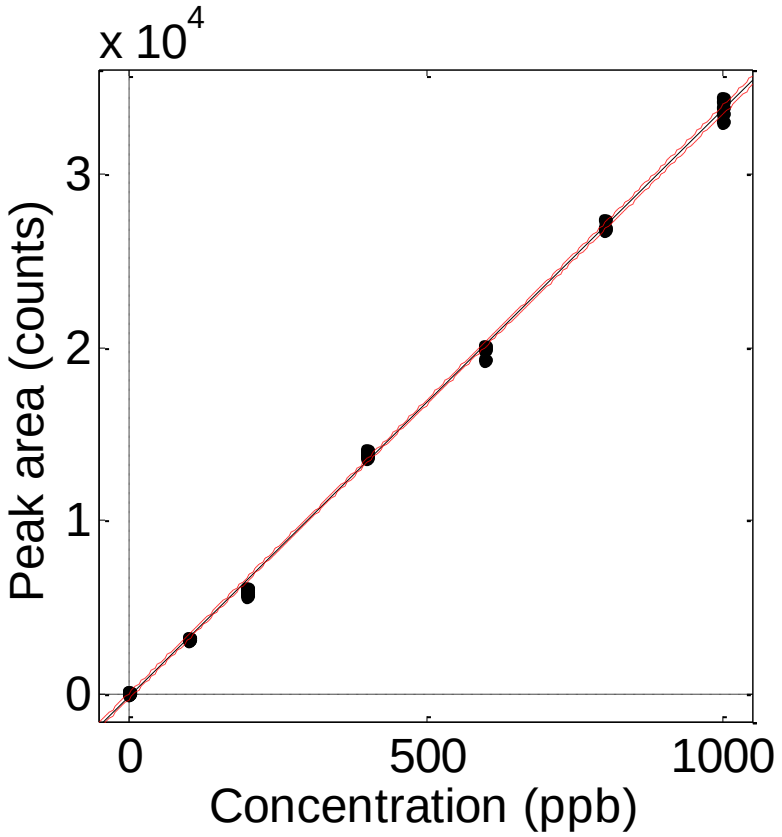

Figure 4.14. Calibration model for Reactive Blue 220.

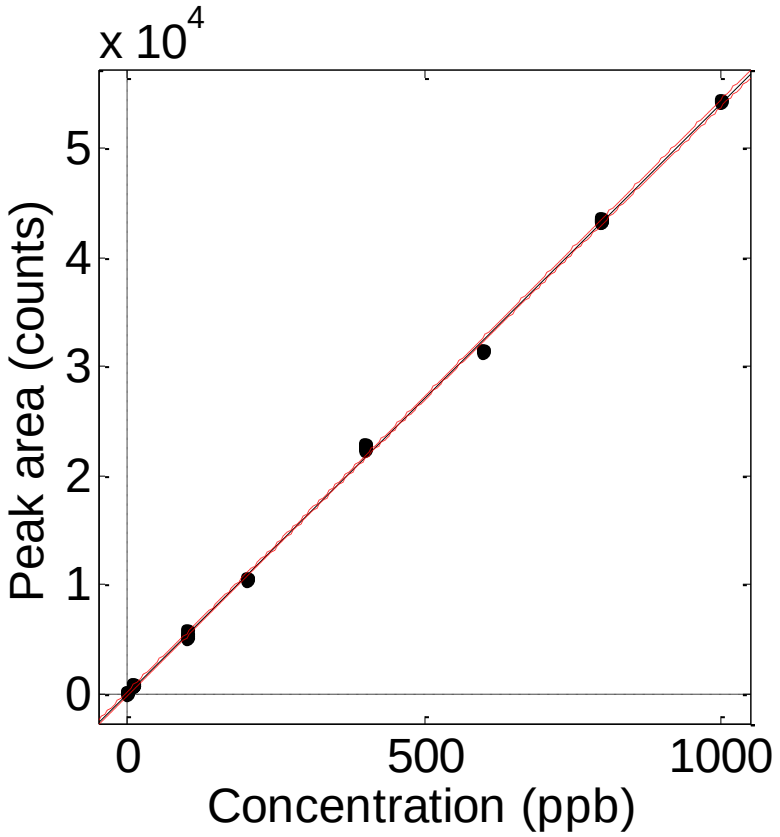

Figure 4.15. Calibration Model for Reactive Orange 72.

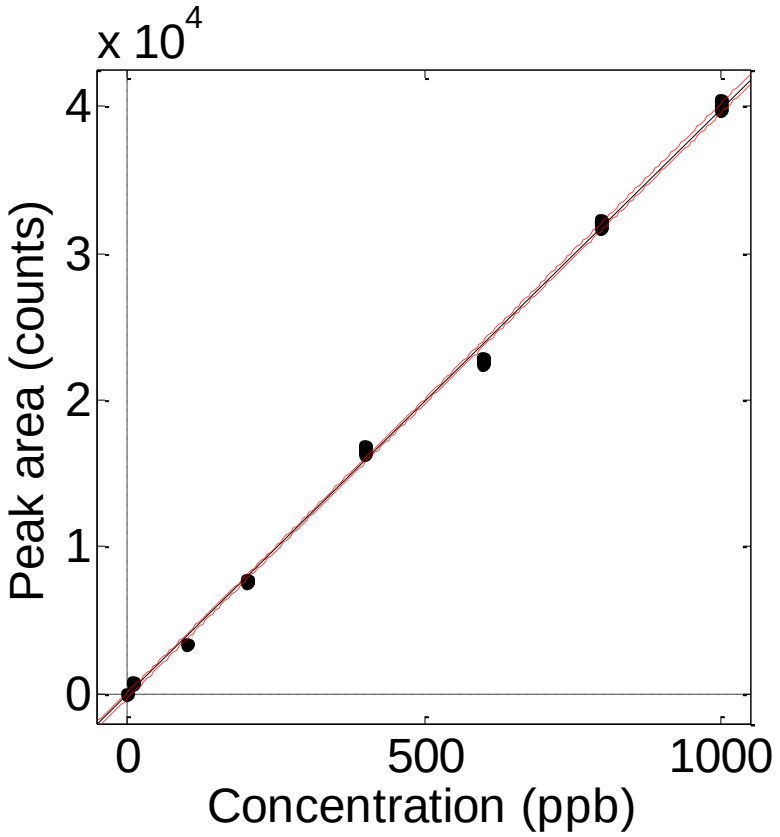

Figure 4.16. Calibration Model for Reactive Yellow 160.

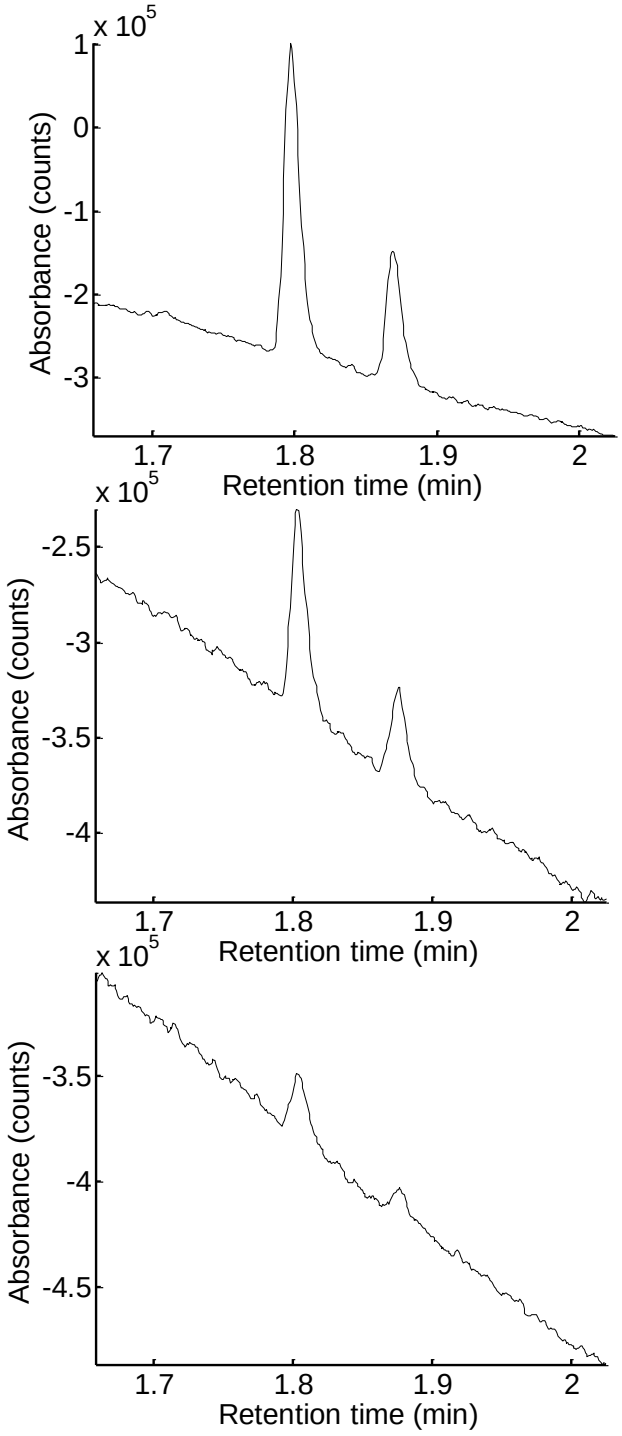

Figure 4.17. UPLC-DAD chromatograms of extracted Reactive Yellow 160 from a 10 mm fiber (top), a 5 mm fiber (middle) and a 1 mm fiber (bottom).

CHAPTER FIVE

MANDEL SENSITIVITY APPLIED TO ANALYTICAL METHOD PERFORMANCE COMPARISONS AND LIMITS OF DETECTION

ABSTRACT

The concept of the sensitivity ratio as an analytical performance characteristic was introduced by John Mandel of the National Bureau of Standards in 1954, but has been not been widely applied in analytical chemistry. The basis for Mandel sensitivity is reviewed here, along with examples of its use. Because the sensitivity ratio is independent of the scale in which measurements are expressed, it is a useful tool for comparisons of variability between different analytical methods.

INTRODUCTION

Validation of a chemical measurement process (CMP) typically involves the reporting of accuracy, precision, limit of detection, and other figures of merit. Such measures are often used to decide which approach should be employed in favor of another. Mandel points out that accuracy comparisons are usually not are contingent on meeting just a few requirements: (a) a monotonic functional relation must exist between what is measured and the property to be determined; (b) reference materials having known values must be available over the target range of the property to be studied; and, (c) the calibration model must be sufficiently free of both random and systematic errors to establish a clear and unbiased relationship.[1,2] Further, statistical measures of calibration accuracy are available for assessing the accuracy performance of a calibration function established by regression.[3,4]

Comparing CMP performance based on estimates of variability from different measurement methods and assigning a level of technical merit to a relevant performance characteristic, however, can be problematic. The oft-recommended approach is to report relative standard deviations (RSDs) or, equivalently, coefficients of variation (CVs) for

the two methods Otto-Hanson, *et al*. provides an illustrative example for which the different measurement scales confound comparison.[5] With two measurements of daily temperature at certain different times and locations expressed in Celsius and Fahrenheit degrees, Assuming that one measurement has a mean of 50 °F with a standard deviation of 10 °F, and the other a mean of 10 °C with a standard deviation of 5.6 °C. With relative standard deviations of 20% and 56%, it might seem that Fahrenheit measurements are more reliable. This comparison is invalid because Fahrenheit and Celsius scales are not proportional to one another because they are interval scale measurements without a meaningful origin, or zero point.[6]. In this case, the relationship between the two measurements is known and the numbers could be converted into the other. In general, the relationship between measurements having different scales may not be known.

Mandel sensitivity can be applied to comparisons of CMPs on different scales because it is a scale independent. The computations are trivial, depending only on the slope of the calibration lines and estimates of the variability of the measurement methods to be compared.

STATISTICAL BACKGROUND FOR MANDEL SENSITIVITY

Conventional sensitivity

The conventional sensitivity (S) of a CMP is defined as the change in the measured signal (Δy) divided by the change in the property being measured (Δx), *i.e.*, the slope of the calibration relationship:

$$S = \Delta y / \Delta x \qquad (1)$$

Figure 5.1 represents the calibration relationship for two different chromatographic methods of determining the same analyte. The first (upper blue line) method has a sensitivity of

$$\frac{\Delta y}{\Delta x} = \frac{100 \text{ counts}}{100 \text{ μg}} = 1.0 \text{ counts } \mu g^{-1} \quad (2)$$

The second method (lower red line) has a sensitivity of

$$\frac{\Delta y}{\Delta x} = \frac{50 \text{ counts}}{100 \text{ μg}} = 0.5 \text{ counts } \mu g^{-1} \quad (3)$$

Because of the steeper slope, it appears that the first method is better (more sensitive).

Mandel response

The straight-line calibration relationships represent idealized models of the real behavior of the chromatographic methods, idealized in the sense that they ignore noise or uncertainty in the measured data. A more realistic view of variation in the chromatographic results for these two methods is shown by the numerous individual data points in Figure 5.2. The calibration lines show what might be expected on the average; the dots show what might be obtained if many individual measurements were made on these two systems. Although the first method has the greater sensitivity ($\Delta y/\Delta x$ = 1.0 count μg^{-1} *vs*. 0.5 count μg^{-1}), it also has greater noise *(*σ_b = 5 counts *vs*. 2 counts).

The noise associated with the first chromatographic method is illustrated in two ways in the Figure 5.3. The point at (25 μg, 25 counts) is shown with a window extending one standard deviation of the blank *(*σ_b = 5 counts) above, and one standard deviation below. The Gaussian curve to the left in the figure is another way of illustrating the uncertainty of the data point at (25 μg, 25 counts). It is a projection of the uncertainty onto the signal axis (chromatographic peak area). The Gaussian curve is centered at 25 counts, with marked lines drawn at $\pm\sigma_b$ as "verticals" within the Gaussian. For the first

chromatographic method, σ_b = 5.0 counts, and the Mandel response for the data point above 25 μg is

$$y_M = \frac{y}{\sigma_b} = \frac{25 \text{ counts}}{5.0 \text{ counts}} = 5.0 \quad (4)$$

The vertical scale at the right of the plot shows the Mandel response. Note that the conventional response of 25 counts corresponds to a Mandel response of 5.

Similarly, the noise associated with the second chromatographic method is illustrated in two ways in Figure 5.4. The point at (50 μg, 25 counts) is shown with another window extending one standard deviation of the blank (σ_b = 5 counts) above, and one standard deviation below. Again, the Gaussian curve to the left in the figure is a projection of the uncertainty onto the signal axis. In this case, the Gaussian is centered at 25 counts, with marked lines drawn at $\pm\sigma_b$ as "verticals" within the Gaussian.

Mandel sensitivity

Mandel defined sensitivity as the ability of a test method to detect a change in the amount of the property under study.[1,2] This ability depends (in part) on the precision of the CMP. Mandel suggested measuring the response as unitless multiples of the standard deviation of the blank (σ_b): $y_M = y / \sigma_b$. The Mandel sensitivity, S_M, is defined in the same way as traditional sensitivity, however, for Mandel response, y_M, replaces Δy in the sensitivity calculation. Thus, the Mandel sensitivity (S_M) is defined as the change in the Mandel response (Δy_M) divided by the change in the property (Δx):

$$S_M = \Delta y_M / \Delta x = \Delta(y/\sigma_b) / \Delta x = (\Delta y/\Delta x)/\sigma_b = S/\sigma_b \quad (5)$$

For the first method (with the steeper slope), the Mandel sensitivity is

$$S_M = S / \sigma_b = \frac{(1.0 \text{ counts } \mu g^{-1})}{5.0 \text{ counts}} = 0.20 \ \mu g^{-1}$$

The second (less sensitive) method, for which σ_b = 2.0 counts, has a Mandel sensitivity (S_M) of

$$S_M = S / \sigma_b = \frac{(0.5 \text{ counts } \mu g^{-1})}{2.0 \text{ counts}} = 0.25 \ \mu g^{-1} \quad (6)$$

The Mandel sensitivity is a slope. It can be interpreted as the number of standard deviations of the blank that the signal changes per unit change in analyte amount. The Mandel sensitivity removes the original response measurement units (peak area), and has units of reciprocal amount (in this case, μg^{-1}).

Although the first method had a larger *conventional* sensitivity (1.0 counts μg^{-1} *vs*. 0.5 counts μg^{-1}), the second method has the larger *Mandel* sensitivity (0.25 μg^{-1} *vs*. 0.20 μg^{-1}). Because Mandel sensitivity is "the ability of a test method to detect a change in the amount of the property under study," the second method (with the shallower slope) will be better able to detect a change in the amount of analyte.

The Mandel response concept lends itself to depicting the performance of two CMPs on a common scale for comparison. When the two chromatographic methods are plotted in Figure 5.5 on the same vertical scale of Mandel response, it is clear that the second method, which had the smaller *conventional* sensitivity, has the larger *Mandel sensitivity* (0.25 μg^{-1}). The first method, which had the larger *conventional* sensitivity, is seen to have the smaller *Mandel sensitivity* (0.20 μg^{-1}). Note that the scaled noise in this plot is the same for both methods (as it should be on this common scale).

Detection decision limits

Mandel's original sensitivity paper was motivated by the concept of deciding whether two CMP responses close to one another can be discriminated—a decision process that is related to calculating decision levels associated with analyte detection. The common

Mandel response scale is an elegant path to calculate such decision limits, because these limits are all based on multiples of the standard deviation of the blank (σ_b), the very quantity that is measured by the Mandel response. Before discussing the application of Mandel sensitivity to CMP detection limits, we review the basis for the common critical decisions limits for analyte detection.

The limit of detection (LD) is specified by calculating the signal level above the mean of the blank at which the fraction risk of concluding that analyte is present, when it actually is not present, is acceptably small. Assuming a Gaussian distribution of noise for measurements of a sample containing no analyte (the 'blank'), an estimate of the standard deviation is obtained by replicate measurements of a blank, or by other statistical approaches, and assumed to have sufficient reliability to be considered a good estimate of the population standard deviation of the CMP. Because the variability of many CMPs is homoscedastic at low levels of analyte, the standard deviation of the blank, $\sigma_{b,}$ is usually a good estimate of the uncertainty around the LD. This decision limit is calculated by finding the number (k) of standard deviations above the mean that provides an acceptably low upper-tailed area above that level. A common choice for this criterion is $k = 3$, which provides an upper-tailed area of $\alpha = 0.0014$. This probability can be interpreted as the false positive risk of obtaining a response as high as or higher than LD from a sample that contains no analyte. Equivalently, the level of confidence associated with correct detection decision at this level is 100% $\times(1 - \alpha)$, or 99.86 %. No single value of k is appropriate for all situations. For example, $k = 3.3$ provides higher detection reliability with a level of confidence for correct detection of 99.95 %, and a fractional false positive probability of $\alpha = 0.0005$. The amount of analyte equivalent to the limit of detection (on

the signal axis) is the limit of detection amount (*LDA*) and is found by inverting the calibration relationship. If a straight line calibration ($y = mx + b$, where y is detector response, x is analyte amount, m is the slope, and b is the y-intercept) is assumed and using k = 3.3,

$$LDA = \frac{3.3 \times s_b}{m} \tag{7}$$

However, at $k = 3$ or k = 3.3 for the LDA, the false negative error rate (β) is unacceptably high: 50% of time samples containing analyte present at that LDA will be falsely declared not detected. Remarkably, the β risk has historically been often ignored, even in standards documents from regulatory authorities.[7,8]

The recognition of false negative (β) risk leads to another critical limit, the minimum consistently detectable amount (MCDA). The MCDA represents the amount at which analyte can be said to be consistently detected, *i.e.*, where the false negative error rate is reduced to be equivalent to the false positive error rate. With the signal domain measurement 6 standard deviations of the blank above the mean of the blank, the fractional risk of encountering a sample giving a signal below the LD is 0.0014. At 6.6 standard deviations of the blank above the mean of the blank, the fractional risk of a false negative result occurring below the LDA is 0.0005. Thus, the MCDA might be calculated as

$$MCDA = \frac{6.6 \times s_b}{m} \tag{8}$$

Analyte amounts above the LDA support the detection decision with high confidence, but do so without controlling the false negative risk. Analyte detected at or above the MCDA are associated with a detection confidence of at least 99.95 % and a false negative β risk

of 0.0005. The low false negative error rate at the MCDA insures that analyte at or above this limit is *consistently* detected.

At an analyte concentration equal to the *LDA*, the expected % relative standard deviation (%*RSD*) of measurements can be calculated from the standard deviation of the blank σ_b projected to the amount axis as the standard deviation of predicted analyte amount, σ_a:

$$\%RSD = 100\%\left(\frac{\sigma_a}{3.3\sigma_a}\right) = 30.30\% \quad (9)$$

The *%RSD* at an analyte concentration equal to the *MCDA* is:

$$\%RSD = 100\%\left(\frac{\sigma_a}{6.6\sigma_a}\right) = 15.15\% \quad (10)$$

These %RSD values are too uncertain for the resulting measurements to be considered quantitative (no analytical chemist would boast of achieving a 30.30 %RSD). The generally accepted signal-to-noise ratio considered to be quantitative is 10:1, or equivalently and %RSD of 10 %. Thus, the limit of quantitation (LQ) is defined as the concentration of analyte that produces a signal 10 times the standard deviation of noise (defined by the standard deviation of the blank),

$$\%RSD = 100\%\left(\frac{\sigma_a}{10\sigma_a}\right) = 10\% \quad (11)$$

At analyte levels between the MCDA and the LQ, analyte is consistently detected with high confidence and low false negative errors, but the %RSD is insufficiently to guarantee accurate quantitation unbiased by experimental uncertainty.

Applying Mandel sensitivity to detection decision limits

Calibrations from the two chromatographic methods discussed earlier are plotted on again on the same vertical scale of Mandel response in Figure 5.6. The LDA (with k = 3.3) for both methods can be calculated from the Mandel sensitivity as

$$LDA = \frac{3.3}{S_m} \tag{12}$$

For the first chromatographic method, with $S_M = 0.20\ \mu g^{-1}$,

$$LDA = \frac{3.3}{0.20\ \mu g^{-1}} = 16.5\ \mu g$$

For the second chromatographic method, with $S_M = 0.25\ \mu g^{-1}$,

$$LDA = \frac{3.3}{0.25\ \mu g^{-1}} = 13.2\ \mu g$$

These LDA values are the analyte amounts (on the x-axis in Figure 5.6) at which the horizontal green line at height $3.3\sigma_b$ intersects with the respective calibration lines.

The MCDA (with $k = 6.6$) for both methods can be calculated from the Mandel sensitivity as

$$MCDA = \frac{6.6}{S_M} \tag{12}$$

For the first chromatographic method, with $S_M = 0.20\ \mu g^{-1}$,

$$MCDA = \frac{6.6}{0.20\ \mu g^{-1}} = 33.0\ \mu g \tag{13}$$

For the second chromatographic method, with $S_M = 0.25\ \mu g^{-1}$,

$$MCDA = \frac{6.6}{0.25\ \mu g^{-1}} = 26.4\ \mu g \tag{14}$$

These MCDA values occur in Figure 5.7 at the intersection of the horizontal green line at $6.6\sigma_b$ with the Mandel response calibration lines.

Finally, the LQ (with $k = 10$) for both methods can be calculated from the Mandel sensitivity as

$$LQ = \frac{10}{S_M} \tag{15}$$

For the first chromatographic method, with $S_M = 0.20\ \mu g^{-1}$,

$$LQ = \frac{10}{0.20\ \mu g^{-1}} = 50.0\ \mu g$$

For the second chromatographic method, with $S_M = 0.25\ \mu g^{-1}$,

$$LQ = \frac{6.6}{0.25\ \mu g^{-1}} = 40.0\ \mu g$$

These MCDA values occur in Figure 5.8 at the intersection of the horizontal green line at $10\sigma_b$ with the Mandel response calibration lines.

Conclusions

Evaluating a CMP form the viewpoint of Mandel response and Mandel sensitivity offers an easy and rapid method for comparison of the calibration performance of analytical methods by use of scale independent approach. The Mandel sensitivity offers an advantage over scale dependent approaches such as RSDs and CVs because it normalizes performance relative to the variability of the measurement method. Mandel sensitivity allows for calculation of detection limit critical values in a universal way that also provides intuitive and visual understanding of the differences among limit of detection amount, minimal consistently detectable amount, and limit of quantitation. We recommend its use for comparing the calibration performance of different analytical methods.

Coauthors of this work include Stanley N. Deming (Statistical Designs, Houston, TX) and Stephen L. Morgan (Department of Chemistry and Biochemistry, University of South Carolina, Columbia, SC 29208). Research in this presentation was supported by award 2010-DN-BX-K245 from the National Institute of Justice, Office of Justice Programs, U. S. Department of Justice. The opinions, findings, and conclusions or recommendations expressed in this publication are those of the author(s) and do not necessarily reflect those of the Department of Justice. Mention of commercial products does not imply endorsement on the part of the National Institute of Justice or the University of South Carolina.

REFERENCES

(1) Mandel, J.; Stiehler, R. D. Sensitivity—A criterion for the comparison of methods of test, *Journal of Research of the National Bureau of Standards* **1954**, *53*, 155-159.

(2) Mandel, J. *The Statistical Analysis of Experimental Data*, John Wiley & Sons, Inc., New York, 1964, pp. 363-389.

(3) Draper, N. R; Smith, S. *Applied Regression Analysis*, 3rd ed., John Wiley & Sons, Inc., New York, 1998.

(4) Deming, S. N.; Morgan, S. L. The use of linear models and matrix least squares in clinical chemistry, *Clin. Chem.* **1979**, *25*, 840-855.

(5) Otto-Hanson, L.; Eskridge, K. M.; Steadman; J. R.; Madisa, G. The sensitivity ratio: A superior method to compare plant and pathogen screening tests. *Crop Sci*. **2009**, *49*(1), 153-160.

(6) Stevens, S. S. On the theory of scales of measurement. *Science* **1946**, 677-680.

(7) Currie, L. A. Detection: Overview of historical, societal, and technical issues. Chapter 1 in: *Detection in Analytical Chemistry: Importance, Theory, and Practice*, L. A. Currie (ed.), American Chemical Society, Washington, DC, 1988.

(8) Currie, L. A. Detection: International update, and some emerging di-lemmas involving calibration, the blank, and multiple detection decisions. *Chemom, Intell. Lab. Sys*. **1997**, *37*, 151-181.

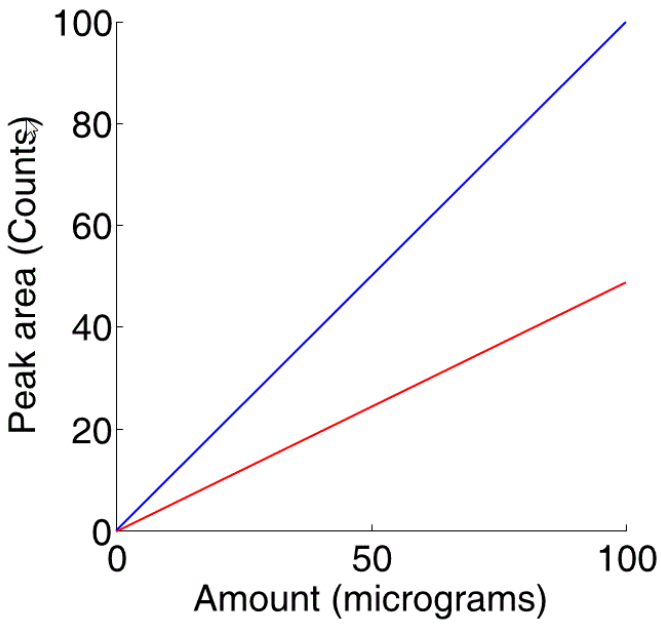

Figure 5.1. Calibration relationship for two different measurement processes.

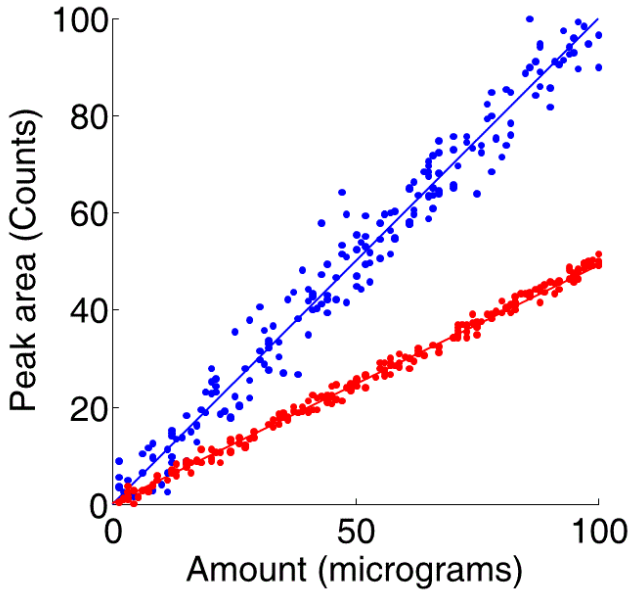

Figure 5.2. Calibration relationship for two different measurement processes with noise; standard deviation for upper (blue) calibration is 5 counts, and the standard deviation for the lower (red) calibration is 2 counts.

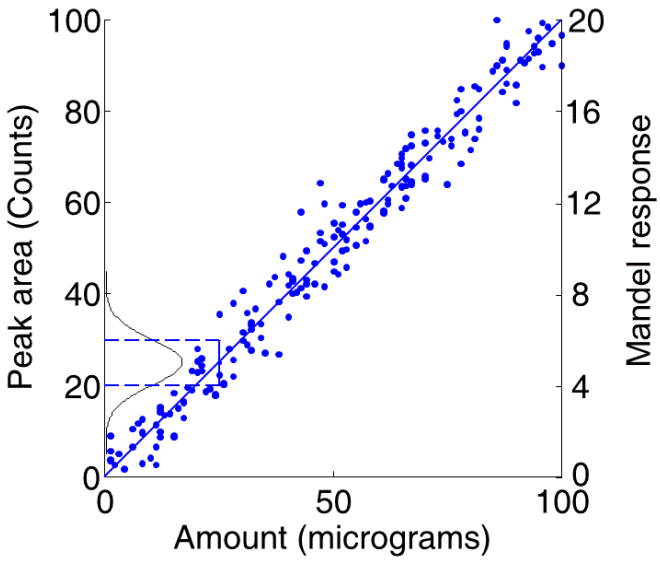

Figure 5.3. Calibration relationship for the first method with plus and minus one standard deviation window about the response of 25 peak counts for 25 micrograms. The right hand scale shows the Mandel response in unitless multiples of the standard deviation.

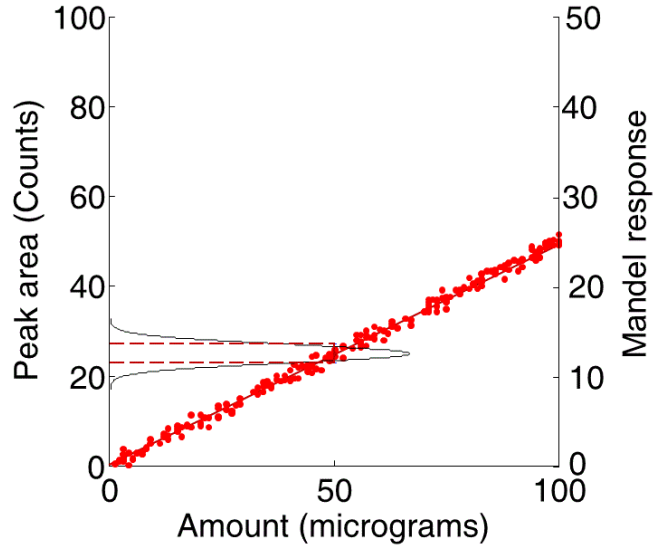

Figure 5.4. Calibration relationship for the second method with plus and minus one standard deviation window about the response at 25 peak counts for 50 micrograms. The right hand scale shows the Mandel response in unitless multiples of the standard deviation.

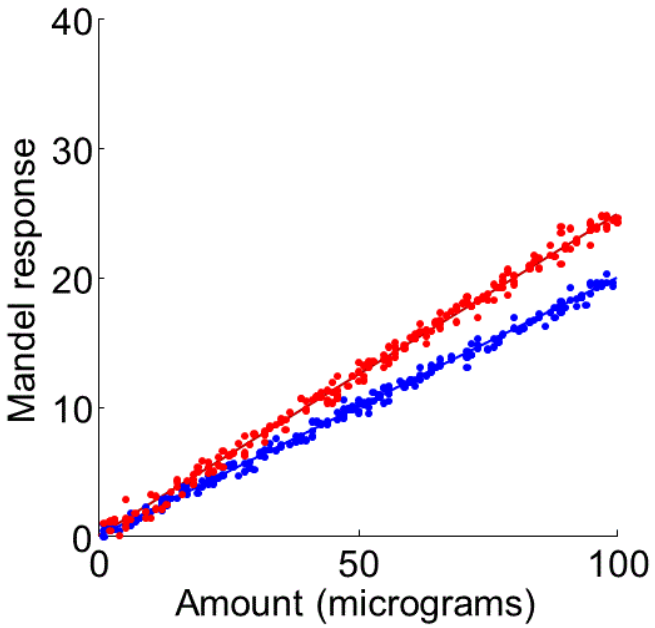

Figure 5.5. Common Mandel response scale for comparison of calibration performance. The second (red) method has larger Mandel sensitivity (0.25 μg^{-1}) than the first (blue) method (0.20 μg^{-1}).

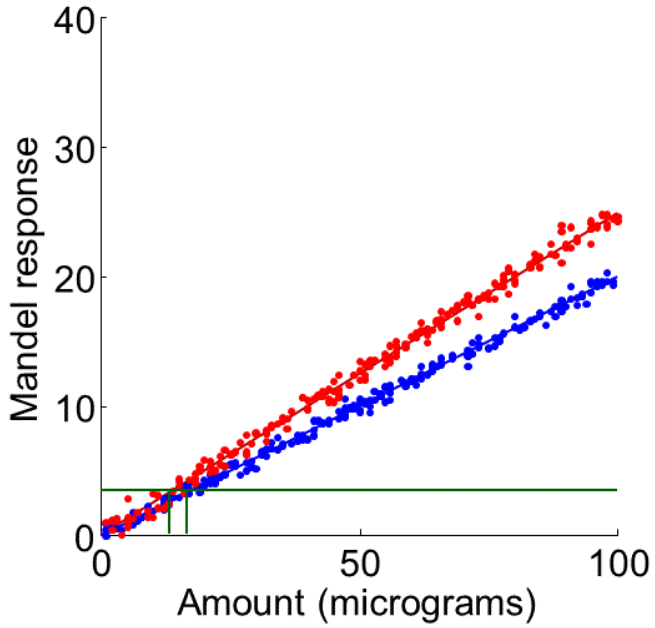

Figure 5.6. Common Mandel response scale for estimation of LDA. The second (red) method has a lower LDA (13.2 µg) than the first (blue) method (16.5 µg).

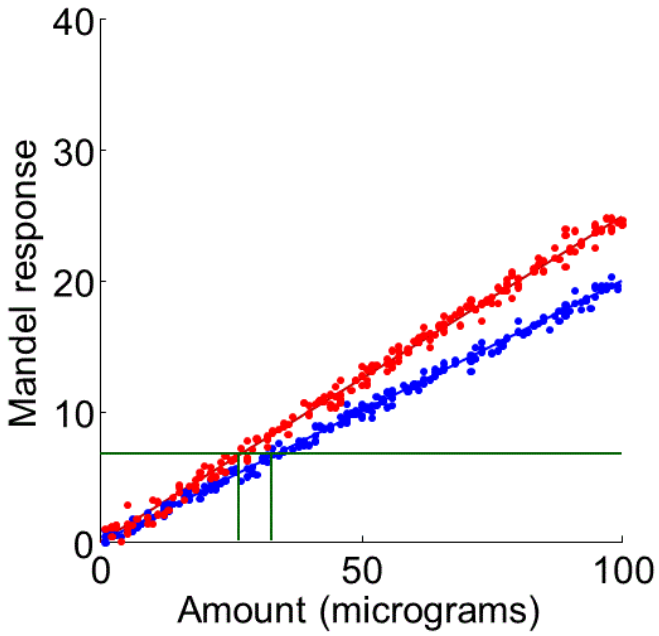

Figure 5.7. Common Mandel response scale for estimation of MCDA. The second (red) method has a lower MCDA (26.4 µg) than the first (blue) method (33.0 µg).

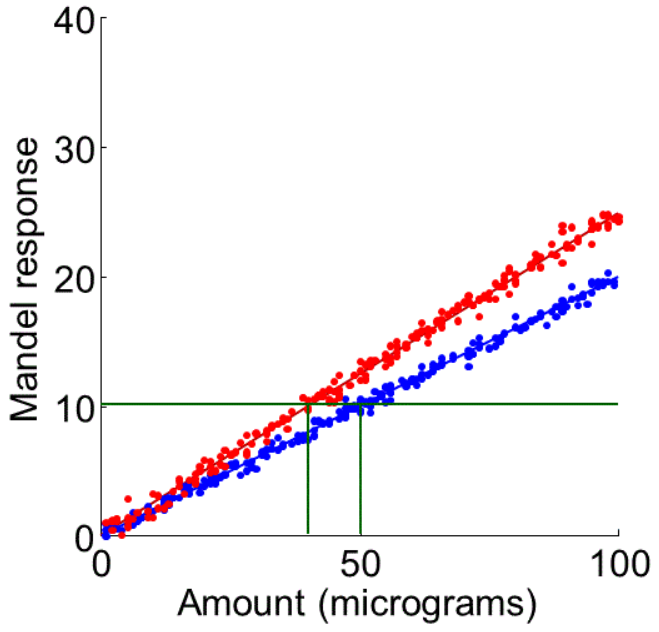

Figure 5.8. Common Mandel response scale for estimation of LQ. The second (red) method has a lower LQ (40.0 µg) than the first (blue) method (50.0 µg).

WORKS CITED

Andreasen, M. F.; Telving, R.; Birkler, R.I.D.; Schumacher, B.; Johannsen, M. A fatal poisoning involving Bromo-Dragonfly. *Forensic Sci. Int.* **2009**, *183*, 91–96.

Beattie, B.; Roberts, H.; Dudley, R. J. The extraction and classification of dyes from cellulose acetate fibers. *J. Forensic Sci. Soc*. **1981**, *21*, 233-237.

Beattie, I.B.; Dudley, R.J.; Smalldon, K.W. The extraction and classification of dyes on single nylon, polyacrylonitrile and polyester fibers. *J. Soc. Dye. Colour* **1979**, *95*, 295-302.

Bendroth, P.; Kronstrand, R.; Helander, A.; Greby, J.; Stephanson, N.; Krantz, P. Comparison of ethyl glucuronide in hair with phosphatidylethanol in whole blood as post-mortem markers of alcohol abuse. *Forensic Sci. Int*. **2008**, *176*, 76-81.

Borros, S.; Barbera, G.; Biada, J.; Agullo, N. The use of capillary electrophoresis to study the formation of carcinogenic aryl amines in azo dyes. *Dyes and Pigm.* **1999**, *43*, 189-196.

Bozic, M.; Kokol, V. Ecological alternatives to the reduction and oxidation processes in dyeing with vat and sulphur dyes. *Dyes and Pigments*, **2008**, *76*, 299-309.

Burkinshaw, S.M.; Graham, C. Capillary zone electrophoresis analysis of chlorotriazinyl reactive dyes in dyebath effluent. *Dyes and Pigm.* **1997**, *34*, 307-319.

Burkinshaw, S.M.; Hinks, D.; Lewis, D.M. Capillary zone electrophoresis in the analysis of dyes and other compounds employed in the dye-manufacturing and dye-using industries. *J. Chromatogr*. *A* **1993**, *640*, 413-417.

Burkinshaw, S.M.; Hinks, D.; Lewis, D.M. The use of capillary electrophoresis for the analysis of several dye classes. In: Special Publication - *Royal Society of Chemistry* **1993**,*122*, 93-100.

Christie, R. *Colour Chemistry.* RSC Paperbacks: Cambridge, England, 2001.

Crabtree, S. R.; Rendle, D. F.; Wiggins, K. G.; Salter, M. T. The Release of Reactive Dyes from Wool Fibers by Alkaline- Hydrolysis and Their Analysis by Thin-Layer Chromatography. *J. Soc. Dye. Colour* **1995**, *111*, 100-102.

Croft, S.N.; Hinks, D. Analysis of dyes by capillary electrophoresis. *Textile Chemist and Colorist* **1993**, *25*, 47-51.

Croft, S.N.; Hinks, D. Analysis of dyes by capillary electrophoresis. *J. Soc. Dye. Colour* **1992**, *108*, 546-551.

Croft, S.N.; Lewis, D.M. Analysis of reactive dyes and related derivatives using high-performance capillary electrophoresis. *Dyes and Pigm.* **1992**, *18*, 309-317.

Currie, L. A. Detection: International update, and some emerging di-lemmas involving calibration, the blank, and multiple detection decisions. *Chemom, Intell. Lab. Sys*. **1997**, *37*, 151-181.

Currie, L. A. Detection: Overview of historical, societal, and technical issues. *Detection in Analytical Chemistry: Importance, Theory, and Practice*, L. A. Currie (ed.), American Chemical Society, Washington, DC, 1988.

Deadman, H. *Fiber evidence and the Wayne Williams trial*, US Government Document J1.14/8a:F44, Federal Bureau of Investigation, US Department of Justice, FBI Law Enforcement Bulletin, March and May, 1984.

Deming, S. N.; Morgan, S. L. *Experimental Design: A Chemometric Approach*, 2nd ed. Elsevier Science Publishers: Amsterdam, 1993.

Deming, S. N.; Morgan, S. L. The use of linear models and matrix least squares in clinical chemistry, *Clin. Chem.* **1979**, *25*, 840-855.

Dockery C. R., Stefan, A. R., Nieuwland, A. A., Roberson, S. N., Baguley, B.M., Hendrix, J. E., Morgan, S. L. Automated extraction of direct, reactive, and vat dyes from cellulosic fibers for forensic analysis by capillary electrophoresis. *Anal. Bioanal. Chem*. **2009**, *394*, 2095-2103.

Draper, N. R; Smith, S. *Applied Regression Analysis*, 3rd ed., John Wiley & Sons, Inc., New York, 1998.

Eyring, M. B.; Gaudette, B. D. An introduction to the forensic aspects of textile fiber examinations. Chapter 6 in: *Forensic Science Handbook*, vol. 2, R. Saferstein, Ed.; Prentice Hall: Englewood Cliffs, NJ, 2005.

Fisher, J. *Forensics under Fire: Are Bad Science and Dueling Experts Corrupting Criminal Justice?* Rutgers University Press: New Brunswick, NJ, 2008.

Gaudette, B. D. The forensic aspects of textile fiber examination. Chapter 5 in: *Forensic Science Handbook*, vol. 2, R. Saferstein, Ed.; Prentice Hall: Englewood Cliffs, NJ, 1988.

Grieve, M. Interpretation of fibres evidence. Chapter 13 in: *Forensic Examination of Fibres*, 2nd edition, Robertson J.; Grieve, M., Eds.; Taylor & Francis: London, 1999.

Hartshorne, A. W.; Laing, D. K. The dye classification and discrimination of colored polypropylene fibers. *Forensic Sci.Int*. **1984**, *25*, 133-141.

Hartzell-Baguley, B.; Stefan, A. R.; Dockery, C. R.; Hendrix, J. E.; Morgan, S. L. Non-aqueous capillary electrophoresis of azo and anthraquinone disperse dyes extracted from polyester fibers for forensic analysis. *Anal. Bioanal. Chem*., **2009**, unpublished manuscript.

Home, J. M.; Dudley, R. J. Thin-layer chromatography of dyes extracted from cellulosic fibers. *Forensic Sci.Int*. **1981**, *17*, 71-78.

Home, J.; Dudley, R. Thin-layer chromatography of dyes extracted from cellulosic fibres. *Forensic Sci.Int*. **1981**, *17*, 71–78.

Houck, M. *Statistics and trace evidence: the tyranny of numbers*, Forensic Science Communications, 1 January 1999.

Huang, M.; Russo, R.; Fookes, B. G.; Sigman, M. E. Analysis of Fiber Dyes by Liquid Chromatography Mass Spectrometry (LC-MS) with Electrospray Ionization: Discriminating Between Dyes with Indistinguishable UV-Visible Absorption Spectra. *J. Forensic Sci*. **2005**, *50*, 526-534.

Huang, M.; Yinon, J.; Sigman, M. E. Forensic identification of dyes extracted from textile fibers by liquid chromatography mass spectrometry (LC-MS). *J. Forensic Sci.* **2004**, *49*, 238-249.

Ji, C.; Feng, F.; Chen, Z.; Chu, X. Highly sensitive determination of 10 dyes in food with complex matrices using SPE followed by UPLC-DAD-Tandem mass spectrometry. *J. Liq. Chromatogr. & Relat. Technol.* **2011**, *34*, 93-105.

Kelly, J. F.; Wearner, P. K. *Tainting Evidence: Inside the Scandals at the FBI Crime Lab*, The Free Press: New York, 1998.

Laing, D. K.; Boughey, L.; Hartshorne, A. W. The standardization of thin layer chromatographic systems for comparison of fiber dyes. *J. Forensic Sci. Soc*. **1990**, *30*, 299-307.

Laing, D. K.; Gill, R.; Blacklaws, C.; Bickley, H.M. Characterization of acid dyes in forensic fiber analysis by high-performance liquid chromatography using narrow-bore columns and diode array detection. *J. Chromatogr*. **1988**, *442*, 187-208.

Laing, D. K.; Hartshorne, A. W.; Bennett, D. C. Thin layer chromatography of azoic dyes extracted from cotton fibers. *J. Forensic Sci. Soc*. **1990**, *30*, 309-315.

Macrae, R.; Dudley, R. J.; Smalldon, K. W. The characterization of dyestuffs on wool fibers with special reference to microspectrophotometry. *J. Forensic Sci*. **1979**, *24*, 117-129.

Macrae, R.; Smalldon, K.W. The characterization of dyestuffs on wool fibers with special reference to microspectrophotometry. *J .Forensic Sci.* **1979**, *24*, 109-116.

Mandel, J. *The Statistical Analysis of Experimental Data*, John Wiley & Sons, Inc., New York, 1964, pp. 363-389.

Mandel, J.; Stiehler, R. D. Sensitivity—A criterion for the comparison of methods of test, *Journal of Research of the National Bureau of Standards* **1954**, *53*, 155-159.

Minioti, K.; Sakellariou, C.; Thomaidis, N. Determination of 13 synthetic food colorants in water-soluble foods by reversed-phase high-performance liquid chromatography coupled with diode-array detector. *Anal. Chim. Acta*, **2007**, *583*, 103-110.

Morgan, S. L.; Vann, B. C.; Baguley, B. M.; Stefan, A. R. *Advances in discrimination of dyed textile fibers using capillary electrophoresis/mass spectrometry*. Trace Evidence Symposium, Clearwater, FL, 2007

National Research Council of the National Academies. *Forensic Analysis: Weighing Bullet Lead Evidence*. The National Academies Press: Washington, DC, 2004.

National Research Council of the National Academies. *Strengthening Forensic Science in the United States: A Path Forward*, The National Academies Press: Washington, DC, 2009.

Needles, H. L. *Textile Fibers, Dyes, Finishes, and Processes: A Concise Guide*. Noyes Publications: Park Ridge, NJ, 1986.

Oien, C. T. *Case management issues from crime scene to courtroom*. Trace Evidence Symposium, Clearwater, FL, 2007 [URL: http://nfstc.org/projects/trace/].

Otto-Hanson, L.; Eskridge, K. M.; Steadman; J. R.; Madisa, G. The sensitivity ratio: A superior method to compare plant and pathogen screening tests. *Crop Sci*. **2009**, *49*, 153-160.

Pawlak, K.; Puchalska, M.; Miszczak, A.; Rosloniec, E.; Jarosz, M. Blue natural organic dyestuffs – from textile dyeing to mural painting. Separation and characterization of coloring matters present in elderberry, longwood and indigo. *J. Mass Spectrom.* **2006**, *41*, 613-622.

Petrick, L.M.; Wilson, T.A.; Fawcett, W.R. High-performance Liquid Chromatography-Ultraviolet-Visible Spectroscopy-Electrospray Ionization Mass Spectrometry Method for Acrylic and Polyester Forensic Fiber Dye Analysis. *J. Forensic Sci*. **2006**, *51*, 771-779

Petroviciu, I.; Albu, F.; Medvedovici, A. LC/MS and LC/MS/MS based protocol for identification of dyes in historic textiles." *Microchemical Journal*, **2010**, *95*, 247-254.

Rafaëlly, L.; Héron, S.; Nowik, W.; Tchapla, A. Optimization of ESI-MS detection for the HPLC of anthraquinone dyes. *Dyes and Pigm.* **2008**, *77*, 191-203.

Rendle, D. F.; Crabtree, S. R.; Wiggins, K. G.; Salter, M. T. Cellulase Digestion of Cotton Dyed with Reactive Dyes and Analysis of the Products by Thin-Layer Chromatography. *J. Soc. Dye. Colour* **1994**, *110*, 338-341.

Rendle, D. F.; Wiggins, K. G. Forensic analysis of textile fibre dyes. *Review of Progress in Coloration and Related Topics* **1995**, *25*, 29-34.

Resua, R. A semi-micro technique for the extraction and comparison of dyes in textile fibers. *J. Forensic Sci*. **1980**, *25*, 168-173.

Riu, J.; Barcelo, D. Determination of linear alkylbenzene sulfonates and their polar carboxylic degradation products in sewage treatment plants by automated solid-phase extraction followed by capillary electrophoresis-mass spectrometry. *Analyst* **2001**, *126*, 825-828.

Riu, J.; Eichhorn, P.; Guerrero, J.A.; Knepper, T.P.; Barcelo, D. Determination of linear alkylbenzenesulfonates in wastewater treatment plants and coastal waters by automated solid-phase extraction followed by capillary electrophoresis-UV detection and confirmation by capillary electrophoresis-mass spectrometry. *J. Chromatogr. A* **2000**, *889*, 221-229.

Riu, J.; Schonsee, I.; Barcelo, D. Determination of sulfonated azo dyes in groundwater and industrial effluents by automated solid-phase extraction followed by capillary electrophoresis mass spectrometry. *J. Mass Spectrom*. **1998**, *33*, 653-663.

Robertson J.; Grieve, M., Eds., *Forensic Examination of Fibres*. 2nd edition. London: Taylor & Francis: 1999.

Robertson, J.; Wells, R.J.; Pailthorpe, M.T.; David, S.; Aumatell, A.; Clark, R. *An assessment of the use of capillary electrophoresis for the analysis of acid dyes in wool fibers.* Advances in Forensic Sciences, Proceedings of the Meeting of the International Association of Forensic Sciences, 13th, Duesseldorf, Aug. 22-28, 1995, 4, 247-249.

Roux, C.; Margot, P. The population of textile fibres on car seats. *Sci Justice* **1997**, *37*, 25-30.

Shaw, I. C. Micro-scale thin-layer chromatographic method for the comparison of dyes stripped from wool fibers. *Analyst* **1980**, *105*, 729-730.

Shore, J. *Colorants and Auxiliaries*, vol. 1, 2nd edition. Society of Dyers and Colourists, West Yorkshire: England, 2002; pp. 18–23.

Sirén, H.; Sulkava, R. Determination of black dyes from cotton and wool fibers by capillary zone electrophoresis with UV detection: application of marker technique. *J. Chromatogr. A* **1995**, *717*, 149-155.

Smith, W. F. *Experimental Design for Formulation*. Cambridge University Press: New York, 2005.

Stefan, A. R., Dockery C. R., Nieuwland, A. A., Roberson, S. N., Baguley, B. M., Hendrix, J. E., Morgan, S. L. Forensic analysis of anthraquinone, azo, and metal complex acid dyes from nylon fibers by micro-extraction and capillary electrophoresis. *Anal. Bioanal. Chem*. **2009**, *394*, 2077-2085.

Stefan, A. R., Dockery, C. R., Baguley, B.M., Vann, B. C., Nieuwland, A. A., Hendrix, J. E., Morgan, S. L. Microextraction, capillary electrophoresis, and mass spectrometry for forensic analysis of azo and methine basic dyes from acrylic fibers. *Anal. Bioanal. Chem*.**2009**, *394*, 2087-2094.

Stevens, S. S. On the theory of scales of measurement. *Science* **1946**, 677-680.

Stoney. D.A. The assumption of relevance and an application to one-trace and two-Relaxation of trace problem. *J. Forensic Sci. Soc*. **1994**, *34*, 17-21.

Szostek, B.; Orska-Gawrys, J.; Surowiec, I.; Trojanowicz, M. Investigation of natural dyes occurring in historical Coptic textiles by high-performance liquid chromatography with UV-Vis and mass spectrometric detection. *J. Chromatogr. A* **2003**, *1012*, 179-192.

Takeda, S.; Tanaka, Y.; Nishimura, Y.; Yamane, M.; Siroma, Z.; Wakida, S. Analysis of dyestuff degradation products by capillary electrophoresis. *J. Chromatogr. A* **1999**, *853*, 503-509.

The Warren Commision Report. St. Martin's Press, New York, 1964; p. 592.

Tuinman, A.A.; Lewis, L.A.; Lewis, S.A. Trace-fiber color discrimination by electrospray ionization mass spectrometry: A tool for the analysis of dyes extracted from submillimeter nylon fibers. *Anal. Chem*. **2003**, *75*, 2753-2760.

Watt, R.; Roux, C.; Robertson, "The population of coloured textile fibres in domestic washing machines. *J. Sci Justice* **2005**, *45*,75-83.

Webb-Salter, M.; Wiggins, K. G. Aids to Interpretation, in: *Forensic Examination of Fibres*. 2nd edition, J. Robertson, M. Grieve, Eds., Taylor & Francis: London, 1999; pp. 364-378.

Wheals, B.B.; White, P.C.; Paterson, M.D. High-performance liquid chromatographic method utilizing single or multi-wavelength detection for the comparison of disperse dyes extracted from polyester fibers. *J. Chromatogr*. **1985**, *350*, 205-215.

Wiggins, K. G. Thin layer chromatographic analysis for fibre dyes. Chapter 11 in: *Forensic Examination of Fibres,* 2nd edition, Robertson J.; Grieve, M., Eds.; Taylor & Francis: London, 1999.

Wiggins, K. G.; Crabtree, S. R.; March, B. M. The importance of thin layer chromatography in the analysis of reactive dyes released from wool fibers. *J. Forensic Sci.* **1996**, *41*, 1042-1045.

Wiggins, K.; Holness, J. A further study of dye batch variation in textile and carpet fibres. *Science & Justice* **2005**, 45, 93-96.

Wiggins, K.G.; Cook, R.; Turner, Y.J. Dye batch variation in textile fibers. J. *Forensic Sci*. **1988**, *33*, 998-1007.

Wood, M.; Laloup, M.; Samync, N.; del Mar Ramirez Fernandez, M.; de Bruijn, E. A.; Maes, R A.A.; De Boeck, G. Recent applications of liquid chromatography-mass spectrometry in forensic science. *J. Chromatogr. A* **2006**, *1130*, 3–15.

Xu, X.; Leijenhorst, H.; Van den Hoven, P.; De Koeijer, J.A.; Logtenberg, H. Analysis of single textile fibres by sample-induced isotachophoresis-micellar electrokinetic capillary chromatography. *Sci. Justice* **2001**, *41*, 93-105.

Yinon, J.; Saar, J. Analysis of dyes extracted from textile fibers by thermospray high-performance liquid chromatography-mass spectrometry. *J. Chromatogr. A* **1991**, *586*, 73-84.

Zhang, X.; Laursen, R. Development of Mild Extraction Methods for the Analysis of Natural Dyes in Textiles of Historical Intersest Using LC-Diode Array Detector-MS. *Anal. Chem.* **2005**, *77*, 2022-2025.